PREPARATION AND CHARACTERIZATION OF CORN ZEIN NANOCOMPOSITE COATED POLYPROPYLENE FILMS FOR FOOD PACKAGING APPLICATIONS

A Thesis Submitted to
the Graduate School of Engineering and Sciences of
İzmir Institute of Technology
in Partial Fulfillment of the Requirements for the Degree of

MASTER OF SCIENCE

in Materials Science and Engineering

by
Onur ÖZÇALIK

July 2010

İZMİR

We approve the thesis of **Onur ÖZÇALIK**

_____
Prof. Dr. Funda TIHMINLIOĞLU
Supervisor

_____
Assoc. Prof. Dr. Banu ÖZEN
Co-Supervisor

_____
Prof. Dr. Devrim BALKÖSE
Committee Member

_____
Prof. Dr. Metin TANOĞLU
Committee Member

_____
Assoc. Prof. Dr. Figen KOREL
Committee Member

13 July 2010

_____ _____
Prof. Dr Mustafa GÜDEN **Assoc. Prof. Dr. Talat YALÇIN**
Head of the Department of Materials Dean of the Graduate School
Science and Engineering of Engineering and Sciences

ACKNOWLEDGEMENTS

ABSTRACT

PREPARATION AND CHARACTERIZATION OF CORN ZEIN NANOCOMPOSITE COATED POLYPROPYLENE FILMS FOR FOOD PACKAGING APPLICATIONS

Feasibility of prepared novel corn zein nanocomposite (CZNC) coated polypropylene (PP) film (CZNC-PP) structures for food packaging applications was investigated. Excellent barrier properties of corn zein nanocomposites were successfully combined with mechanically strong PP as an eco-friendly promising alternative to conventional barrier packaging systems. In this study, the effect of nano-sized layered silicate amount, type and processing of CZNC layer on the barrier, mechanical, optical and surface properties of the CZNC-PP films were investigated. Incorporation of organomodified montmorillonite (OMMT) by solution intercalation into zein coating matrix improved barrier and mechanical properties of PP films. The properties of single CZNC layers and interactions between layered silicates and zein matrix were also investigated. Fine delamination of OMMT in zein coating was found to be responsible for the improvements in oxygen and water vapor barrier of single corn zein layers due to more tortuous path formed for permeation of oxygen and water vapor. Prepared CZNC-PP films achieved nearly 4 times reduced oxygen permeability while WVP of the films were reduced by 30% with 5 wt% OMMT content in 5.9 µm corn zein coating. Meanwhile, improvements were less significant for unmodified nanoclay loadings due to the incompatibility between unmodified MMT and corn zein. Hydrophobicity of CZNC surface increased with increasing OMMT loading in accordance with WVP results. Permeation data was fitted to various phenomenological models predicting the permeability of polymer nanocomposites as a function of clay concentration and aspect ratio of nanoplatelets. While significant improvements in mechanical properties including doubled elastic modulus and 75% higher yield strength of PP films were obtained, incorporation of OMMT in CZNC layer did not change the color of CZNC-PP films significantly.

ÖZET

GIDA AMBALAJI UYGULAMALARI İÇİN MISIR PROTEİNİ NANOKOMPOZİTLERİ KAPLI POLİPROPİLEN FİLMLERİN HAZIRLANMASI VE KARAKTERİZASYONU

Gıda ambalaj uygulamalarına yönelik mısır proteini nanokompozitleri ile kaplanmış (MPNK) polipropilen (PP) filmlerin hazırlanması ve karakterizasyonu incelenmiştir. Biyobozunur bir polimer olan mısır proteininin yüksek oksijen bariyer özellikleri ile mekanik olarak dayanıklı olan PP filmlerinin özellikleri mevcut bariyer filmlerine çevreci bir alternatif oluşturabilecek şekilde başarılı bir biçimde birleştirilmiştir. Bu çalışmada mısır proteini nanokompozit tabakasının hazırlanmasında kullanılan nano boyutlu kil miktarının, tipinin ve nanokompozit hazırlama metodunun MPNK kaplı PP filmlerin (MPNK-PP) bariyer, mekanik, optik ve yüzey özellikleri üzerine olan etkileri incelenmiştir. Sıvı yaklaşımı metodu ile polimer yapıya dahil edilen organomodifiye tabakalı silikat nanokillerinin (OMTS) MPNK-PP filmlerin bariyer ve mekanik özelliklerini belirgin biçimde iyileştirdiği gözlemlenmiştir. MPNK tabakalarının tekbaşına özellikleri ve içeriğindeki killer ile polimer matrisinin etkileşimi de bu çalışmada incelenmiştir. Oksijen ve su buharı bariyer özelliklerinde elde edilen iyileşmelerin nanoboyutlu silikat tabakalarının etkili biçimde açılması sonucu artan dolambaçlı difüzyon yoluna bağlı olarak gerçekleştiği belirlenmiştir. 5.9 mikrometre kalınlığındaki, kütlece %5 OMTS içeren MPNK katmanı ile kaplanan filmler baz PP filmler ile karşılaştırıldığında oksijen geçirgenliği değerlerinin 4 kat, su buharı geçirgenliklerinin ise %30 oranında azaldığı görülmüştür. Su buharı bariyeri ile uyumlu olarak, MPNK kaplı yüzeylerin hidrofobik özellikleri OMTS ilavesi ile artmıştır. Bunun yanında, modifiye olmayan doğal kil ve sonikasyon yerine karıştırma ile hazırlanan filmlerde gözlemlenen iyileşmelerin daha az belirgin olduğu gözlemlenmiştir. Bariyer iyileştirmelerine ek olarak; OMTS ilaveli mısır proteini kaplamalı filmlerde baz PP filmlere kıyasla elastik modülüs 2 kat artarken, akma mukavemeti %75 oranında artmış, filmlerin renginde çıplak göz ile ayırt edilebilecek herhangi bir değişiklik gözlemlenmemiştir.

TABLE OF CONTENTS

LIST OF FIGURES

LIST OF TABLES

CHAPTER 1

INTRODUCTION

Food packaging deals with the preservation of food quality during the period from its production to its end use by the consumers. Synthetic polymers are the main packaging materials today since they offer versatile solutions for several needs of food packaging. Conventional packaging polymers are begun to be questioned due to increasing environmental concerns and their petroleum based sources. Research on sustainable alternative materials for food packaging is a hot topic for over a decade. Biopolymers are being draw attention of many researchers especially because of their petroleum independent sources and eco-friendliness. Most of biopolymers are synthesized from microorganisms or extracted directly from biomass. Their incomparably shorter degradation in the nature than the conventional synthetic polymers makes them attractive for food packaging applications.

Protein based biopolymers such as corn zein, soy or whey proteins extracted from by-products of food industry have noticeable properties suitable for food packaging. The most important feature of protein based biopolymers is their excellent barrier to oxygen, comparable to that of ethylene vinyl alcohol (EVOH) or polyvinylidine chloride (PVDC) (Padua and Wang, 2002; Miller and Krochta, 1997). Protein based polymers are soluble in light solvents such as ethanol depending on the type of the protein. Extensive research was reviewed concerning the preparation and characterization of stand-alone protein based biopolymer films. (Padua and Wang, 2002,; Tharanathan, 2003; Cuq et al., 1998). The processability of these polymers using plasticizers with different polymer processing techniques was also studied (Hernandez-Izquerdo and Krochta, 2008).

Particularly among proteins, corn zein; obtained from the corn gluten that is a by-product of corn wet milling industry; has great potential to be used in food packaging applications. Protein based polymers are heterogeneous polymers owing their functionality to amino acids in their structures (Padua and Wang, 2002; Lawton, 2002; Shukla and Cheryan, 2001). Proteins are mostly hydrophilic, being very sensitive to humidity and mostly soluble in water constituting for an important limitation for their

use in food packaging applications. On the contrary, zein is not soluble in water although its properties are still being dependent on relative humidity. Corn zein is relatively hydrophobic due to its high content of non-polar amino acids (Padua and Wang, 2002; Gioia and Guilbert, 1999). Although corn zein is a better barrier to moisture compared to other proteins and an excellent barrier to oxygen, use of corn zein standalone films in food packaging applications seem impossible with current status due to poor mechanical properties. Various plasticizers were used to solve the brittleness problem of corn zein. In addition to use of plasticizers; many hybrid strategies were developed to put corn zein in use in order to utilize its sustainability and excellent barrier to oxygen. These include lamination of zein with other proteins and lipids (Ghanbarzadeh and Oromiehi, 2008; Ryu et al., 2002; Cho et al., 2002; Weller et al., 1998), blending with synthetic polymers or biopolymers (Herald et al., 2002; Wu et al., 2003; Corradini et al., 2004) and coating polyolefin surfaces with corn zein (Tihminlioglu et al., 2010; Lee et al., 2008). Biopolymer coatings such as corn zein are attractive in environmental aspects, since identification and separation of layers for recycling of synthetic films are problematic and multilayer structures used for barrier applications constitute for an important amount of waste (Marsh and Bugusu, 2007; Cutter, 2006).

In this study, feasibility of further improvements in layered silicate loaded biopolymer coatings on commercial polypropylene films were investigated. Layered silicate nanocomposites (LSNC) were successfully used to improve the properties of synthetic polymers and are currently being put in use by food packaging industry (Lange and Wyser, 2003). Unique improvements brought in by clay nanoplatelets intercalated or exfoliated within the polymer matrix were well reviewed in the literature (Pavlidou and Papaspyrides, 2008; Paul and Robeson, 2008; Alexandre and Dubois, 2000; Ray and Bousmina, 2006). Improved elastic modulus and tensile strength at break due to strong interactions between high surface area LS and polymer matrix and improvements in barrier properties due to enhanced tortuosity are also promising features of biopolymer nanocomposites (DeRocher et al., 2005; Nielsen, 1967; Lape et al., 2006; Herrera-Alonso et al., 2009; Choudalakis and Gotsis, 2009). Therefore, the primary objective of this study was to develop a corn zein nanocomposite (CZNC) coated polypropylene (PP) film structure and to investigate the effect of coating on oxygen and water vapor permeability of the films. The CZNC was prepared by solution intercalation method using organomodified montmorillonite (OMMT), Cloisite 10A, as

nanofiller. Beside barrier properties, mechanical, surface hydrophobicity and color properties of the coated films were also discussed for various OMMT concentrations.

The thesis report consists of seven chapters, which altogether aim at covering preparation and characterization of corn zein nanocomposite coated polypropylene films for food packaging applications. Chapter 1 gives a general introduction to the background of this study. Decisive factors such as barrier and mechanical durability together with environmental aspect of food packaging were outlined in Chapter 2, in order to present the point of view of this thesis. Biodegradable alternatives of conventional polymers and strategies to utilize desirable properties of corn zein for food packaging applications were summarized in Chapter 3. Chapter 4 of the thesis was dedicated to nanocomposites and their applications. Desirable improvements in biodegradable polymer properties that can be achieved by layered silicate nanocomposites were also discussed in this chapter. Materials and methods used for the preparation of corn zein nanocomposite coated polypropylene films were given in Chapter 5 together with the characterization methods employed to investigate effect of CZNC coatings on polypropylene films. Mechanical, oxygen and water vapor barrier performance of CZNC coatings on PP films and effect of OMMT loading on barrier and properties of single CZNC layers were also evaluated in Chapter 6. Interactions between OMMT layered silicate and corn zein matrix as followed by FTIR-ATR as well as optical and surface characteristics of the prepared films were also discussed. Finally in Chapter 7, conclusions of this study were outlined.

CHAPTER 2

GENERAL INFORMATION ABOUT FOOD PACKAGING MATERIALS

Food packaging is one of the major application areas of polymers. Polymers in rigid forms or in films replaced other materials such as glass and metals due to their ease of production and versatility in food packaging applications. Food packaging deals with safely preparation of food for transport, distribution, storage and retailing end use.

Today, most of the food products are consumed months after their production and far from their production origin as well. During this period, prevention of food from deterioration is crucial. Food either in its processed form or in the raw material stage is highly perishable depending upon its water activity and temperature of storage and therefore it needs a careful technological intervention to preserve it longer (Tharanathan, 2003). For example; the post harvest losses of farm products such as fruits and vegetables are significantly high, ranging from 15 to 20% (Tharanathan, 2003). Similar to unprocessed farm products, processed food products are also sensitive and need protection until consumer use. Improper or poor packaging of these goods is responsible for high losses as well as improper distribution and storage.

The purpose of food packaging is to preserve the quality and safety of the food that it contains from the time of manufacture to the time it is used by the consumer (Cutter, 2006). Foods are sensible products that may undergo biological, chemical and physical deteriorations during storage and distribution. Deteriorations in packed food may be caused from many sources but mainly due to the transport of solutes through the packaging such as gases - like oxygen and carbon dioxide or water vapor. Resistance of the packaging material to the transport of solutes is called barrier property of the material. Deterioration of sensory attributes, reduction of nutritional content and impairing safety of foods is caused principally by physical and chemical changes in the food during storage and by microbial spoilage. Packaging should minimize these deteriorative changes in food products (Haugaard et al., 2001).

Packaging is directly related to food safety; firstly, if the packaging material does not provide a suitable barrier around the food, then microorganisms might

contaminate the food and make it unsafe. However, microbial contamination can also arise if the packaging material permits the transfer of, for example, moisture or O_2 into the package. In this situation, microorganisms that are present in the food, but present no risk because of the initial absence of moisture or O_2, may subsequently be able to grow and present a risk to the consumer (Robertson, 2006). As in the case of microbial deteriorations, enzymatic reactions are also favored by water content and ingress of O_2 into a package entailing deteriorations in food.

Food quality is also affected by chemical and physical reactions within the packaging. There are numbers of possible deteriorative chemical reactions adversely affecting the quality of food especially favored by transferred O_2 and water vapor. Lipid oxidation (autoxidation) initiated by molecular O_2, non-enzymatic browning, color changes related with the presence or absence of O_2, and reactions of vitamins or proteins with O_2 decreases the nutritional value of packaged food. Chemical changes of food also results in physical changes. Some physical changes deteriorating the food quality can be listed as softening, caking especially in powder products, toughening, emulsion breakdown, swelling/shrinkage and crushing/breakage that can be altered by controlling water uptake as well as protecting from physical impacts.

Mechanical properties of the packaging materials are important as well as barrier properties to ensure the success of the packaging. A packaging material must be durable itself in order to coat and protect the food product inside. An important function of a packaging is to resist some degree of impact without significant/permanent changes during the distribution of the product. An ideal packaging material must be strong and flexible at the same time in order to protect the product that it contains. Mechanical properties are also important for the other functions of packaging such as barrier properties. Resistance to solutes of the material is also related with the microstructure of the packaging material and durable mechanical properties also guarantee homogeneous barrier to solutes.

Packaging of raw or processed food is critical. Beside packaging technology, the materials used for food packaging must include a list of properties: low cost, lightness, toughness, flexibility, impact resistance, fabrication easiness, inertness, barrier to oxygen and water vapor, high wet-strength, etc. (Smith, 2005). Today the most well-known polymeric packaging materials that meet these criteria are polyethylene and polypropylene which have been in use by the food industry for over 50 years (Cutter, 2006). Polypropylene has good resistance to chemicals and water vapor, but not to

oxygen gas. Therefore, multilayer structures of PP is used with an oxygen barrier such as ethylene vinyl alcohol or polyviniylidene chloride, to improve the oxygen barrier properties (Marsh and Bugusu, 2007). In 2000, polypropylene represented 23% of the thermoplastic consumed in Western Europe. Its sales in tonnage is the third most important amongst plastics in the world (Brachet et al., 2008).

Global production of packaging materials is estimated at more than 180 million tones per year, with growth and demand increasing annually (Tice, 2003). Within the plastic packaging market, food packaging is the largest sector. It is estimated 125 million tones of plastics are produced throughout the world annually and 25% of this amount is used for food packaging purposes (Weber et al., 2002). It is estimated that of the 100$ billion packaging market in the United States, 70% is attributed to beverage and food production (Comstock et al., 2004).

It seemed, more than ten years ago, that it was time to add one more characteristic to the list of desirable properties for plastics that usually have a service life of 18 months or less (Smith, 2005). Environmental concerns become more important in the last decades for the selection of packaging materials; and additional to above mentioned characteristics of an ideal food packaging material, environmental impact is added to list. In contravention of high usage and economical value of polymers the recovery of plastic materials are very low. Most of the polymer based packaging materials end in land fills, which is the cheapest and the most common solution for generated wastes. Packaging wastes constitute for 5.7% of total discarded waste and only 9.4% of the plastic packaging materials were recovered in United States according to EPA (2006) statistics. This percentage is very low compared to other packaging materials that of 58.8% for paper and paperboard, 51.3% for metals and 25.3% for glass (Marsh and Bugusu, 2007). Reason of this low recovery ratio was attributed to difficulty in identification and separation of polymeric packaging materials (Marsh and Bugusu, 2007; Cutter, 2006; Tice, 2003). The identification and separation issue can be more easily seen in recovery statistics for polymeric resins of EPA (2006). While recovery ratio of polyethylene terephthalate (PET), which is mostly used for plastic bottle production that is easier to separate from wastes is around 18% (this ratio is also low compared to other non-polymer packaging materials). Recycling of polyolefins is especially problematic. For example, the recovery of polypropylene which is extensively used in multilayer barrier films and coating applications together with other polymers is just about 0.25% (Marsh and Bugusu, 2007).

Land filling is still the most common application for the waste packaging materials. Beside landfills, combustion or incineration is a way of waste management. By burning polymeric wastes, besides generating electricity or heat; the waste volume can be decreased by 70% to 90% (Marsh and Bugusu, 2007). But still the remaining waste must be land filled and the emissions given to atmosphere are another problem. Biobased food packaging idea was emerged at the point of waste management. Biobased (biopolymer) packaging is defined as packaging containing raw materials originating from agricultural sources, i.e. produced from renewable biological raw materials such as polysaccharides like starch chitosan, animal or plant derived proteins like corn zein, soy, whey, casein and bioderived monomers like polylactate (PLA) (Petersen et al., 1999; Cutter, 2006).

Biopolymers have opportunity to be used as food packaging materials. Plant derived biopolymers such as chitosan, corn zein and starch is known to be effective barrier to oxygen, comparable to that of EVOH and OVDC. Most of the biopolymers are thermoplastics that can be shaped into solid articles or processed into films. Recent technological advances also have allowed biopolymers to be processed similarly to petroleum based plastics whether in sheets, by extrusion, spinning, injection molding, or thermoforming (Cutter, 2006). In spite of their excellent barrier to oxygen and other gases, biopolymers are poor water vapor barrier and moreover, their barrier and mechanical properties are dependent to moisture which is not desirable especially for the packaging of certain food types. One of the challenges facing the food packaging industry in its efforts to produce biobased primary packaging is to match the durability of the packaging with the product shelf life. The biopolymer packaging material must remain stable without changes of mechanical and/or barrier properties and must function properly during storage until disposal (Petersen et al., 1999).

Poor mechanical properties and dependency to moisture of biopolymers should be overcome in many ways. For example, use of plasticizers such as glycerol, ethylene glycol, sorbitol etc. in the film formulations or composites is advantageous to impart pliability and flexibility which improves handling (Tharanathan, 2003). Bilayer packaging applications of biopolymers are also a solution. Coating the water sensitive material with wax would add hydrophobicity to the biopolymer and maintain structural stability against moisture (Petersen et al., 1999).

In food packaging technology, application of bilayer and multilayer structures is a common and well known technique. Multilayer films are produced by coextrusion of

different types of polymers. Mechanically durable but low barrier polymers and high barrier-low strength polymers are widely coextruded to satisfy different needs of food packaging. Multilayer co-extruded film applications are especially common in production of barrier films such as metallized PET-LDPE for the packaging of instant coffee in elastic vacuum bags and polyvinyl alcohol/ethylene vinyl alcohol coated polypropylene used in many products for producing barrier to oxygen combined with polypropylene's strength (Robertson, 2006).

Despite the availability of a variety of excellent synthetic oxygen barriers, the disadvantages of any such composite polymeric structures are the difficulties entailed in their recycling. Existing composite films containing layers of different plastic materials may not be recycled, because typically only single component plastics are recyclable (Hong and Krochta, 2006). Since biopolymers could also be processed using extrusion, biopolymer –biopolymer and/or biopolymer-synthetic polymer bilayer or multilayer films can be produced in order to utilize the O_2 barrier of a biopolymer and mechanical strength of a synthetic polymer as well as to maintain heat sealability. In environmental aspect of view, multilayer films containing synthetic polymers are not favorable since it is hard to separate layers and recover. But in the case of biopolymer coated conventional synthetic polymers, desired barrier properties would be achieved by using less amount of synthetic polymer leading to light weighting the disposed packaging after decomposition of biobased part in much shorter time.

For a decade, one of the most important research topics is the nanotechnology applications in materials science. Nanoscale manipulations successfully done on materials have potential to give effective and superior results. Nanocomposite systems offer great opportunities in biobased food packaging polymers. Characteristic disadvantages such as poor mechanical properties, or low barrier to water vapor can be improved by using nanocomposite technology.

Nanocomposites are a new class of composites, which are particle-filled polymers with at least one dimension of the dispersed particles, is in the nanometer range (Alexandre and Dubois, 2000). Blending or creating composite structures with inorganic fillers is a widely used method to improve polymer properties in today's polymer industry. Replacing conventional fillers with nanofillers were proved to give many successful results such as improvements in mechanical properties, weight reduction, technological improvements such as resistance to fire, adding antimicrobial properties and one of the most promising – to improve barrier properties to gases and

water vapor. Nanocomposite applications have potential to make biopolymers a stronger environment friendly alternative of petroleum based polymeric food packaging materials.

Multilayer films and standalone films produced by using biopolymers and biopolymer-nanocomposites are favorable in terms of associating excellent barrier to gases of a synthetic polymer or improving the properties of a single biopolymer. They are also favorable in terms of bringing in positive public opinion for marketing. Since one function of the packaging material is communication, the environment friendly biopolymer packaging is a message itself. It is generally accepted that consumers are becoming more conscious of the environment. Indeed, recent consumer surveys show that the consumers are willing to pay more for food, packaged in biomaterials which are friendlier to the environment (Petersen et al., 1999).

2.1. Mass Transfer in Food Packaging

Barrier to permeating solutes in order to ensure the quality of food requires dealing with mass transfer phenomena in food packaging. Mass transfer phenomena occurring in food packaging involves absorption of any gas, water vapor, or solute from surrounding to the packaging which is also defined as solubility; and diffusion that is the transport of any absorbed solute within the polymeric media due to concentration difference. Permeability is the steady-state rate of transport of a permeant molecule through a polymer of unit area per unit thickness as a result of combined effects of diffusion and solubility (Miller and Krochta, 1997).

For many packaging materials, the relation between solubility, diffusion and permeability can be described by using the expression:

$$P = D * S \qquad\qquad (2.1)$$

where P is the permeability coefficient, D is the diffusion coefficient, and S is the solubility coefficient related with the absorption of a gas to a solid surface.

2.1.1. Solubility of Permeants in Packaging Film

Solubility is the partitioning behavior of a permeant molecule between the surface of a polymer and the surroundings. It is a measure of the mass of permeant molecules sorbed by a unit of polymer mass per unit of partial pressure. The solubility coefficient *S* describes the dissolution of a permeant in a polymer, and thus represents a thermodynamic property of the polymer-permeant system (Miller and Krochta, 1997). The solubility coefficient can be represented as:

$$S = \frac{C}{p}$$ (2.2)

where *p* is the vapor pressure of the permeant, *C* is the concentration of the permeant and *S* is the solubility coefficient.

2.1.2. Diffusion through the Packaging Film

Diffusion is the process, by which permeant molecule moves through the polymer matrix as a result of random molecular motions, representing the kinetic property of polymer-permeant system. There are two processes by which gases and vapors may pass through polymeric materials:

- A pore effect, in which the gases and vapors flow through microscopic pores, pinholes and cracks in the materials
- A solubility diffusion effect, in which the gases and vapors dissolve in the polymer at one surface, diffuse through the polymer by virtue of a concentration gradient, and evaporate at the other surface of the polymer. This "solution-diffusion" process (also known as "activated diffusion") is described as true permeability (Robertson, 2006).

Activated diffusion is described as the opening of a void space among a series of segments of polymer chain due to oscillations of the segments. Then, this active state is followed by translational motion of the permeant within the void space before the segments return to their normal state. Both active and normal states are long-lived, as

compared with the translational of the permeant. Factors affecting the structure of a polymer have a direct effect on segmental mobility, and therefore, influence its mass transport properties (Miller and Krochta, 1997). A schematic representation of activated diffusion process is given in Figure 2.1 below:
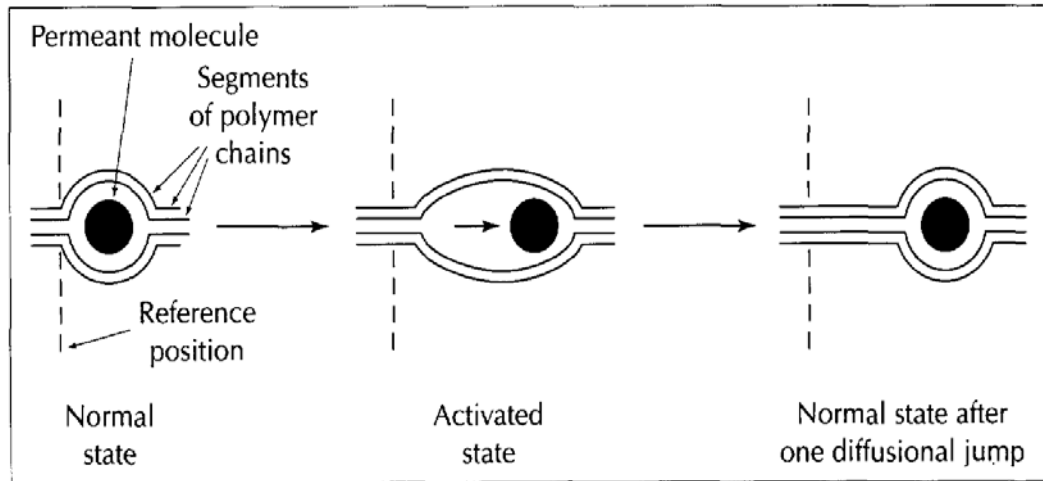
Figure 2.1. The activation process for diffusion (Resource: Miller and Krochta 1997)

The mathematical theory of diffusion called Fick's first law is based on the hypothesis that the rate of transfer of diffusing substance through unit area of a section is proportional to the concentration difference;

$$J = -D\frac{\delta c}{\delta x} \tag{2.3}$$

where J is the diffusive mass transfer rate of permeant per unit area, c is the concentration of permeant, x is the length and D is the diffusion coefficient.

2.1.3. Permeability of Packaging Films

Permeability is the steady-state rate of transport of a permeant molecule through a polymer of unit area per unit thickness as a result of combined effects of diffusion and solubility (Miller and Krochta, 1997). The permeability coefficient, P, includes both thermodynamic and kinetic properties of polymer-permeant system as expressed in equation 2.1. Barrier properties of polymeric films are generally reported in terms of

permeability because of its simplicity rather than their diffusion or solubility constants. Permeability of a film is determined by the steady state rate of mass transport through the films with constant D and S. Permeability coefficient can be defined by integrating equations 2.2 and 2.3 to obtain:

$$P = \frac{(dM/\,dt)_{steady-state} \times L}{A \times \Delta p} \tag{2.4}$$

where M is mass or volume of permeating substance, t is time, L is length, A is the cross-sectional area that permeation takes place and Δp is the partial pressure difference of permeate across the film. It is more convenient to use partial pressures rather than concentrations in the formula. Because sorption of gas component into a film generally has a linear relationship with the partial pressure of the gas as shown in Henry's law under conditions where the gas concentration is lower than its saturation concentration or maximum solubility (Han, 2005; Miller and Krochta, 1997). The term *(dM/dt)* is the slope of the permeate transmission curve and is required to be at steady-state.

Any type of monolayer, bilayer or multilayer packaging film permeability can be measured by the permeation cell technique consisting of two chambers at different solute concentrations separated by sample film. With the knowledge of intrinsic thickness and permeabilities, the permeability of multilayer film or single layers can be calculated by using the equation below by using permeability (P) and thickness (L) of multilayer film (Robertson, 2006; Han, 2005):
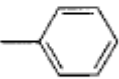
$$\frac{L}{P} = \sum_{i=1}^{n} \frac{L_i}{P_i} \tag{2.5}$$

where n is the number of layers in the film, while L_i and P_i is the thickness and permeability of each layer respectively.

Diffusion in polymers is influenced by many factors. Characterizing the relations between permeability of solute and polymer structure is crucial in terms of designing barrier films in food packaging. Chemical structure of the polymer is one of the most important factors in polymers controlling the permeation of solute. Substituent groups existing in the polymer structure result in differences in the cohesive energy density of the polymer; which is a measure of how polar the polymer is. In general, polar polymers

are effective on resisting the permeation of non-polar gases such as O_2, and polymers with non-polar character are classified as good barriers to water vapor. Effect of substituent groups tied on the same backbone on water vapor and oxygen permeability can be followed in the Table 2.1 below. On the contrary, existence of some polar groups; as in the case of most of the biobased polymers; could result in absorption of moisture from the atmosphere and may lead to swelling and plasticizing of the polymer diminishing the barrier properties (Robertson, 2006).

Table 2.1. Effect of substituent groups on polarity (Cohesive Energy Density-CED) and oxygen - water vapor permeabilities of polymers (cm^3 $\mu m/(m^2$ d kPa)) (Source: Miller and Krochta, 1997)

Backbone: $\{CH_2 - CH\}$ with X

Substituent group (X)	Polymer	CED (cal/cm³)	Permeability at 25°C[b]	
			Oxygen	Water
–H	Polyethylene	66	0.188	100
(phenyl ring)	Polystyrene	85	0.168	1100
–OCOCH₃	Poly(vinyl acetate)	88	0.023	8500
–Cl	Poly(vinyl chloride)	94	0.0036	250
–CN	Polyacrylonitrile[c]	180	0.000039	300
–OH	Poly(vinyl alcohol)	220	0.0000016 (dry)	[d]

The types of substituent groups present in a polymer can also have a tremendous effect on the variability of the permeability coefficient by influencing two main factors: how tightly the polymer chains are bound together and how much free volume exists between the chains (Miller and Krochta, 1997). Interstitial spacing between the molecules in a polymer also affects the movement of any solute through the polymer. Increase in free volume; decreases the resistance of polymer to a permeating solute. Although free volume is a characteristic of the polymer, it might be manipulated by the addition of plasticizers. Plasticizer addition to a polymer during processing increases the free volume and enhances the flexibility of the polymer packaging product in expense for decrease in barrier properties.

Polymer chain structure and alignment also effects the permeation of solutes. Close chain-to-chain packing ability brought by molecular symmetry, order or

crystallinity slows down the moving molecules and enhances the barrier properties. Linear, isotactic polymers have good chain packing; and could limit the permeation more than the polymers with bulky side groups. Crystalline phases within a polymer acts as impermeable barriers to solutes and are more effective in limiting permeants than amorphous phases in semi-crystalline polymers.

As in the case of crystalline parts of the polymer, crosslinks between polymer chains limit the movement of the permeant. Crosslinks formed by curing the polymer and by addition of chemicals improves the barrier property of the polymer. Another parameter affecting the mobility of the permeating molecules is the glass transition temperature (T_g) temperature of the polymer. Below T_g, the segments have little mobility and there is also a reduction in "free volume". Thus not only are there fewer voids, but, in addition, a diffusing molecule will have a much more tortuous path through the polymer. Therefore, if a polymer has a high T_g, then it is likely that its temperature of use will be below its T_g and it will consequently have improved barrier properties (Robertson, 2006).

2.2. Mechanical Properties of Packaging Films

Mechanical properties are critical as barrier properties for a packaging material. Along the travel of the packaged food, from its packing to use, packaging must be durable and free from minor defects to ensure the safety of food. Sufficient mechanical strength of packaging material is critical in terms of preventing food to be effected from physical impacts and also to satisfy the barrier properties required. Among many properties considered for polymeric packaging films such as barrier, clarity, etc.; mechanical properties are the most frequently considered and primary property controlled in the industry. Interactions between hydrocolloids and small molecules, including water, plasticizers, lipids, and other additives dispersed in the space of the matrix contribute to the mechanical behavior of films (Olabarrieta, 2005).

Mechanical properties of polymer films are mainly evaluated using tensile testing that gives useful data such as yield and tensile strength, elongation at break and elastic modulus (Young's modulus). The tensile behavior of a polymer should be examined in two sections according to their deformation characteristics. The initial deformation of a polymer under applied load is elastic. Although the specimen deforms,

it would regain its initial shape after the load is removed. Elastic deformation of a polymer is characterized by the initial linear curve obtained in tensile testing. From the slope of this line the elastic (Young's) modulus is obtained. Modulus is the ratio of stress per strain before elastic limit and gives information about the stiffness of the material. As applied force is increased, the polymer deformation becomes plastic and the deformation becomes irreversible.

At the initial steps of plastic deformation polymer chains get close to each other and the resulting stress caused by elongation increases. After the yield strength point, polymer chains relax and the resulting stress decreases. The yield point of a polymer is important since it would provide information on the maximum allowable stress before plastic deformation. Other two important properties of a polymer film, the tensile strength at break (maximum strength) and elongation at break is obtained at the point at which the film looses its structural integrity and breaks down. The maximum tensile strength and elongation of a film is important since, after that point the package would not be available to protect the product inside.

The mechanical properties of polymers are diverse. Depending on the polymer type, processing conditions and the rate at which load is applied, mechanical properties changes (Olabarrieta, 2005). The most widely used packaging materials polyolefins are characterized by good maximum strength and high elongations. The mechanical properties of polymers can also be manipulated by adding different chemicals or fillers. Plasticizer addition as generally used to make a stiff polymer more flexible also results in decreased yield and maximum strength and decreased modulus values as well. On the other hand, cross-linking agents can be used to increase the modulus and maximum strength (Smith, 2005).

The fillers added to the polymer during processing for cost reduction, improvement of barrier properties, etc. also affects the mechanical properties. In this case the effect is dependent on the interaction between the filler and the polymer matrix. While a good interaction between filler and polymer matrix enhances maximum strength and modulus at the expense of reduced flexibility, insufficient interaction diminishes the mechanical properties. At the point of interaction between filler and polymer matrix, nanoparticles are reported to give better results because of the increased interaction due to high available surface area in contact with the polymer.

2.3. Optical and Surface Properties of Packaging Films

Food packaging has also communication aspect additional to barrier and mechanical properties required to ensure the quality of food until final consumer use.. In terms of marketing purposes, the appearance and design of the packaging is very important. The name, properties or trademark of the product must always be printed on the packaging. In some cases, food packaging is better to be transparent in order to directly present the food inside.

Surface properties of the films, surface energy or surface tension are critical for food packaging films. Surface energy of the films depends on variations on the homogeneity and roughness of the surface as well as composition and crystal orientation of the packaging material (Smith, 2005). Surface energy of the films cannot be measured directly. Surface energy parameters are obtained from contact angle analysis of several probe liquids such as water. Contact angle measurements can give an idea about the surface characteristics such as hydrophobicity. Level of surface hydrophobicity is important since interactions with other layers such as printing ink applied on packaging films or coatings require compatibility with the surface for good adhesion. Besides, surface characteristics are also important in production processes such as blending or co-extrusion applications.

Another feature of packaging films is their optical properties. Transparency, ability of a material to let light through a film is important. Transparency of packaging films are required in applications which product visibility from outside is desired. Consumer surveys showed better acceptance of products are obtained by transparent packaging of fresh vegetables and fruits and also for snacks (Petersen et al., 1999). Most of the synthetic polymers like PET, PP, PE are well known transparent materials. Beside transparency, appearance of the films is important. Haze; simply scattering of light which results into cloudy appearance, is not desired in food packaging (Hong et al., 2003). Color of the films is also important since details of the product may deteriorate when deviances to more yellow or green colors exists in packaging. Color of the pristine film is also important in terms of printing applications.

CHAPTER 3

BIOBASED AND BIODEGRADABLE POLYMERS IN FOOD PACKAGING

Biodegradable and biobased polymers are the materials that have ability to be totally decomposed in the nature by the microorganisms in the soil. Advances in the production of biodegradable polymers and their processing led to the idea of green polymer packaging materials. Today, nearly all the polymer based packaging materials are produced from petroleum based synthetic non-degradable materials. Replacement of synthetic polymers by biodegradable polymers has been taken seriously for a decade. Research and some early applications proved that biodegradable polymers have potential to be used for packaging as blends with synthetic or natural polymers, composites or as stand-alone films. Although there is extensive research and investment in the biodegradable polymer area, biopolymers are still not competitive to commonly used synthetic polymers (Petersen, 1999; Weber, 2002; Cutter, 2006).

The terms biobased and biodegradable polymers are often used together, but they define different characteristics. In order to call a polymer "biodegradable", all the carbon in its structure should be accounted for carbon balance, and all residues left should be nontoxic in the environmental assessments. In addition, the residue and microbial biomass should eventually be incorporated into the natural geochemical cycle (Nayak, 1999). On the other hand; biobased polymer definition is used to define the type of polymers that have natural and renewable origins. The biobased materials may have biodegradability as one of their properties, whereas biodegradable materials not necessarily are biobased. Since the aim of this section is to discuss biodegradable polymers with biological origins; the terms biopolymer and biobased are going to be used to define biobased-biodegradable polymers.

Biopolymers should be classified into three categories according to their origin and method of production:

I. Polymers produced by microorganisms or genetically modified bacteria such as polyhydroxyalkonates (PHAs)

II. Polymers produced by chemical synthesis from renewable bio-derived monomers like polylactic acid (PLA)

III. Polymers directly extracted from biomass such as proteins like corn zein and polysaccharides such as starch

These categories are further outlined in the Figure 3.1:
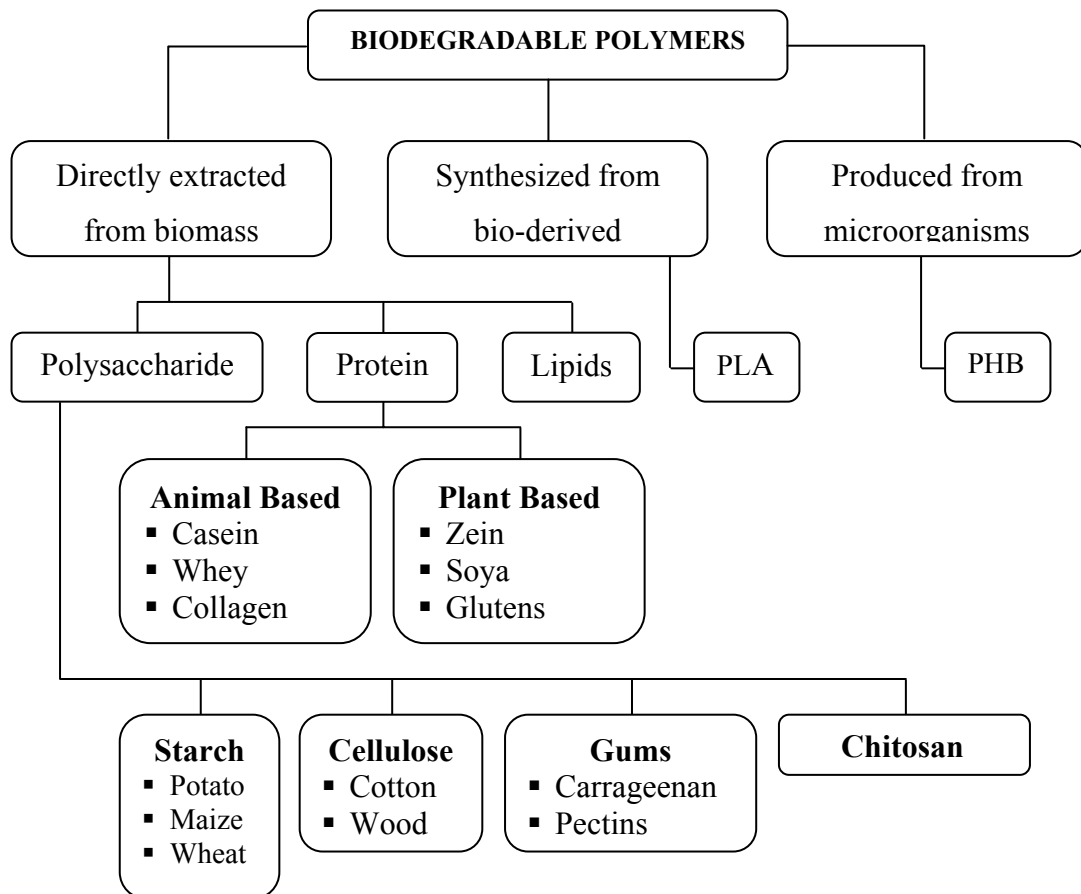
Figure 3.1. Biodegradable polymer families (Source: Weber, 2000; Kolybaba et al., 2003)

Depending on the structure of the biopolymer, these polymers have different interesting properties for food packaging. Bio-derived PLA and microorganism produced PHB are known to be mechanically durable and good barrier to water vapor. Biodegradable polymers extracted from biomass are known to be good oxygen barriers due to their polar structure. Next sections are going to be dealing with the biomass extracted proteins in more detail.

3.1. Biopolymers Extracted from Biomass

Biopolymers extracted from biomass counts for the largest and diverse group of biodegradable polymers. All the polymers in this group are "truly green" since they all have biological origins and they completely decompose in the nature. Biomass originated biopolymers are mostly obtained from by-products and characterized as effective gas-especially oxygen barriers. On the other hand, major drawback is this group is their low mechanical strength and hydrophilicity affecting their barrier properties. Because of this, real potential of biomass derived polymers lies in their blends with other polymers and in multilayer structures. This group can be investigated in major sub-groups of polysaccharides such as starch or chitosan and proteins like corn zein, whey, etc.

Polysaccharides are an important group of biomass extracted biopolymers since they are constitute for the most abundant form of biopolymers in the nature. Among polysaccharide biopolymers, starch attracts the most interest in biodegradable packaging. Starch is a highly crystalline material like cellulose. Although it is tough and not processable in its granule form, starch may have thermoplastic properties upon disruption of its molecular structure by dissolving in boiling water or processing by extrusion (Tharanathan, 2003). In its thermoplastic form, starch has desirable properties for food packaging. It is biodegradable in the nature and it has excellent barrier to oxygen and carbon dioxide better than the widely used PP and PE polymers. On the other hand, unmodified starch; also in thermoplastic form; suffers low mechanical properties and water sensitivity.

Polysaccharide based chitosan and chitin together are the second most abundant polymer in the nature. Generally chitosan is characterized as an excellent barrier to oxygen and carbon dioxide (Weber, 2000). Although chitosan has film forming ability and has excellent barrier to gases, its use conventional in packaging is limited due to its high price even compared to other biopolymers and its moisture sensitivity coming from its hydrophilic nature (Weber, 2002).

3.1.1. Protein Based Biopolymers

Protein based biopolymers are classified under the main group "biopolymers extracted from biomass". Protein based biopolymers are truly green. First they are produced from totally renewable, mostly annual crops or animal based compounds. Second no residue will be left to nature after their complete degradation. Another important environmental feature of this class of biopolymers is their short degradation time. Degradation of protein based biopolymers complete in a couple of months to years depending on the protein type; that is nearly negligible compared to thousands of years degradation cycle of synthetic polymers such as PP or PE.

Protein based biopolymers are being obtained from two main sources. These sources are animal based and plant based agricultural sources. Whey protein is the best example for the animal based protein biopolymers. Whey is extracted from the byproducts of cheese industry (Weber, 2000). Like most of the other plant based biopolymers, whey suffers from brittleness and due to its hydrophilic nature; it is very sensitive to humidity; even soluble in water. The most promising feature of whey protein makes it a topic of interest is its low oxygen permeability. Whey protein has been topic of many studies in the literature including its coatings on PP or PE films (Hong et al., 2004; Hong and Krochta, 2006; Lee et al., 2008). Casein, gelatin, collagen, keratin are the other elements of animal based protein films.

Plant based proteins constitute for a very large and versatile group of biopolymers. All members of this group are being extracted from by-products of industry. Members of this group are corn gluten, wheat gluten as examples to direct by-products of industry; and further processed forms such as corn zein, soy protein isolate.

Plant based protein compounds can be processed with melt processing techniques such as extrusion or injection molding with appropriate modifications generally held by plasticizers (Hernandez and Krochta, 2008). They are characterized as polar and hydrophilic compounds sensitive to humidity and soluble in water except corn zein. Polar character of plant protein biopolymers also bring in excellent oxygen barrier comparable to that of widely used EVOH and PVDC synthetic polymers. In the following sections, characteristics and properties of corn zein protein which is the subject of this study is going to be discussed in more details.

3.2. Plant Protein Based Corn Zein

Corn zein is another type of biopolymer with film forming ability. Commercial corn zein proteins are obtained by extraction of the corn wet-milling industry by products named corn gluten meal. Biologically it is classified as a prolamin found in corn endosperm and it is alcohol soluble (Lawton, 2002). Corn zein has a unique and complex structure compared to other biobased polymeric materials.

Corn zein has some sort of thermoplasticity that makes it a promising candidate in industrial polymers world. Corn zein is characterized as a hydrophobic polymer due to its high content of non-polar amino acids in its structure. Although, it is hydrophobic and it is not soluble in water unlike some other biopolymers such as starch, humidity deeply affects the properties of corn zein such as mechanical and barrier to gases, as well as its processability. Like other protein based biopolymers, corn zein is an excellent barrier to gases; especially its barrier against oxygen and carbon dioxide makes it an attractive polymer together with its hydrophobicity and thermoplasticity for food packaging applications.

The earliest uses of corn zein in the industry go until the beginning of the 20th century. The first patents were introducing zein as a novel type of binder. Zein's resistance to grease was utilized in lacquers, varnishes and coatings instead of shellac. Despite being used in coatings, zein was also used in inks for a while (Lawton, 2002). Recently corn zein is commonly used in controlled drug delivery applications. Drugs are usually incorporated in to zein micro spheres and in order to delay the release of drugs utilizing the zein's strength to stomach acid (Shukla and Cheryan, 2001).

3.2.1. Corn Zein as a Packaging Material

Corn zein has potential to be used in barrier food packaging applications for oxygen sensitive foods alone or in combination with other synthetic polymers in multilayer applications. The films formed by drying of alcoholic aqueous dispersions are not water soluble, but are relatively brilliant and grease resistant (Nayak, 1999). Another advantage of zein over conventional synthetic polymers is that corn zein is completely biodegradable and it is annually renewable since it is produced from the by-product of corn milling industry. Corn zein offers relatively good mechanical properties

and good barrier to water vapor permeability compared to other biomass based polymers and interestingly, it does not swell in water.

Despite having ideal and strong properties, corn zein suffers the known disadvantages of protein based biopolymers. Corn zein is brittle especially at low water activity and its properties are widely affected by high moisture contents. Brittleness of the corn zein could be overcome by addition of plasticizers that also improves the processability of the corn zein, which is extensively investigated in the literature. Since obtaining sufficient mechanical strength in single corn zein films is hard, the most promising application of corn zein appears to be its use together with mechanically strong films.

3.2.2. Plasticizers for Corn Zein Films

Brittleness is an important characteristic of plant based protein biopolymers. Brittleness of corn zein constitutes for the most important challenge to be solved for their industrial packaging film applications. A packaging film must be durable from its production to end-use in order satisfy mechanical strength required for the packed products' mechanical stability, and to maintain critical functions such as barrier to oxygen and water vapor without significant changes.

Brittleness and problematic melt processing of corn zein is due to the existence of strong intermolecular forces within the structure. In almost all cases, manufacturing and industrial use of protein-based films and coatings requires plasticization of the protein in order to improve the flexibility of films and to make them processable (Gao et al., 2006). Many theories have been proposed to account for the mechanisms of plasticizer action; roughly relaxing the strong interactions in polymer structure which results in more flexible materials and significant changes in barrier properties (Padua and Wang, 2002; Hernandez and Krochta, 2008; Hong and Krochta, 2006; Tillekeratne and Eastel, 2000).

Gioia and Guilbert (1999) discussed three of these plasticizing theories. In the "lubricity theory", the plasticizer acts as a lubricant to facilitate movements of the macromolecules over each other, whereas the "gel theory" considers the disruption of polymer-polymer interactions (hydrogen bonds and van der Waals or ionic forces). The "free volume theory" states that a study of plasticization is a study of ways to increase

free volume and is useful to clarify the lowering of the glass transition temperature (T_g) by a plasticizer. In their study concerning the effect of polar and amphiphilic plasticizers on corn gluten meal, glycerol found to be more effective due to its small molecule size than other larger molecule plasticizers. The authors concluded that regardless of which theory is the most appropriate, the action of a plasticizer is to interpose itself between the polymer chains and alter the forces holding the chains together (Gioia and Guilbert, 1999). Another conclusion from the same study was that, polar plasticizers, such as water and glycerol are more effective than amphiphilic plasticizers such as octaonic acid on mass basis for the plasticization of corn protein.

In the literature many compounds were studied as plasticizers for protein based biopolymers. Some of the common plasticizers used for the formation of corn zein films were also given in the Table 3.1 below.

Table 3.1. Common plasticizers used for formation of corn zein films (Gioia and Guilbert, 1999; Tillekeratne et al., 2000; Padua and Wang 2002; Santosa and Padua, 2000; Lee et al., 2008)

Plasticizer Type	Plasticizer Type
Glycerol (GLY)	Polypropylene Glycol (PPG)
Water	Dibutyl Tartrate
Polyethylene Glycols (PEGs)	Sugars (glucose, fructose)
Triethylene Glycol	Sorbitol
Propylene Glycol (PG)	Stearic Acid (SA)
Oleic Acid (OA)	Lauric Acid (LA)

Glycerol ($C_3H_8O_3$) is a polar and hydrophilic plasticizer and belongs to polyols group. It is the most common used plasticizer in corn zein and other protein based biopolymer studies, since the protein conformation is stabilized to a large extent by hydrogen bonds (H-bonds) and nonpolar interactions. Because of this, plasticizers must be polar (Hernandez and Krochta, 2008). Glycerol is a miscible compound with zein and has ability to plasticize corn zein effectively. Effectiveness of glycerol due to its small molecule size and good interaction with corn zein and other protein based biopolymers compared to various plasticizers was reported by many authors (Gioia and Guilbert, 1999; Lawton, 2004; Ghanbarzadeh et al., 2007; Hong and Krochta, 2003;

Gao et al., 2006). Ghanbarzadeh and coworkers (2007) investigated the surface of plasticized corn zein films. AFM results obtained in the study proved the effective plasticization with glycerol. Smoother surfaces with glycerol compared to sorbitol and mannitol was observed.

Plasticization and extend of plasticization can be followed by the changes in the thermal properties of polymer. Plasticization is always characterized by significant depressions in the glass transition temperature – a polymeric material property stating whether the polymer is in rubbery state or more ordered and tough glassy state. Glass transition temperature changes with plasticization and extend of plasticization were investigated in the literature (Madeka and Kokini, 2006; Santosa and Padua, 2000; Wang et al., 2004; Gioia and Guilbert, 1999; Gillgren et al., 2009; Lawton, 2004).

Plasticizing efficiency of the initial concentrations of plasticizers are more effective and property determining than higher concentrations (Gioia and Guilbert, 1999; Gillgren et al.,2009; Lawton, 2004). Some of the mentioned studies concerning thermal analysis of the plasticized corn zein also reported significant effect of water on the plasticized corn zein. The following section discusses the plasticizing effect of water in more details.

3.2.3. Water as a Plasticizer for Corn Zein Films

Although glycerol is the most commonly used plasticizer in corn zein films, water has also a significant effect on the properties. Protein based polymers are generally hydrophilic and dramatically effected and even decompose by the presence of water. Despite the fact that corn zein is classified as hydrophobic and is not soluble in water, still presence of water changes its film properties significantly due to polar parts in its structure. Another importance of water is that it may be used to enable zein melt processed. Water is also used as a plasticizer in its melt processing operations such as extrusion and molding in order to improve processability of corn zein (Hernandez and Krochta, 2008; Selling et al., 2004).

Generally use of water for plasticization is not common and studies concerning water alone are limited. Gioia and Guilbert (1999) studied glycerol and water separately as plasticizers in their study using corn gluten meal (CGM). Concentration of the plasticizers was in 0-30% in mass basis. More significant glass transition temperature

depression for water was reported compared to other plasticizers obtained by MDSC analysis. The effectiveness of water as a plasticizer was attributed to water's small molecule size, enabling it to easily enter between CGM chains and its polar structure compatible with protein structure.

Gillgren and coworkers (2009) also studied water and glycerol plasticization of corn zein using FTIR and DMA for the determination of Tg up to 50% (w/w) in terms of plasticizer concentration. In accordance with the results of Gioia and Guilbert (1999), the group reported higher plasticizing effect of water and glycerol for small concentrations – 5% for water and 15% for glycerol - and moderate effect of plasticizers up to 40% (w/w) from the Tg data obtained from DMA. Interaction of water and glycerol with zein protein structure was also reported in the study (Gillgren et al 2009).

Lawton (2002) reported another important aspect of water for the plasticization of corn zein in his review. A group of plasticizers including glycerol were classified as secondary plasticizers and noted their effectiveness should be increased by using other compounds. Lawton (2004) also studied the coupling of water with glycerol and other plasticizers in the previously mentioned study dealing with the relative humidity effect on zein. In the study, zein already containing 5%(w/w) water was further plasticized by additional 5%(w/w) plasticizer. Glass transition temperature decrease followed by DSC was higher in the samples containing both water and plasticizer than the samples containing 10%(w/w) plasticizer alone. It was also reported that for higher plasticizer concentrations, water and glycerol was competing for the plasticization of zein. The additional plasticizing effect of water did not exist for hygroscopic plasticizers such as glycerol for plasticizer concentrations over 30% (w/w) (Lawton, 2004).

All plasticizers used for corn zein, as well as water, impose different changes in the mechanical and barrier properties of the plasticized polymers. In the following parts, these changes are going to be discussed.

3.2.4. Mechanical Properties of Plasticized Corn Zein Films

Plasticizers affect the structure of polymers by loosening the interactions between polymeric chains. Changes in the structure can also be followed from the mechanical properties of the materials. Changes in mechanical properties of plasticized protein based corn zein were generally reported as decreases in maximum tensile

strength and Young Modulus while significant improvements in percent elongation at break were observed. For mechanical testing of corn zein, appropriate relative humidity is critical since water and relative humidity acts like a plasticizer as discussed before. Degree of effects observed due to relative humidity and water content is also different for the type of plasticizer used. Because of this, as in the requirements of the ASTM D 882 standard for thin films testing, the samples must be conditioned at least 48 hours at the desired humidity (50% RH for ASTM D 882)

Lawton's study (2004) is important in terms of showing the humidity dependence of corn zein films in plasticized or unplasticized form. Lawton investigated effect of water (relative humidity) on the properties of corn zein films. The effect of several plasticizers such as glycerol, triethylene glycol (TEG), polyethylene glycol 300 (PEG300), and oleic acid on corn zein films prepared by casting plasticized zein solutions on glass plates was investigated. Mechanical properties of the unplasticized zein films (tensile strength and elongation at break, Young's modulus) were observed to be diminishing significantly for increasing %RH values in 0-90% RH range. Plasticized films also exhibited the same decrease trend seen for the unplasticized zein films. Another important feature of the study was that, plasticizing corn zein resulted in more stable films without sharp mechanical property changes due to relative humidity. Similar findings were also reported by Selling and Sessa (2007) for TEG plasticized zein films.

Gioia and coworkers (2000) studied mechanical properties of octaonic acid (OA) and glycerol (GLY) plasticized corn gluten meal and effect of water content in plasticized samples. Samples both plasticized by OA and GLY exhibited improved tensile strength and elongation at break up to 20% (w/w) plasticizer content and decrease in tensile strength at 30% (w/w) plasticizer content. Young modulus of the glycerol plasticized samples also decreased as in the case of OA plasticization, but the decrease was less significant. Effect of water content resulted in more dramatic decreases in mechanical properties of OA plasticized samples. These changes were attributed to the more water sensitive character of OA plasticization since water absorption of OA plasticized samples were higher compared to GLY plasticization.

Ghanbarzadeh and coworkers (2007) studied the effect of different plasticizers (glycerol, sorbitol and mannitol) at high concentrations (50%-70%-100% (w/w)) on corn zein films. Decrease in Young's modulus and improved elongation at break values were reported as expected. Glycerol was found to be the most effective plasticizer

relaxing the strong interactions between zein polymer chains due to its smaller molecular size. Glycerol addition improved strain at break and decreased modulus more significantly than the other plasticizers.

3.2.5. Barrier Properties of Plasticized Corn Zein

Relaxation of interactions between zein polymer chains due to use of plasticizers causes permeants to travel more easily throughout the films. As for other polymers, plasticizers used to improve processability and flexibility of corn zein results in higher water vapor and oxygen permeability. For corn zein protein, proper selection of plasticizer and its amount are critical to produce barrier polymers.

Plasticizers results in important changes in water vapor permeability of corn zein polymer. Since corn zein is known to be a moderate barrier to water vapor, plasticizers introduced to the system increase water vapor permeability. Water contact angle of polymers can also accepted as an indication to WVP of a polymer due to hydrophobicity of the material (Ghanbarzadeh et al., 2006). Relationship between water vapor permeability and water contact angle can be seen in water barrier materials. Polymers such as PP and PVDC or oil based lipids used for water vapor barrier in food packaging are known as highly hydrophobic polymers and characterized by high contact angles (Smith, 2005).

Ghanbarzadeh and coworkers (2006) studied the hydrophobicity of zein films plasticized by high concentrations (50%-70%-100%w/w zein) of glycerol, sorbitol and mannitol. The plasticizers used were all hydrophilic and decreased the contact angle of water at the surface of the zein film between 15% - 25%. Among the plasticized films, zein-glycerol films had the most hydrophobic character. Addition of glycerol decreased the contact angle to 52.48^0 from 62.3^0 of unplasticized zein. Their findings were in good agreement with another study comparing glycerol and sorbitol as plasticizers. Plasticization resulted in more hydrophilic structures and similar trends were reported by Muthuselvi and Dhathathreyan (2006).

Corn zein films without plasticizers were reported to have lower water vapor permeability than the films plasticized by glycerol or its mixtures with PEG or PPG (Padua and Wang, 2002). Paramawati and coworkers (2001) studied the effect of polyethylene glycol (PEG) and lauric acid (LA) on WVP of corn zein. Plasticizing

effect of PEG was found to be more significant since films become more flexible and WVP was higher. Mixtures of PEG and LA plasticizers resulted in significant decreases in water vapor permeability of the films.

Gioia and coworkers (2000) studied water absorption and water transmission rates of CGM and its plasticized samples. Octaonic acid plasticized samples absorbed nearly 20% more water than unplasticized CGM samples. Also the time required to reach equilibrium was also reported to increase 4 times for octaonic acid plasticization. Water transmission of glycerol plasticized samples increased 2 fold. Similar findings were also given by Wang and Padua (2004) who reported effect of relative humidity in extruded corn zein samples. 2 fold increase in WVP was observed for the samples tested at 50% relative humidity instead of 100%.

Oxygen permeability is also strongly affected by the plasticizer addition and relative humidity that also acts like a plasticizer. In the literature, there is not enough data and study concerning the oxygen permeability of corn zein polymer. Plasticizers and increased relative humidity was reported to increase oxygen permeability of zein and other biopolymers in the reviews. Another parameter affecting oxygen transport throughout the corn zein films is the temperature at which permeability analysis conducted. Temperature effect on oxygen permeation was studied by Padua and Wang (2002) at 0% relative humidity. The results were well fitting Arrhenius activation energy model.

3.3. Biopolymer Coating Applications of Packaging Materials

In the literature, there are studies conducted to investigate the properties of laminated biopolymer structures. Insolubility of corn zein in water convinced researches to coat zein on other water soluble biopolymers or prepare laminates using hot press molding. Ghanbarzeadeh and Oromiehi (2008) investigated glass transition temperatures of laminated whey and zein films using DMA and DSC. Ryu and coworkers (2002) coated water soluble starch with zein and investigated the mechanical properties of the coatings. Whey powder-Sodium caseinate mixtures were coated with zein layers (Cho et al., 2002). In another study, corn zein was used as a substrate and coated with water resistant compounds (sorghum wax and carnauba wax) to modify its barrier to water (Weller and et al.,1998).

In the recent years, coating the surfaces of synthetic polymers with biopolymers has begun to draw attention of many researchers looking for new types of packaging materials. Biopolymer coating on synthetic polymers is attractive since the amount of non-degradable waste disposed could be decreased.

Biopolymer coatings on economical synthetic polymers, as being alternative to conventional multilayer polymeric structures; attracted many research. Hong and coworkers (2004) examined the optical and surface properties of whey protein isolate (WPI) coatings on conventional PP and PVC films with different plasticizers (Glycerol, polyethylene glycol, polypropylene glycol, sorbitol and sucrose). WPI is a hydrophilic protein based polymer similar to corn zein. WPI coatings resulted in good adhesion between polar PVC substrate and WPI. On the contrary, WPI coatings on PP were not uniform and showed poor adhesion. Authors attributed poor adhesion to the nonpolar character of the PP substrate with low surface energy. Since WPI is polar, nonpolar PP didn't have enough binding sites for the polymer. Corona treatment was applied on the surface of PP in order to impart some degree of oxidation and increase surface energy of the polymer.

Surface treatment of polymer is a widely used technique in the production of multilayer polymeric films. In the applications where polar and nonpolar polymers desired to be used together, surface modification of nonpolar polymer is used to increase possible binding sites for good adhesion of layers. Surface treatment could be done by several methods such as corona discharge, flame treatment, and chemical etching.

In the latter part of the study, researchers reported good adhesion between PP and WPI after corona treatment of PP film. The color differences were insignificant and gloss of the films was improved. Only films plasticized with glycerol showed small gloss loss. Lower contact angles with respect to base PP and PVC were also reported regardless of the plasticizer type. Decrease in the contact angle values were attributed to hydrophilic character of plasticized WPI coatings (Hong et al., 2004).

Hong and Krochta (2003) investigated changes in oxygen barrier properties of WPI coated PP (corona treated) films using different plasticizer types (glycerol, sorbitol, sucrose, propylene glycol (PG) and polyethylene glycol 200 (PEG200)), at various temperatures, and relative humidities (RH). Significant increase in film thickness was obtained as high molecular size plasticizers were used. WPI coatings plasticized by glycerol and PG showed highest barrier to oxygen per unit thickness

indicating the importance of the plasticizer type in oxygen permeability. WPI coated PP films showed significant exponential increase in oxygen permeability (4 fold in the temperature range); good fitting the Arrhenius model in the temperature range of 15 to 45 $^\circ$C. It was found that PP layer was more responsible for the increase in oxygen permeability. Relative humidity at which permeability analysis were conducted showed serious effect on oxygen barrier of WPI and WPI-PP films. Especially over 60% RH, oxygen permeability of WPI film increased 6 fold. Finally, the group reported 15% improvement in oxygen barrier at 25C and 50%RH (6μm WPI - 51μm PP).

In a later study of Hong and Krochta (2006); WPI and whey protein concentrate (WPC) were coated on corona treated PP and PE films. The effects of temperature and relative humidity on oxygen permeability of coated films were again investigated. The same trends mentioned above were observed for PE and WPC. Calculated oxygen permeabilities of WPI and WPC were reported to be nearly the same.

Lee and coworkers (2008) studied mechanical properties of SPI, WPI and corn zein biopolymers plasticized by different plasticizers (glycerol, sorbitol, PEG400, PEG200, glycerol, PG) coated PP films. Corn zein coated films plasticized by PG and GLY showed poor mechanical properties. Meanwhile, PEG200/400 plasticized films showed better properties by diminishing the flexibility of the films in lesser extend.

Atik and coworkers (2007) investigated the optical, barrier and mechanical properties of corn zein coated PP films. Ethanol concentration, plasticizer type and level in the coating formulations were examined. Zein coatings applied resulted in insignificant color changes and transparency decrease depending on the coating formulation. Barrier to water vapor and oxygen of the resulting films improved significantly depending on the coating formulation. Some improvements in mechanical properties were also observed such as tensile strength and Young modulus of the films improved due to stiffer mechanical character of the zein coating. Interestingly, no decrease in elongation values was reported (Atik et al., 2007; Tihminlioglu et al. 2010).

Additional to coating of synthetic polymers, researchers also studied coating of paperboards in order to utilize water and grease barrier properties of biopolymers. Rhim and coworkers (2006) coated SPI films on paperboards and investigated effect of cross-linking agents and mixed OMMT on water contact angle and water vapor permeability. WVP of SPI coated paperboards showed consistent trend with the contact angles measured. Samples with lower contact angles (higher hydrophilic character) showed higher WVP. Another study investigated relationship between water vapor permeability

and oil absorption with water and oil contact angles in paperboards coated with hydrophobic starch and starch plasticized by stearic acid. Authors reported improved water vapor and grease barrier with starch coating and increased stearic acid concentration. Again a relationship between permeability and measured contact angles were reported (Butkinaree et al., 2008).

Biopolymer coatings on synthetic polymers were studied by many researchers and showed potential to be used as an alternative to conventional multilayer food packaging. Biopolymer barrier to oxygen could be utilized in combination with the mechanically durable synthetic polymers. At the same time, faster decomposition of multilayer structure could be achieved due to biodegradability of biopolymer layer after disposal.

Another possible strategy to utilize high performance films from corn zein is its nanocomposites. Strong interactions of nanofiller and corn zein can improve mechanical and barrier properties. Excellent barrier properties of zein nanocomposites (CZNC) could be utilized by coating CZNC on synthetic polymers in order to combine barrier of corn zein with high mechanical strength of synthetic polymers.

CHAPTER 4

LAYERED SILICATE POLYMER NANOCOMPOSITES AND PROPERTIES

There exist several strategies to put in use when properties of polymeric materials are found to be inadequate or desired to be further improved. Blending with other polymers, treating with various chemicals such as plasticizers or cross-linking agents, designing multilayer structures are the examples of these strategies discussed in the previous chapter. Beside these methods, composting inorganic fillers within polymer matrices is a widely used method. Polymer composites are also being applied in the industry today to improve mechanical properties of a polymer such as stiffness or toughness; to obtain better barrier properties against water vapor and various gases; to improve thermal properties or to enhance their resistance to fire and ignition, to introduce functional properties such as antimicrobial activity, or just to reduce the costs of the product. Composite applications are known and widely used in many fields of polymer world for a long time however; the nanocomposite applications are quite new and nowadays accepted as one of the most promising areas in polymer research.

Polymer nanocomposites are a new class of composites which are filled with particles whose at least one dimension is in the nanometer range (Alexandre and Dubois, 2000). Conventional composites impart some drawbacks to the resulting materials, such as weight increase, brittleness or opacity (Pavlidou and Papaspyrides, 2008) that are generally attributed to high filler content required to obtain desired properties. The important difference of nanocomposites over conventional composites is that nanocomposites are able to achieve same level of improvement with less amount of nanofiller. The first successful nanocomposites were prepared in 1993 using nylon 6 and organically modified montmorillonite (OMMT). Although several attempts were made by many research groups previously, none could achieve satisfactory results due to the level of inefficient exfoliation (Okamoto, 2005).

High level interactions between polymer matrix and properly dispersed nanofiller are the key point in nanocomposites. Nanocomposites offer higher level of improvements, since nanofiller-polymer matrix interactions in nanocomposites are far

stronger compared to conventional composite structures. Polymer nanocomposites can be synthesized from a variety of nanometer size particles. Nanoparticles can be classified in three main families with respect to number of dimensions being in nanometers. The first nanoparticle family is the isodimensional nanoparticles, such as spherical silica obtained by in situ sol-gel methods. This family is characterized with their both three dimensions being in nanoscale. The second and one of the most promising families for exceptional mechanical properties are called nanotubes or whiskers. They are widely researched for utilizing high performance yielding materials. Two dimensions of nanotube particles are in nanometers and have an elongated structure in their third dimension (Ray and Bousmina, 2005).

The third and the most extensively researched group of nanoparticles are the layered silicate family. Layered silicates (LS) - or generally so called nanoclays - differ from the other nanoparticles by being in nanometer scale with their single (thickness) dimension. Layered silicates are in the form of platelets and characterized by having very large surface area available for interaction with polymer matrix. Good examples of layered silicates are forms of natural clays; montmorillonite (MMT), hectorite and saponite. In the following section, structure and properties of the layered silicates will be discussed.

4.1. Properties of Layered Silicates

Among nanoparticles; layered silicates are the most widely used family among the nanoparticles since their polymer interactions are well known and they are easy to access (Alexander and Dubois, 2000). Among number of natural or synthetic origin layered silicates, 2:1 type (phyllosilicates or smectide family) clays are the most suitable candidates for reinforcing polymer matrices since their structural properties were reported to be suitable for utilization in nanocomposites.

Layered silicates (LS) have high surface areas around 400–700 m^2 per gram of layered silicate (Goettler et. al., 2007). Obviously, high surface area is owing to high aspect ratios of LS being in the range of 30-1000 (Ray and Bousmina, 2005). High surface area of LS should be utilized optimally when they are well exfoliated in polymer matrix. Layered silicates have two unique characteristics that make them an important candidate for preparation of nanocomposites. Although LS are generally found in

stacks, they have ability to disperse into individual layers which allows better dispersion of layered silicate particles. Second; surface characteristics of layered silicates can be manipulated depending on the matrix polymer type. These two characteristics are related to each other, since degree of dispersion of layered silicates depends on interlayer charge (cation) of the clay and polymer character (Ray and Okamoto, 2003; Paul and Robeson, 2008).

Crystal structure of layered silicates consists of layers made up of two tetrahedrally coordinated silicon atoms fused to an edge-shared octahedral sheet of either aluminum or magnesium hydroxide (Ray and Bousmina, 2005). The thickness of the above mentioned layer is about 1 nanometer in thickness and its lateral dimensions vary from 30 nm to several microns depending on the type of the LS. Stacking of the layers leads to regular van der Waals gaps between the layers called the interlayer or gallery. Structure of montmorillonite as an example to 2:1 layered silicates is given in the Figure 4.1.

In the case of tetrahedrally substituted layered silicates, the negative charge is located on the surface of silicate layers. Hence, the polymer matrices can interact more readily with these than with octahedrally-substituted material (Alexandre and Dubois, 2000). Pristine layered silicates usually contain hydrated Na^+ or K^+ ions. Since the surface contains negative charges in the pristine state, layered silicates such as montmorillonite are only miscible with hydrophilic polymers such as poly(ethylene oxide) (PEO), poly(vinyl alcohol) (PVA), etc. (Ray and Bousmina, 2005; Alexandre and Dubois, 2000; Okamoto, 2005). To improve miscibility with other polymer matrices, one must convert the originally hydrophilic silicate surface to organophilic, which enables intercalation of layered silicates within hydrophobic polymers.

Hydrophilic layered silicates such as montmorillonite can not be effectively exfoliated within most of the polymers because of the hydrophobicity of the polymers. Degree of exfoliation and performance of layered silicate nanocomposites (LSNC) depends on compatibility of interlayer charge (cation) of the clay and polymer matrix since opening of stacks and their alignment in different directions is driven by intermolecular interactions (Goettler et al., 2007). Surface characteristics of hydrophilic montmorillonites are generally changed in order to achieve efficient dispersion within hydrophobic polymers. Changing the surface characteristic of LS from hydrophilic to organophilic is called organomodification. By organomodification, surface energy of LS is reduced and the surface becomes more compatible with hydrophobic polymers.

Generally, change in surface charge of layered silicates is obtained by ion-exchange reactions with cationic surfactants, including primary, secondary, tertiary, and quaternary alkylammonium or alkylphosphonium cations (Alexandre and Dubois, 2000). Beside improved miscibility with the matrix polymer; organomodification also leads to higher interlayer spacings between individual clay platelets exhibiting more available space for the penetrating polymer chains within LS stackings. XRD analysis of several OMMT particles showed increases in the interlayer spacings (Cervantes-Uc et al., 2007).

4.2. Layered Silicate Nanocomposite Structures and Characterization

4.2.1. Layered Silicate Nanocomposite Structures

Introduction of layered silicates to the polymer matrix may result in several structures due to penetration level of polymer chains between the silicate layers. These structures could be overviewed in three types: phase separated, intercalated and exfoliated. As mentioned in previous section, structure's reliance on filler-polymer matrix interactions is obvious. In the case of relatively strong interactions among silicate layers rather than matrix, nanofillers tend to stay in stacks within the polymer defined as phase separated. Phase separation is generally observed for the composites of unmodified or inadequately modified silicates with hydrophobic polymers (Choudalakis and Gotsis, 2009, Ray et al., 2003). If the polymer chains can not penetrate efficiently between layers of silicates, the interface for bonding with matrix would be less and the resulting structures will have similar properties to that of microcomposites.

Second LSNC structure is the intercalated state of layered silicates within polymeric matrix. Better penetration of polymer chains due to stronger interactions lead to increased opening of clay stacks, concurrently is not enough to completely degrade the original conformation of nanoclays. Intercalated structures tend to take position within the matrix in stacks rather than single platelets.

The targeted structure in a nanocomposite is the exfoliated structure which is characterized by the random and disordered dispersion of silicates within the polymer matrix. As the interaction between silicate layers become weaker, matrix polymer penetrates strongly inside stacks and diminishes the ordered formation of LS stackings.

This conformation maximizes the interaction between polymer and filler, and leads to enhanced properties in the nanocomposite. An illustration for the possible layered silicate nanocomposite structures was given in Figure 4.1. In a LSNC, one or more of the nanocomposite structures may exist together. Beside mentioned structures, also there also exist mid-structures. In some conditions, intercalated silicate layers may also flocculate and extend the length of stacking in x-axis denoted by L_{clay} as can be seen in the Figure 4.2. The flocculation of nanoclay platelets was attributed to interactions between organically modified silicate and polymer matrix (Okamoto, 2005). Each structure is formed depending on the level of miscibility and interactions that have different extend of influence on the performance of nanocomposites. Therefore, it is critical to characterize the structure in order to evaluate the performance of nanocomposites.
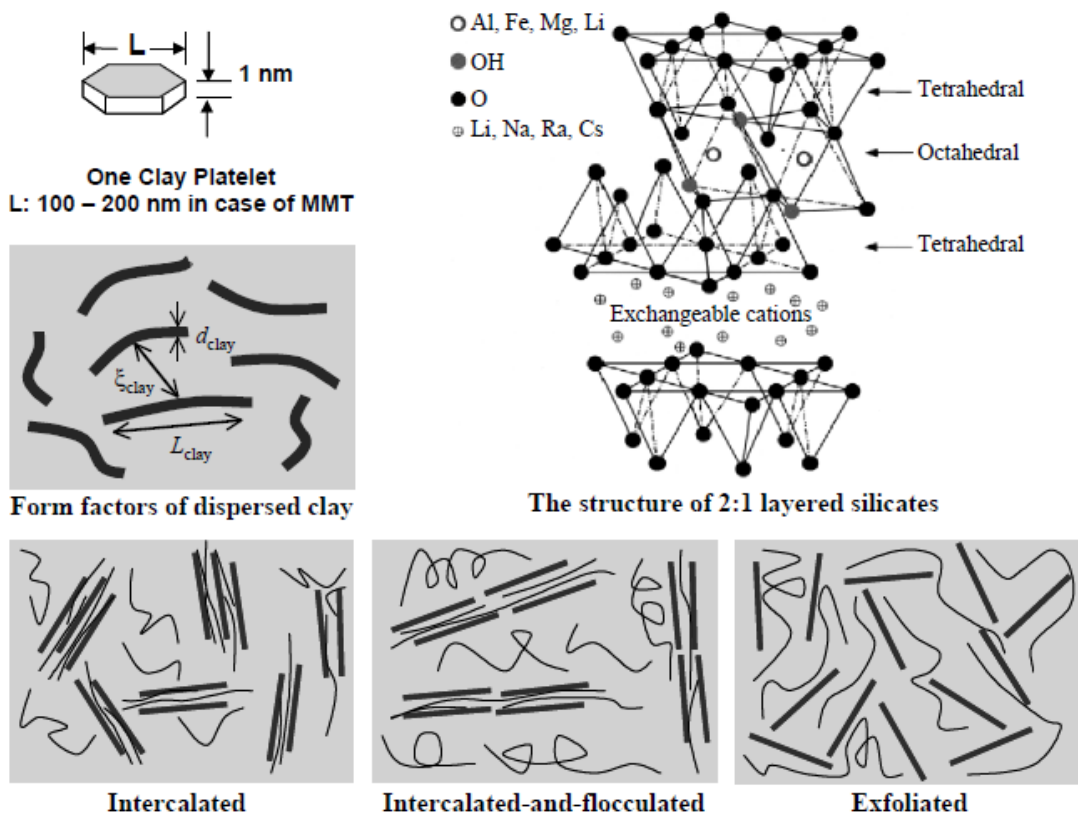
Figure 4.1. Schematic illustration of three different types of thermodynamically achievable polymer/clay nanocomposites (Source: Ray et al., 2003, Okamoto, 2005)

4.2.2. Characterization of Nanocomposite Structures

Characterization of nanocomposite structures is a key issue in nanocomposite research, since extend of the dispersion of layered silicate nanoparticles within the polymer matrix governs the possible modifications and additional unique properties Characterization of nanocomposites has been primarily done by joint use of X-ray diffraction (XRD) and transmission electron microscopy (TEM) techniques. Some other techniques have also been used such as FTIR and NMR in combination to support XRD in terms of molecular interactions (Ray et al., 2003).

In the XRD analysis, X-rays send on a sample –especially those having regular crystal structures- are collected and analyzed as peaks from different atom positions. Most of the layered silicates generally have ordered structures that give reflection when diffracted beams send on them. After incorporation of nanosized layered silicates into the polymer matrix, extend of nanofiller dispersion in the nanocomposite structure can be followed from XRD analysis by monitoring the position, shape, and intensity of the basal reflections from the distributed silicate layers (Ray and Bousmina, 2006).

The dispersion of silicate layers in the polymer matrix generally resulted in increased gallery height or d-spacing. The changes in the d-spacing can be investigated quantitatively by using the Bragg's law (Equation 4.1) where λ corresponds to the wavelength of the X-ray source used, θ is the diffraction angle measured and d is the spacing between diffractional lattice planes.

$$\lambda = 2d \sin\theta \qquad (4.1)$$

As interlayer spacing between planes increases, the characteristic peak of the clay in the XRD chromatogram shifts to lower angles. Intercalated structures are identified by broader and smaller diffraction peaks in XRD. This is reflected in 2θ values observed in lower angles, since the d-spacing of silicate layers are also expected to increase. In the case of intercalation with flocculation; the new arrangement of silicate layers may lead to appearance of new basal reflections at lower angles.

As extend of intercalation increases and exfoliation of silicate layers occurs within the polymer matrix, it can be expected that all reflections disappear and the obtained XRD analysis (crystallogrophy) of the nanocomposites is observed just like a

noise. Disappearance of peaks was attributed to large gallery height; beyond the maximum d-spacing value can be determined by XRD (Ray and Bousmina, 2005). Also exfoliation results in disordered dispersion of layered silicate stacks in several directions and loose their ordered structure that enables them to be detected (Paul and Robeson, 2008).

As discussed in the beginning of this section; XRD technique is generally used in combination with TEM. XRD results should be supported by some other techniques since XRD signal strength is strongly dependent on many factors like clay loading and layer orientation (Ijdo et al., 2006). In some cases it is very difficult to understand the peak broadening. In addition; layered silicates initially do not exhibit well-defined basal reflections, thus peak broadening and the decrease in intensity is difficult to study systematically (Ijdo et al., 2006). Therefore, TEM is used to make sure the real picture of the nanocomposite structure. TEM allows a qualitative understanding of the internal structure, spatial distribution and dispersion of the nanoparticles within the polymer matrix. Views of the defect structure through direct visualization could also be obtained. (Ray and Okamoto, 2003; Goettler et. al., 2007). Representative XRD chromatograms and corresponding TEM images for several types of structures were given in Figure 4.2.
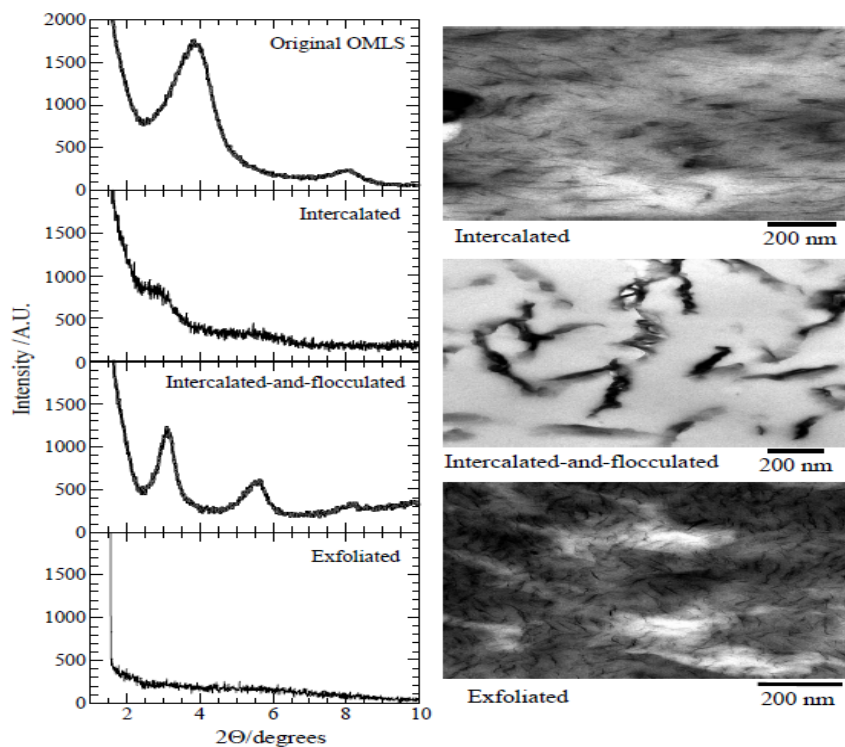
Figure 4.2. XRD patterns, and TEM images of three different types of nanocomposites
(Source: Okamoto, 2005)

4.3. Preparation Techniques of Layered Silicate Nanocomposites

Performance of a nanocomposite lies in the degree of dispersion of nanofillers in the polymer matrix. Highly dispersed - exfoliated nanoparticles within the polymer matrix allows enhancement of many properties of polymer and by this way, unique nanocomposites could be obtained for different applications. Several nanocomposite preparation methods exist depending on the polymer type or desired application.

4.3.1. In-situ Intercalative Polymerization

In this method; polymerization reaction is held in the liquid monomer or in the liquid monomer solution that layered silicates were previously swollen. In situ intercalative polymerization is advantageous since polymers are synthesized together with nanofillers. Another advantage of this technique is to facilitate the lower molecular weight of monomer or oligomer solution for enhanced dispersion efficiency of layered silicates. Some examples of intercalative polymerization method include the polymerization of a polyamide thermoplastic from its monomers, the cross-linking of a thermosetting epoxy and the vulcanization of rubber (Ray and Okamoto, 2003).

4.3.2. Melt Intercalation

Melt intercalation method is the most practical and industrially promising method for inserting polymer chains into the silicate galleries. Different than solution intercalation, melt intercalation is specific for each polymer type. It also eliminates solvent related cost and waste problems and can be used in combination with the entire industrial polymer processing methods. Melt intercalation method includes penetration of polymer chains into silicate galleries above softening point of polymer by means of shear forces (Ray and Bousmina, 2005). As shear introduced to the system increases, intercalation of silicates followed by exfoliation became more effective. This causes better interaction between LS and polymer matrix and results in more significant property improvements. Melt processing of nanocomposites is generally held in twin-screw extruders either in co-or counter rotating configurations.

4.3.3. Direct Intercalation from Solution (Solution Intercalation)

Direct intercalation of polymer chains into the layered silicates from solution or shortly solution intercalation method is the basic and easiest way to prepare nanocomposites. Although there are many different procedures reported in the literature; the first step in solution intercalation is the swelling of nanoparticles in the solvent phase. Initial swelling of layered silicates in the solvent before polymer addition resulted in better dispersion (Pandey and Singh, 2005; Kvien et al., 2007) due to the fact that solvent molecules have ability to penetrate into layered silicate stacks and increase the d-spacing (Ray and Okamoto, 2003). Several studies also showed that each solvent has different capability of swelling silicates. Surface energies of solvent and clay type have an important role on the swelling of layered silicates (Tran et al., 2006). Compatibility of solvents and nanoclays were also reported to affect modified layered silicate swelling and d-spacing within organic solvents depending on the type of organomodification agent used (Burgentzle et al., 2004). Once silicate particles swelled within the solvent; replacement of solvent molecules with polymer molecules come to the fruitition by the addition of individually dissolved polymer mixture in the same solvent or just by dissolving polymer in the LS swelled solution. Most effective method to achieve layered silicate swelling is sonication. Generally, further sonication is applied to polymer-swollen silicate solution in order to enhance penetration of polymer chains within nanoclay stackings. Use of plasticizers is also important in solution intercalation method since plasticizers may compete with polymer to bond with layered silicates (Pandey and Singh, 2005; Kvien et al., 2007).

Addition of swelled silicates and dissolved polymer solution is held around dissolution temperature specific to polymer type in order to utilize the low viscosity and free movement of polymer chains. Since most of the biopolymers dissolves in light solvents such as hexane, ethanol or water, solution intercalation is an ideal method to prepare layered silicate nanocomposites especially in the laboratory conditions. Solution intercalation can also be used in combination with other methods; such as in situ intercalative polymerization and prior to melt intercalation to prepare masterbatch stocks for further exfoliation.

4.4. Barrier Properties of Layered Silicate Nanocomposites

Among several interesting properties of polymer layered silicate nanocomposites (LSNC), the most attractive one from food packaging aspect is the availability of nanocomposites for unique improvements in gas and water vapor barrier of packaging films. Composting inorganic fillers with polymers is a common application in the industry to improve barrier properties of packaging materials. Micro size filler content required for adequate improvements is generally high, and may lead to deteriorations in mechanical strength and optical properties of produced films (Lu and Mai, 2007). Besides, possible problems such as higher processing temperature and poor melt rheology may occur. In the case of nanocomposites, level of barrier improvement is higher and such adverse effects are less likely to occur.

Improvements in barrier properties by the introduction of fillers in the polymer matrix are primarily attributed to the tortuous path formed for the permeating molecules. A diffusing molecule tends to travel in the path where it will face with least resistance. Any source of resistance, such as crystalline domains within the structure or irregularities in the sequence of the polymer molecules results in longer path that a permeant must travel reducing the permeability as discussed in the previous chapters. Tortuosity concept where the inorganic fillers are assumed to be impermeable for gas and liquid molecules (Eitzman et al., 1996) is analogous to above mentioned transport properties of molecules.

Basically, nanocomposites also improve barrier of polymers by creating more tortuous path for diffusing molecules due to incomparably higher aspect (length to width) ratio of nanofillers. While conventional composites are accepted to improve the barrier properties of polymers due to increased tortuosity; several additional factors were also proposed for nanocomposites. Small particle size and enormous surface area offered by layered silicates (LS) reported to alter matrix structure and change the permeation properties. Restrained polymer chain mobility resulted in decrease of free volume fraction of rubber/hectorite nanocomposites due to interactions in LS-polymer matrix and decrease in gas permeability (Sun et al., 2008). Nanoscale dimensions of nanocomposites may act as seeds for the creation of crystalline domains in the structure. MMT exfoliation within Nylon 6 increased matrix crystallinity and improved barrier properties (Ray and Bousmina, 2006).

LSNCs offer unique improvements in barrier properties of polymers due to their special geometry and properties. Polymer chains can be inserted between the LS stackings by several preparation methods and LS surface can be modified to enhance compatibility with the polymer matrix. Fine distribution of LS platelets, defined as exfoliation, may give aspect ratios in the range of several hundreds (Bharadwaj, 2001; Choudalakis and Gotsis, 2009; Ray and Okamoto, 2003). Schematic explanation of more effective tortuous path formation in LSNC in comparison to conventional composites was given in Figure 4.3.

(a)   (b)
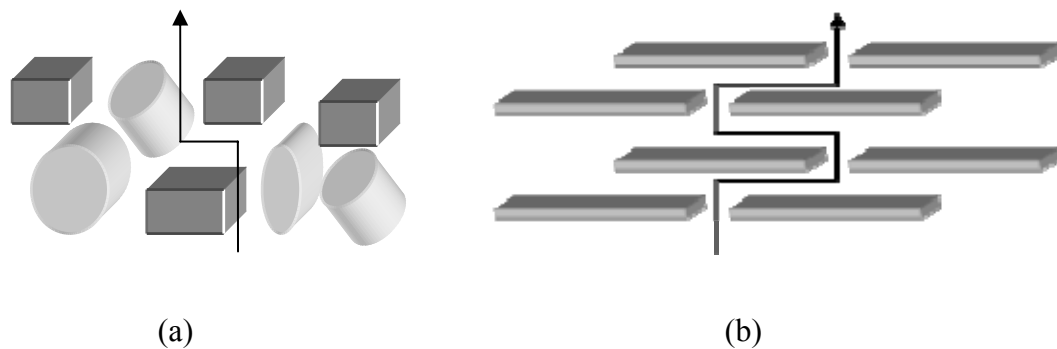
Figure 4.3. Schematic illustration of formation of highly tortuous path in nanocomposite. Conventional filler reinforced composites at left and, polymer/layered silicate nanocomposites at right.

Petersson and Oksman (2006) compared bentonite/PLA LSNC and microcrystalline cellulose (MCC)/PLA microcomposite by fixing the weight percent of filler. Results showed very significant differences in oxygen permeability values approving the effect of aspect ratio. Oxygen permeability of bentonite LSNC decreased while MCC composites destructed polymer structure and resulted in high permeability to O_2; even three times higher than the value for neat PLA. The most important feature of LSNC is the availability to achieve the same level of barrier improvement with small concentrations of nanofiller around 1-5 wt% without altering the mechanical strength of polymeric films due to high length to width ratio of LS compared to conventional fillers.

Though single LS platelets are characterized in nanometers, poor exfoliation may lead to agglomerates, decreasing the effectiveness of nanocomposites beyond a critical level of nanoclay content specific to each system. Heterogeneous wheat gluten biopolymer and MMT nanocomposites showed insignificant changes beyond 5 wt% LS content despite sharp improvements obtained in WVP up to 5% wt (Tunc et al., 2007). Similarly, starch and gelatin LSNCs showed decreased efficiency in improving WVP

and oxygen barrier beyond 7 wt% of unmodified MMT (Tang et al., 2008; Bae et al., 2009).

In the literature, barrier property improvements obtained by LSNC were mostly interpreted by the extensive tortuosity formed due to exfoliation of LS. Changes in polymer structure such as crystallinity, directed by LS platelets are hard to follow, and some polymer classes such as protein based biopolymers are amorphous. Several models based on tortuosity exist in the literature proposed to explain the effect of dispersed LS within the polymer matrix. Although these models were well defined before the development of nanocomposite concept, they are also applicable to LSNC since a very broad range of dimension definitions (i.e. aspect ratio) are used in the models (Paul and Robeson, 2008). Most of the permeability models applicable to LS systems were generally constructed by ignoring any possible structure change in the polymer as a result of nanocomposite formation (Pavlidou and Papaspyrides, 2008; Ray and Bousmina, 2006; Sorrentino et al., 2006).

The earliest attempt to construct a model to investigate permeability of gases and water vapor in layered silicate systems was done by Nielsen (Nielsen, 1967). The model was constructed on regular arrangement of 2 dimensional, rectangular platelets; aligned perpendicular to diffusion direction creating the highest tortuosity. Any structure change in the polymer which could alter the permeability in the matrix due to exfoliation of LS was ignored. Relative permeability of dilute LS systems with respect to pristine polymer could be analyzed according to volume fraction of layered silicates up to 10 v% Nielsen model successfully explains the level of decrease in permeability of LSNC by the formation of highly tortuous path due to higher aspect ratio of nanosize LS. Since Nielsen Model is one of the basic models, the derivation of the model was given below to give an idea about tortuosity based permeability models.

Due to above mentioned assumptions, solubility (S) and diffusion (D) parameters of Fick's Law (Equation 4.2) was modified considering the presence of layered silicates:

$$P = D * S \qquad\qquad (4.2)$$

$$S = S_0 * (1 - \phi) \qquad\qquad (4.3)$$

$$D = D_0 / \tau \qquad\qquad (4.4)$$

where φ is the volume fraction of nanoparticles in the matrix; τ is the tortuosity factor; and D_0 and S_0 denotes for diffusion and solubility coefficients of neat polymer. Tortuosity is dependent to aspect ratio (length of particle (L)/thickness of particle (W)) and the shape and orientation of nanoplatelets as well. Tortuosity can be defined as:

$$\tau = l'/l \tag{4.5}$$

While l denotes for membrane (film) thickness, l' is the distance a solute must travel in the presence of nanoplatelets. Estimation of l' is done by thinking each nanoplatelet increases the diffusion length by L/2 from the definition of aspect ratio (α):

$$l' = l + N*(L/2) \tag{4.6}$$

where N is the number of platelets on the path:

$$N = \frac{l*\phi}{W} \tag{4.7}$$

Then l' becomes as;

$$l' = l*\left(\frac{l*\phi}{W}\right) \tag{4.8}$$

By combining Equations 4.6 and 4.8, l' and tortuosity (τ) become:

$$l' = l*\left(1+\frac{l*\phi}{2W}\right) \tag{4.9}$$

$$\tau = 1+\left(\frac{l*\phi}{2W}\right) \tag{4.10}$$

Then diffusion parameter of modified Fick's Law (Equation 4.4) becomes:

$$D = \frac{D_0}{\left(1+\dfrac{l*\phi}{2W}\right)} \tag{4.11}$$

and by inserting Equations 4.3 and 4.11 into Equation 4.2; composite permeability equation is derived as;

$$P = \frac{D_0}{\left(1 + \frac{l * \phi}{2W}\right)} * S_0 * (1 - \phi) \qquad (4.12)$$

Dividing the composite permeability definition given in Equation 4.12 by permeability of neat polymer and rearranging by considering aspect ratio (α); relative theoretical permeability of a polymer can be calculated by the Nielsen Model:

$$\frac{P}{P_0} = \frac{1 - \phi}{1 + \frac{\alpha}{2}\phi} \qquad (4.13)$$

Theoretical permeability of LS systems predicted by Nielsen Model for several aspects ratios were plotted in the Figure 4.5. As seen in the Nielsen plot, when assumptions of the model satisfied, aspect ratio of the LS significantly affects the permeability of the system. As aspect ratio increases, the marginal improvement obtained for smaller clay contents is more explicit since path required to be traveled by a diffusing molecule become significantly longer as seen in Figure 4.4.
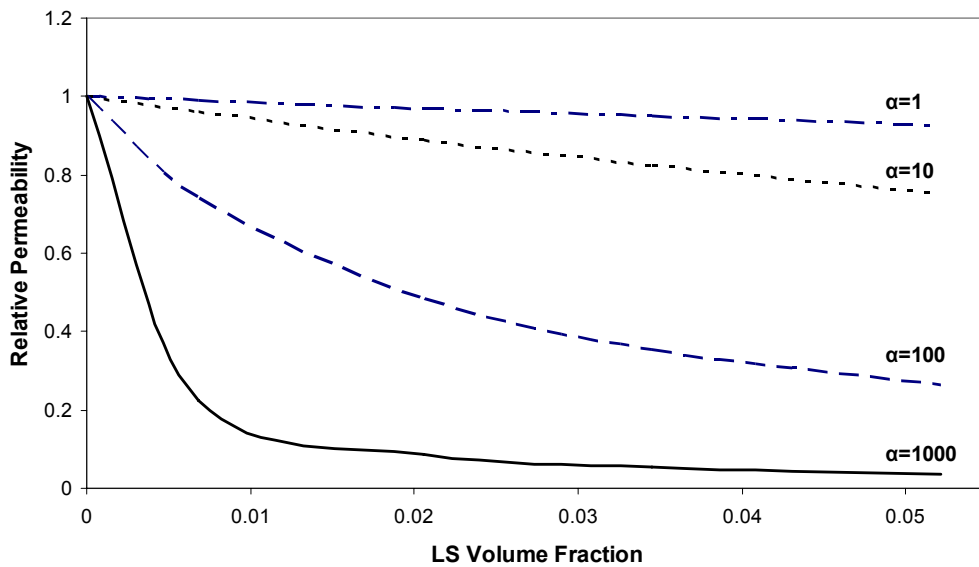
Figure 4.4. Relative permeability predictions according to Nielsen Model as a function of layered silicate volume fraction for different aspect ratios

Another two widely used models to predict permeability in LSNC systems are Cussler regular and random models. The first model is an alternative to Nielsen model, considering regular alignment of LS in the polymer matrix and proposed using the same assumptions. Difference of Cussler regular array model over Nielsen model is that; the model also includes area available to permeation of molecules (Eitzman et al., 1996, Lape et al, 2004). The model equation derived is:

$$\frac{P}{P_0} = \frac{1-\phi}{1+\frac{(\alpha\phi)^2}{4}}$$ (4.14)

The volume fraction of nanofillers in a composite or nanocomposite matrix can be calculated by using the formula for all models:

$$\phi = \frac{1}{1+\left(\frac{\rho_c * (1-M_c)}{\rho_p * M_c}\right)}$$ (4.15)
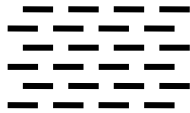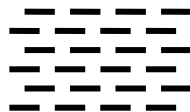
where ρ_p and ρ_c are densities of matrix polymer and filler respectively and M_c denotes for mass fraction of filler.

Cussler model for regular alignment of rectangular platelets predicts the permeability better especially for low nanoclay loadings below 0.5 v% (Sun et al., 2008, Choudalakis and Gotsis, 2009). This property of model is beneficial for more accurate predictions in some LSNC systems while the area included estimation is ineffective for some systems.

Random positioning of rectangular platelets aligned normal to diffusion direction was also modeled by Cussler (Eitzman et al., 1996; Lape et al., 2004; DeRocher et al., 2005). Assumptions and considered platelet positioning was tabulated in Table 4.1 together with other models discussed in this section. The derived model equation for random positioning of rectangular platelets is:

$$\frac{P}{P_0} = \frac{1-\phi}{(1+\frac{\alpha}{3}\phi)^2}$$ (4.16)

Table 4.1. Most common permeability models used to investigate nanocomposite barrier performance

Model	LS Array	Formula	Assumptions
Nielsen (Nielsen, 1967)		$\dfrac{P}{P_0} = \dfrac{1-\phi}{1+\dfrac{\alpha}{2}\phi}$	2D, rectangular platelets, regular array, platelets align normal to diffusion direction
Cussler (regular) (Eitzman et al., 1996)		$\dfrac{P}{P_0} = \dfrac{1-\phi}{1+\dfrac{(\alpha\phi)^2}{4}}$	2D, rectangular platelets, regular array, platelets align normal to diffusion direction
Bharadwaj (Bharadwaj, 2001)		$\dfrac{P}{P_0} = \dfrac{(1-\phi)}{1+\dfrac{2}{3}\dfrac{\alpha}{2}\phi(S+\dfrac{1}{2})}$	2D, rectangular platelets, random array, platelets align in different directions to diffusion
Cussler (random) (Lape et al., 2004)		$\dfrac{P}{P_0} = \dfrac{1-\phi}{(1+\dfrac{\alpha}{3}\phi)^2}$	2D, rectangular platelets, random array, platelets align normal to diffusion direction

Although Nielsen and Cussler models reported to evaluate the permeability decrease of nanocomposites well in the literature, their ability to reflect exfoliated state of nanocomposites is controversial. For example, an aspect ratio of 70 was found by using Nielsen Model for the WVP data of PCL nanocomposites although successful exfoliation of LS was observed by TEM (Ray and Bousmina, 2006). This was attributed to the low aspect ratio to alignment of platelets in several directions rather than the direction proposed by Nielsen Model. Several studies showed alignment of LS platelets in various directions for exfoliated LSNC structures as observed by TEM images.

A platelet orientation included extension of Nielsen model is Bharadwaj model (Bharadwaj, 2001). The model equation is:

$$\frac{P}{P_0} = \frac{(1-\phi)}{1+\frac{2}{3}\frac{\alpha}{2}\phi(S+\frac{1}{2})} \qquad (4.17)$$

An order parameter S was introduced to Nielsen equation to quantify the average degree of particle deviation from diffusion direction. Parameter S can be calculated by using Equation 4.18. In the equation θ is the angle between diffusion direction and the orientation of platelet. The S value may have a value between 0 and 1.

$$S = \frac{1}{2}\left\langle 3*\cos^2\theta - 1\right\rangle \qquad (4.18)$$

While S=1 case considers the same alignment with Nielsen Model, the S=0 case accounts for completely random orientation of platelets as seen in Table 4.1. Effect of LS platelet orientation on permeability decrease especially for shorter exfoliated platelets can be more easily seen by the model (Bharadwaj, 2001).

Permeability estimations done by using different models may lead to various results depending on whether the clay content is in the dilute region and aspect ratio of LS employed during the calculations. Theoretical permeability values predicted by discussed models for aspect ratios of 50, 200 and 1000 was plotted in Figure 4.6 for comparison. The differences related to the model assumptions were discussed in more detail for broad ranges of LS loadings and aspect ratios in the review of Choudalakis and Gotsis (2009).

Accepted permeability models are generally applicable to dilute and/or semi-dilute clay contents in nanocomposites since models assume good level exfoliation in their predictions. Herrera-Alonso and coworkers (2009) investigated He and O_2 permeability of polyurethane-OMMT nanocomposites up to very high LS content of 50 wt%. Their results were fitted to several models gave very low aspect ratios between 10 and 40 for used OMMT, which should be attributed to nanoclay agglomerates and out-of range model fitting. It should also be noted that LS platelets exist in a range of aspect ratios rather than a single homogeneous ratio (Paul and Robeson, 2008). The aspect ratio estimated by using the permeability models is a normalized value for overall system.

4.5. Mechanical Properties of Layered Silicate Nanocomposites

The potential of polymeric layered silicate nanocomposites in materials science was first evidenced by the effective reinforcing capability of exfoliated layered silicate nanoclays in polymer matrix. Improvements in mechanical properties of polymers could be achieved in a larger extend by employing nanocomposites compared to conventional composites prepared by using micro size fillers. As in the case of barrier improvements of layered silicate nanocomposites, several factors were proposed for the performance of LSNC. These factors can be sum up in two headings; factors that can be explained by composite theory and nano-effects occurred in polymer structure due to efficient distribution of nanofillers in the polymer matrix (Paul and Robeson, 2008; Ray et al., 2003).

Reinforcing mechanism of fillers such as fibers can be put in use to understand the effect of LSNC on mechanical properties. High moduli rigid fillers within the relatively soft polymer matrix create a mechanically restrained area of polymer, particularly adjacent to filler. Reinforcing mechanism of fillers was given in the Figure 4.5 below. As long as adequate bonding between polymer and filler phases exists, the structure would tend to act as a stronger material than the pristine polymer. At this point, the enormous surface area (characterized in several hundred meter squares) benefited due to effective distribution of layered silicate platelets can be used to explain the more expressed improvements in a LSNC than a conventional composite (Pavlidou and Papaspyrides, 2008; Paul and Robeson, 2008; Ray and Bousmina, 2006).
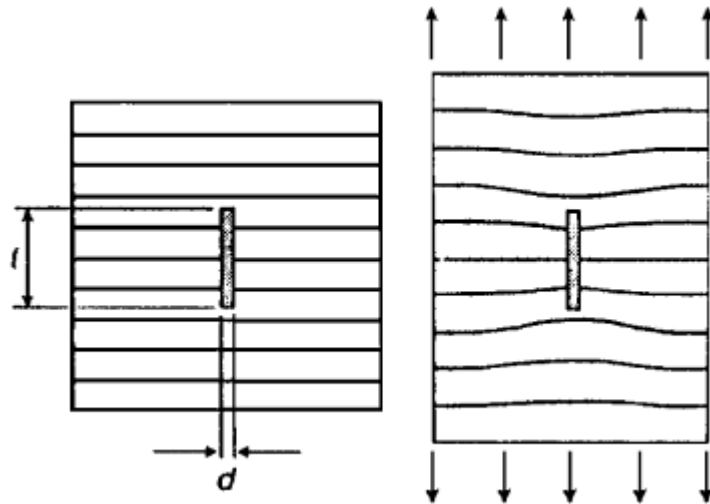
Figure 4.5. Reinforcement mechanism in composite materials
(Source: Pavlidou and Papaspyrides, 2008)

Several reviews and studies discussed the successful stiffening of polymers by LSNC with less filler content compared to conventional composites to achieve same degree of improvement. Paul and Robeson (2008) reviewed comparison of PE/MMT nanocomposites with PE/Talc composites and Nylon6/MMT nanocomposites with Nylon6/glass fiber composites. The required amount of MMT to double elastic modulus of neat polymers was reported to be 4 and 3 times lower than talc and glass fibers; indicating a significant weight reduction for the same performance (Paul and Robeson, 2008). Petersson and Oksman (2006) studied PLA nanocomposites prepared by bentonite LS and PLA microcomposites prepared by microcrystalline cellulose. Concentration of both fillers was 1 wt% with respect to polymer. Authors reported 50% increase in elastic modulus and yield strength for LSNC of PLA while cellulose composites slightly reduced the modulus of films without significantly improving the yield strength.

Beside improvements in stiffness, the addition of LSNC increased the maximum tensile strength of polymers. While elastic modulus increase in LSNC was mainly attributed to existence of stiffer layered silicates platelets, improvements in tensile strength of LSNC were attributed to degree of bonding between nanoclay and polymer matrix (Ray and Bousmina, 2005; Pavlidou and Papaspyrides, 2008). Dean and coworkers (2008) improved the tensile strength of PVOH/Starch blends by using MMT. Higher increase in tensile strength in PVOH blends compared to single starch films

were attributed to enhanced bonding between PVOH and MMT as evidenced by FTIR. Many reviews concerning the mechanical properties of LSNC reported that tensile strength improvements in LSNC are more sensitive to nanoclay content than modulus changes due to level of interactions between nanofiller and polymer (Okamoto, 2005; Ray and Okamoto, 2003; Pavlidou and Papaspyrides, 2008).

Maximum elongation of polymeric films under tensile load is another important mechanical aspect of nanocomposites. It is well known that polymeric composites improve modulus and tensile strength at the expense of flexibility of the material. Decreased flexibility is generally observed in nanocomposites as well. Nanocomposites are thought to alter flexibility of polymers in lesser extend than conventional composite systems that results in better interactions between filler and polymer matrix due to higher surface area available for bonding (Okamoto, 2005; Paul and Robeson, 2008; Ray and Bousmina, 2006).

4.6 Nanocomposites of Agricultural and Protein Based Biopolymers

Successful nanocomposite applications of synthetic polymers encouraged many researchers to develop biodegradable nanocomposite systems for food packaging applications. Currently, there is an extensive literature available about the nanocomposite applications of biopolymers. Most biopolymer nanocomposite research is focused on microorganism and bio-derived monomer synthesized polymers such as PHAs, PCL and PLA that have homogeneous and similar structure to polyolefins.

Agricultural based biopolymers were also being subject to nanocomposite applications. Many researches was conducted on starch, and in less extend on other proteins like soy, wheat gluten, gelatin and whey to improve their inherent mechanical brittleness and high permeability to water vapor by utilizing strong interactions between layered silicate nanoclay platelets and polymer matrix. As in the case of synthetic polymers and other biopolymers, nanoclays intercalated and exfoliated within the polymer matrix showed enhanced mechanical and barrier properties for agricultural biopolymers. Today, nanocomposite applications are one of the hottest topics for the property improvements in protein based and other types of renewable biopolymers.

Tang and coworkers (2008) compared the performances of unmodified and modified nanoclays on plasticized starch nanocomposites. While unmodified MMT was

exfoliated or intercalated depending on the clay content, all concentrations of modified MMT showed no increase in interlayer spacing. In consistent with the XRD results, modified 130E MMT resulted in lower tensile strength and percent elongation at break, even showing poorer mechanical properties than the pristine starch. This was attributed to the disturbed structure of starch due to ineffective dispersion of modified clay. Meanwhile, the unmodified MMT being compatible with the starch matrix resulted in improved mechanical and water vapor barrier properties. These results were in good agreement with the level of exfoliation interpreted from XRD analysis. Huang and Netravali (2006) investigated nanocomposite performance of unmodified cloisite Na^+ on highly hydrophilic soy protein cross-linked by phytagel. Iimproved tensile strength (TS) and Young modulus was reported due to observed exfoliated structure up to 7 wt% nanoclay with a slight decrease in elongation at break. Further clay loading resulted in intercalated structures and a decrease in TS (still being higher than the pristine soy film) and percent elongation. On the other hand modulus of the samples continued to increase. DMA of the nanocomposite samples also showed enhanced storage modulus, especially for lower temperatures. A slight increase in T_g (from 186.7 to 193.4 ^{o}C) of nanocomposite samples was observed.

Protein based biopolymers, as well as most of the plant based polymers require plasticizer treatment in order to prevail over the inherent brittleness of films. Plasticizers loosen the bonds among polymer chains by entering between and creating new interactions as well. As biopolymers have tendency to form new bonds with layered silicates, plasticizers may also compete with polymers to interact with nanoclays. Pandey and Singh (2005) investigated the effect of processing sequences in solution intercalation method together with interactions between glycerol and MMT in starch nanocomposites. Authors proposed that glycerol and starch compete for bonding with MMT. This competition results in a decrease in the efficiency of starch chains' entering between layered silicate platelets according to FTIR analysis. Plasticization, following the mixing of layered silicates and starch improved the elongation at break of samples in spite of significant decreases observed for simultaneous or former plasticization with starch/LS mixing. More flexible and stronger films resulted due to mixing of LS and biopolymer prior to plasticization which was also observed in the study of Kvien and coworkers (2007).

Nanocomposite preparation by using solution intercalation involves use of stronger mixing techniques. While early studies utilized long ultrasonic bath treatments,

probe type ultrasonic processors gave better results as observed in this study. Dean and Yu (2005) investigated effect of ultrasonic treatment time on layered silicate delamination by using XRD analysis. Increased period of ultrasonic treatment was resulted in a small increase in d-spacing due to swelling effect of water. Improved delamination of LS stackings was reported for longer ultrasonic treatment and plasticization effect of glycerol.

Chen and Zhang (2006) investigated interactions between glycerol plasticized soy protein and unmodified MMT as well as mechanical properties of produced nanocomposites. Authors foresee H-bonds were formed between nanoclay platelets and soy protein according to FTIR analysis results. While intensity of FTIR bands at Amide I and II regions increased for intercalated and exfoliated structures, high clay loading did not change the peak intensities. This was interpreted; as occupation of all free sites results in inefficient dispersion of further added nanoclay, as also considering XRD results. Changes in the "in- and out-of-plane" Si-O stretching bands of MMT were also observed. Higher exfoliation of clay platelets were resulted in narrower and less intense Si-O bands as well as better identified out-of-plane band due to efficient dispersion of MMT. Interestingly, very high clay contents compared to other polymers were reported. Exfoliated nanocomposite structures up to 8 wt% of MMT and intercalation around 16 wt% was obtained. High interaction of nanoclays was resulted in dramatic decrease in elongation at break and significant increase in Young modulus. Tensile strength at break of the molded films doubled at 16 wt% clay loading

Depending on the polymer chains entering within the layered silicates and degree of stack opening give improved properties to the nanocomposites. The stack opening – or interlayer spacing- of the layered silicate is also critical as well as the interactions between nanoclay and polymer itself. Yu and coworkers (2006) studied soy protein nanocomposites prepared by dispersing unmodified rectorite, another type of layered silicate, characterized by twice the interlayer spacing of unmodified MMT. TEM images showed exfoliated structures for 4 wt% clay and intercalated structures without agglomeration for 12 wt% samples. TEM images were also supported by XRD peaks disappeared or shifted to left indicating increased interlayer spacing. FTIR analysis of the nanocomposites gave similar results to that of Chen and Zhang's (2006) study. Researchers reported highly increased Young modulus up to 20 wt% clay and doubled tensile strength for 12 wt% clay loaded sample. Further increase in clay content resulted in decreased tensile strength close to that of pristine polymer's for 24 wt% clay

concentrations. Decrease in tensile strength was attributed to brittleness caused by clay agglomerates. Also flexibility of the prepared samples decreased dramatically. The glass transition of the nanocomposites were hindered due to limited chain motion caused by polymer chains entering between clay layers according to the thermal analyses results (Chen and Zhang, 2006).

Rao (2007) compared two different gelatin - layered silicate nanocomposites prepared by nanoclays with different aspect ratios. Layered silicates having higher aspect ratios gave better results for synthetic polymers. Cloisite Na^+ characterized by aspect ratio of 200 increased modulus and tensile strength at break more than the Laponite layered silicate with aspect ratio of 30. DSC scans of the nanocomposites resulted in slightly increased melting temperatures and decreased melting enthalpy of the nanocomposites which was attributed to depressed crystallinity by the presence of the nanoclays in the structure. Transparent films with very little changes compared to pristine gelatin film for both nanocomposites were also reported.

Effect of layered silicate nanoclays on optical properties of whey protein composites was studied by Sothornvit and coworkers (2010). In contrast to unchanged optical properties in gelatin nanocomposites (Rao, 2007), cloisite 30B layered silicate incorporated composites hindered optical properties of whey protein films. Transparency and gloss of whey protein films decreased due to the clay introduced. Authors also reported improvements in the haze of composite samples indicating reduced homogeneity on the surface. Diminished optical properties in whey modified MMT nanocomposites can be attributed to poor dispersion of clays in the structure.

An important aspect of nanocomposites is their potential to have improved barrier properties compared to that of neat polymers. Many nanocomposite studies showed that layered silicates can decrease water vapor permeability (WVP) and oxygen permeability (OP) depending on the level of dispersion of nanoclays. Bae and coworkers (2009) studied water vapor and oxygen permeability of fish gelatin nanocomposites prepared by unmodified Cloisite Na^+ montmorillonite. Increment in MMT content resulted in continuous decrease in both OP and WVP, following the same trend. The decreases were slightly sharper for clay content up to 5%. Improvements in tensile strength in expense of percent elongation at break were reported as well. Authors also investigated effect of sonication on the nanocomposites produced. OP of sonicated samples was lower, together with better improvements in mechanical properties. Among samples stirred at different speeds, no significant difference in OP was observed. It was

concluded that, mechanical forces, other than sonication are ineffective for the preparation of nanocomposites.

Layered silicates introduced to polymer matrix would affect permeability characteristics in several ways. Since permeation has solubility and diffusion aspects, effect nanoclays may exist in one of them or both. Tunc and coworkers (2007) prepared glycerol plasticized wheat gluten/MMT nanocomposites and investigated their barrier to water vapor, oxygen and carbondioxide; as well mechanical performance of the nanocomposites. Surface hydrophilicity of wheat gluten was affected by the clay content in the 0-10 wt% range. While contact angle of the nanocomposites observed to decrease significantly by the increasing clay concentration, the water absorption rate was decreased interestingly. Authors attributed these changes to clay content. Clays dispersed within the polymer formed a barrier to penetrating water vapor while hydrophilic character of clays increased the wettability of the wheat gluten polymer. No change in oxygen and carbondioxide permeabilities were obtained while WVP of the films reduced to half of neat gluten. Considering all permeability results together; authors predicted the effect of clays in the films as limiting the solubility of water molecules to surface rather than decreasing diffusivity.

Changes in hydrophobicity of biopolymers due to introduction of hydrophobic OMMT were also reported in several studies. Magalhaes and Andrade (2009) studied corn starch nanocomposites prepared by organomodified Cloisite 30B. Authors observed very significant increases in hydrophobicity of hydrophilic starch, depending on the clay content. Organomodified Nanomer 1.34TCN incorporated soy protein coatings as a conventional filler on paperboards resulted in increased hydrophobicity measured by higher contact angle of water on soy protein layer (Rhim et al. 2006).

Very recently in the literature, Corn zein OMMT nanocomposites prepared by using solution intercalation and blown film extrusion methods were studied by Luecha and coworkers (2010). Improved elongation at break was reported for extrusion blown samples, while the samples prepared by solution intercalation increased the brittleness. Tensile strength and elastic modulus of prepared films showed discontinuous improvements. Water vapor permeability of nanocomposites showed improvements in small OMMT concentrations whereas, WVP of samples with OMMT content higher than 3 wt% were very close to that of pristine corn zein. Additionally, better thermal stability was obtained from TGA analysis.

CHAPTER 5

EXPERIMENTAL

5.1. Materials

Corn zein used in this study was obtained from Sigma-Aldrich. Ethanol (Ethyl alcohol) (lab-grade, >99.5%) used as solvent for corn zein was supplied from Panreac. Dilution of lab-grade ethanol to 95%(v/v) was done with ultra pure water. Nanocomposites were prepared by using the commercial organomodified layered silicate montmorillonite Cloisite 10A (125 meq/100g clay) and natural montmorillonite Nanofil 116 (116meq/100g clay) were obtained from Southern Clay – Rockwood. Glycerol (MW: 92 g/mol) obtained from Fluka was used as plasticizer to overcome the brittleness of corn zein. Plasticized corn zein nanocomposites were casted on commercial corona treated 40 µm thickness polypropylene (C11/40 µm) films, supplied by Polinas Company (Manisa/Turkey).

5.2. Preparation of Corn Zein Nanocomposite Coated PP Films

Corn zein nanocomposite coatings were prepared by solution intercalation method. Different amounts of commercial nanoclays (1-3-5-7.5%w/w corn zein) were first dispersed in 50 ml of aqueous (95%v/v) ethanol by stirring for 15 minutes. Then, in order to open clay stackings, stirred solution was sonicated for 60 minutes by using a ultrasonic probe sonicator (Sonix Vibracell 505) working at 40% capacity of its 20±0.05 kHz output. 2.5g corn zein was dissolved within the clay dispersion at 50^0C. After complete dissolution of zein, 0.64µl of glycerol was added to plasticize the corn zein, and then sonication was applied for 60 minutes in order to obtain further penetration of plasticized biopolymer chains inside clay platelets. Sonication steps were done in a cooling water bath operating at 15^0C in order to prevent overheating and decomposition of corn zein. The prepared CZNC solution was then immediately casted on corona discharged commercial polypropylene (PP) films with 40 µm thickness (C11/40) with a custom blade of 500µm in height by using automatic constant speed film applicator

(Sheen 1133N). Then, the prepared corn zein nanocomposite coated polypropylene films (CZNC-PP) were first put in to a vacuum oven at 50^0C, and -200mbar for 120 minutes and then the temperature was raised to 120^0C for 24 hours in order to achieve complete evaporation of solvent. All films were kept in a desiccator to prevent films from absorbing water vapor until testing.

5.3. Determination of Film Thickness

Thicknesses of prepared CZNC-PP films with various clay contents were measured with an electronic digital micrometer (293-821, Mitutoyo) with 0.001mm sensitivity. The thicknesses used in permeability analysis and mechanical testing evaluations were determined by taking at least five different measurements from random sections of films. Thicknesses of individual CZNC layers used in oxygen and water vapor permeability calculations were determined by subtracting the thickness of polypropylene film (40 µm) from the measured total thickness.

5.4. Fourier Transform Infrared (FTIR) Analysis of CZNC-PP Films

Infrared spectra of the prepared films were obtained by using a FTIR spectrometer (Perkin Elmer Spectrum 100) equipped with ATR accessory. Film spectra were collected at a resolution of 4 cm^{-1} and averaging 64 scans by using ZnSe crystal and DTGS detector in the 4000-650 cm^{-1} wave number range. Spectra of the films below 650 cm^{-1} wavenumber range were also obtained by using a FTIR spectrometer (Shimadzu FTIR 8201) in transmission mode. FTIR analysis of nanoclay powders were done by preparing pellets with KBr. Regular FTIR spectra were collected by averaging 64 scans at resolution of 4cm^{-1}.

5.5. X-Ray Diffraction (XRD) Analysis of CZNC-PP Films

X-Ray diffraction (XRD) analyses of the films were carried out by using X'pert PRO MRD X-Ray diffractometer (PANalaytical) suitable for thin film analysis.

Samples were scanned for diffraction angles $2\theta = 0.25 - 8^o$ from the CZNC coated surfaces.

5.6. Oxygen Transmission Rate Analysis of CZNC-PP Films

Oxygen transmission rates (OTR) of CZNC coated PP film samples were determined by using gas permeation instrument (Dansensor Lyssy, L-100-5000 Manometric Gas permeability Tester) according to ASTM D3985 standard. OTR measurements were conducted at 23^0C and 0%RH. Gas permeation instrument was consisting of two chambers separated by the test film. Analysis was conducted based on the concentration difference created by passing oxygen at the upper chamber and by creating vacuum in the lower chamber. Before analysis, lower chamber was vacuumed to a predefined value controlled by number of undervac cycles. When desired vacuum value was reached, the applied vacuum was cut and oxygen was let to permeate through lower chamber. Since tester was running in manometric principle, the pressure probe was insensitive to type of the gas. Time required to increase the lower chamber pressure to predefined value was measured and the transmission rate of the testing gas was calculated by the tester by using reference film data. The output of the analysis was oxygen transmission rate in ml gas (oxygen) per area (m^2) time (day). OTR of films were determined by testing three different samples and their average was recorded.

Oxygen transmission rates of single CZNC layers was calculated from the CZNC-PP results by using the following multilayer permeability model since all measurements were conducted in the same pressure range and oxygen gas flow.

$$\frac{L}{P} = \sum_{i=1}^{n} \frac{L_i}{P_i} \tag{5.1}$$

where n is the number of layers, L and P are the thickness and oxygen transmission rate of the multilayer film. L_i and P_i on the left hand side of the formula are the thickness and oxygen transmission rate of each layer, respectively.

5.7. Water Vapor Permeability Analysis of CZNC-PP Films

A water vapor permeability analyzer (Mocon Permatran 3/33) was used to investigate the effect of nanocomposite coating layer on water vapor permeability of CZNC coated PP films. All water vapor permeability tests were conducted at 37.8 ^{0}C and 90% RH according to ASTM F1249 standard. The test film was placed between two test cells. While test (upper) chamber was continuously flushed with dry nitrogen, lower chamber was washed with carrier nitrogen. Carrier nitrogen, was passed through ultra pure water to adjust the RH and flowed into the lower cell. As the water vapor diffused through the test film, it was carried by nitrogen to the detector in the upper chamber. Nitrogen flow rate was set to 100 cm^3 per minute. The data was recorded as water vapor transmission rate (WVTR). Permeability of the samples (10^{-2} g (water vapor) thickness (mm) per area (m^2) time (day) pressure (mmHg)) was calculated by using Equation (5.2):

$$Permeability = \frac{WVTR}{S(R_1 - R_2)} * L_{film} \qquad (5.2)$$

Where, R_1 is relative humidity at the source expressed as a fraction ($R_1 = 0.9$ for 90% RH chamber), R_2 is relative humidity of the vapor sink expressed as a fraction ($R_2 = 0$ for the 0% RH chamber (dry side)), S is the vapor pressure of water at the test temperature in inches of mercury and L_{film} is the thickness of the tested film. All films were tested for three different samples and the average was reported as the water vapor permeability data. WVP of single CZNC layers were calculated by using the multilayer permeability equation (Equation 5.1).

5.8. Mechanical Property Determination of CZNC-PP Films

A texture analyzer (TA XT Plus) equipped with a 5 Kgf load cell was used in tensile mode to determine the mechanical properties of prepared films according to ASTM D-882 standard. Tested films were cut in 10 mm width and 75 mm in length in order to provide enough space for film holding. The initial gauge length and testing speed were fixed at 25 mm and 10 mm/min, respectively. Reported tensile strength at

break and yield strength values were the stress value at the rupture of the films and the value when yielding begins, respectively. Percent elongation at break values were directly read from stress-strain curve and denotes for the ratio of length of the sample at rupture of film to initial length of the sample. Elastic (Young) moduli of films were calculated from the slope of linear portion of stress-strain curve. Sample stress – strain diagram was given in Figure 5.1. At least five films were tested and the average was reported.

5.9. Contact Angle Measurements of CZNC-PP Films

Contact angle analysis of prepared CZNC coated PP films were conducted using the initial contact angle method. Initial contact angle of water in air on the CZNC-PP surfaces was measured with a contact angle analyzer (Attension Theta Optical Tensiometer, KSV Instruments) by dropping a constant 6μl of water on to the CZNC surface of the films by using an automatic micro syringe. Distilled water was used a probe liquid. An image of water drop was recorded immediately just after dropping from the syringe and the contact angle of water drop analyzed digitally by using the software of the device. Initial contact angle values of at least ten measurements were reported as the average of left and right contact angles.

5.10. Color Measurements of CZNC-PP Films

The color of corn zein nanocomposite coated PP films was assessed using a colorimeter (Avantes). PP film having no CZNC coating (L = 90,56, a = 0,35, b = 0,55) was used as a background for color measurements of the coated films. In the Hunter system, color is represented as a position in a three-dimensional sphere, where the vertical axis L indicates the lightness (ranging from black to white), and the horizontal axes, indicated by a and b, are the chromatic coordinates (ranging from a: greenness to redness and b: blueness to yellowness). Hunter L, a, and b values were averaged from five readings across for each coating replicate. The total color difference (ΔE) can be calculated by the following equation;

$$\Delta E = \sqrt{(\Delta L)^2 + (\Delta a)^2 + (\Delta b)^2}$$ (5.3)

For each film, at least five measurements on different positions of film surface were made. The results were expressed as ΔE values, with the substrate PP having no CZNC coatings as reference

CHAPTER 6

RESULTS AND DISCUSSION

Corn zein nanocomposites (CZNC) were prepared by solution intercalation method by using layered silicate nanoclays. Prepared CZNC solutions were coated on to commercial Polinas C11/40μm polypropylene (PP) films. The effect of modification of clay on the properties of CZNC coated films (CZNC-PP) and as well as single CZNC layers was investigated. CZNC solutions were also prepared by using stirring instead of sonication processing steps in order to follow the effects of sonication on the final properties. Organically modified layered silicate clay Cloisite 10A (CLO10A), and unmodified Nanofill 116 (NF116) were used as nanofillers. Resulting films were named according to their clay content in CZNC layer such as CLO10A-1% to Clo10A-7.5% and NF116-1% to NF116-5% as seen in Table 6.1. Sample codes PP and PPZ were used for the commercial polypropylene film and plasticized corn zein coated polypropylene film, respectively. Samples starting with CLO10A(Stir) code denotes for the CZNC-PP films with CZNC layers prepared by employing stirring instead of sonication step.

Effects of nanoclay content, nanoclay type and preparation technique of nanocomposites on the oxygen transmission rate (OTR) and water vapor permeability (WVP) of the coated CZNC layer on the overall film and single CZNC layer were investigated. In addition, mechanical, surface and optical properties of prepared CZNC-PP films were studied. Structural characterizations of the nanocomposites were also carried by FTIR and XRD analysis.

Prepared CZNC were successfully coated onto films since substrate PP was a corona treated film for good adhesion of zein coatings. Depending on the nanofiller concentration, different film thicknesses in the CZNC layer were observed and tabulated in Table 6.1. According to thickness calculations, no direct relationship between nanofiller content and CZNC coatings thickness was observed. But it should be noted, thicker coatings were obtained for NF116 and CLO10A(Stir) samples. Tabulated film thicknesses were used in the evaluation of mechanical properties, oxygen and water vapor permeability analysis.

Table 6.1. The measured thicknesses of CZNC coated PP films and single CZNC coatings according to nanoclay content and type

Sample Code	OMMT Concentration (%wt)	Coated Film Thickness (µm)	Coating Thickness (µm)
PP	-	40	
PPZ	-	46±0.89	6±0.89
CLO10A-1%	1	46.8±1.17	6.8±1.17
CLO10A-3%	3	46.8±0.75	6.7±0.75
CLO10A-5%	5	45.9±0.66	5.9±0.66
CLO10A-7.5%	7.5	47.6±0.80	7.6±0.80
NF116-1%	1	47.68±0.62	7.68±0.62
NF116-3%	3	47.16±0.69	7.16±0.69
NF116-5%	5	48.34±0.76	8.34±0.76
CLO10A(Stir)-3%	3	50.46±0.97	10.46±0.97
CLO10A(Stir)-5%	5	49.76±1.63	9.76±1.63

6.1. Structural Characterization

Structural characterization of prepared corn zein nanocomposite coated polypropylene films were done in order to understand the effect of CZNC structure on the performance of films. Nanocomposite structure of the CZNC layers were done by using X-Ray Diffraction (XRD) and Fourier Transform Infrared (FTIR) analysis.

X-Ray diffraction is the most commonly used technique to investigate nanocomposite structures. Depending on the shape, intensity and position of <001> diffraction of layered silicate nanoclays, some idea about the structure of nanocomposites can be obtained. Peak shifts to lower angles and broader peaks are attributed to intercalated or exfoliated structures depending on the level of changes in the XRD chromatograms. Depending on the clay type, XRD analysis can be conducted down to 1 or lower theta values in order to achieve proper characterization of nanocomposites.

Characteristic (001) peak of Cloisite 10A nanoclay powder was obtained at 4.65 theta value indicating a basal spacing of 19.02Å. Position of characteristic Cloisite 10A peak was in agreement with the value reported by the producer. XRD analyses of the CZNC-PP films were suitable to investigate nanocomposite structure in CZNC layers,

since substrate PP films and corn zein matrix of nanocomposite layers gave no reflection in the analyzed range. XRD results of CZNC-PP films were given in Figure 6.1. Primary reflection of Cloisite 10A was disappeared after dispersion of nanoparticles within corn zein matrix for all samples as it is seen in the XRD results.
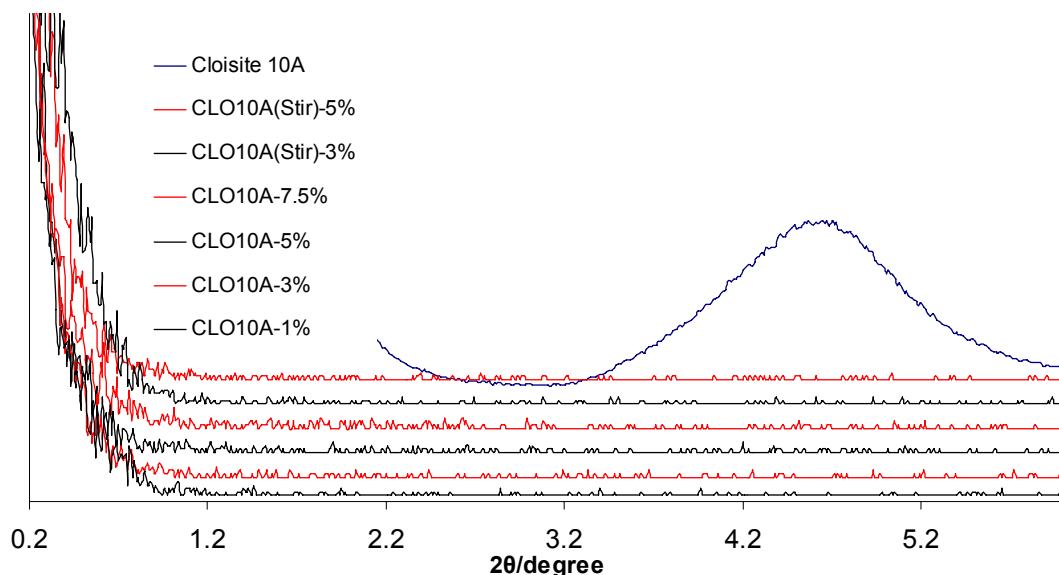
Figure 6.1. XRD results of Cloisite 10A nanoclay and CZNC coated PP films. Order of samples from top to bottom follows the order given in the legend of the plot

In the literature, disappearance of layered silicate peak is attributed to complete exfoliation of nanoclays in the polymer matrix. In the complete exfoliated state of nanocomposites, single layered silicate platelets are dispersed in the polymer matrix at several directions and far from each other beyond the detection limit of XRD. (Pavlidou and Papaspyrides 2008; Yu et al., 2007; Chen and Zhang, 2006; Okamoto, 2005). As can be seen from the XRD results of CZNC-PP films, characteristic peak of nanoclay was disappeared for all clay concentrations. Even high layered silicate content of 7.5% and samples prepared without sonication seem to achieve complete exfoliation which is inconsistent with the previous studies in the literature. Many biopolymers showed partially exfoliated or intercalated nanocomposite structures for concentrations higher than 5 wt% (Tang et al., 2008; Rao, 2007; Kvien et al., 2007; Ray et al., 2003). Mechanical stirring forces such as stirring and homogenization was also shown to be ineffective for delamination of layered silicates resulting in phase separated or partially intercalated structures (Bae et al., 2009; Dean and Yu, 2005).

In the existence of literature findings, for higher concentrations of Cloisite 10A, intercalated structures that can be identified by small shift of main nanoclay peak to lower angles and quite broader peak were expected due to FTIR and permeability results. In addition, for the samples prepared by stirring instead of sonication treatments; no change in the <001> peak except a slight decrease in peak intensity was expected. There might be several reasons for the improper XRD results. XRD is strongly dependent to amount of filler content and orientation of fillers in the structure (Ijdo et al., 2006). Besides, the thickness of the nanofiller containing CZNC layers was very low compared to 40μm PP film, that lead to very small nanoclay contents to be detected in the analyzed samples.

6.1.2. Fourier Transform Infrared (FTIR) Analysis

Structural changes occurred due to exfoliation/intercalation of layered silicate nanoplatelets can also be followed by FTIR analysis. Composite systems include dispersion of filler materials in the polymer matrix and definitely these particles interact with the matrix. Bonding of filler with the polymer matrix can be followed from the appearance of new bands in the FTIR spectra. Since nanofillers in the nanocomposite systems have stronger interactions with the polymer matrix compared to conventional composites, FTIR can be used in combination with XRD to examine nanocomposite structures.

CZNC-PP films were analyzed qualitatively by using FTIR-ATR from the CZNC coated side of the films. Since CZNC-PP films could not be grinded to prepare pellets with KBr, quantitative analysis could not be made on samples. FTIR spectra of Cloisite 10A nanoclay were also obtained in order to interpret the changes in nanocomposite system. Qualitative FTIR discussions were done in 850-1150 cm^{-1} and in 1450-1800 cm^{-1} regions where significant changes were observed (Figure 6.2 and Figure 6.4 respectively).

The most representative changes in FTIR spectra of CZNC layers were observed in 850-1150 cm^{-1} region. As can be seen in Figure 6.3, Cloisite 10A nanoclay has a single broad band at this interval, but corn zein does not have any peak in this region. Even small concentrations of nanoclay leads to arising of a small band at around wave number of 1040 cm^{-1} that is generally assigned to in-plane Si-O bands (bonds oriented

parallel to clay layer) (Yu et al., 2007; Ijdo et al., 2006; Chen et al., 2001). Layered silicates, in their clay powder form, give a large band in the region 750-1350 cm^{-1} as seen in Figure 6.3, consisting of several Si-O-Si bands overlapping with each other depending on the clay type and origin (Cervantes-Uc et al., 2007; Madejova, 2003; Johnston and Premachandra, 2001). Opening of layered silicate galleries leads to appearance of new Si-O bands (Ijdo et al., 2006; Johnston and Premachandra, 2001). Existence of several Si-O bands can be more easily seen in CLO10A-5% spectra due to the increase in the nanoclay content. Another in plane Si-O band at 1122 cm^{-1} with a small shoulder was observed Figures 6.2 and 6.3. A new band at 1023.43 cm^{-1} was observed in CLO10A-7.5% coated films which could be attributed to a new Si related bond due to changing structure with increasing organomodified nanoclay (Ijdo et al., 2006; Johnston and Premachandra, 2001).
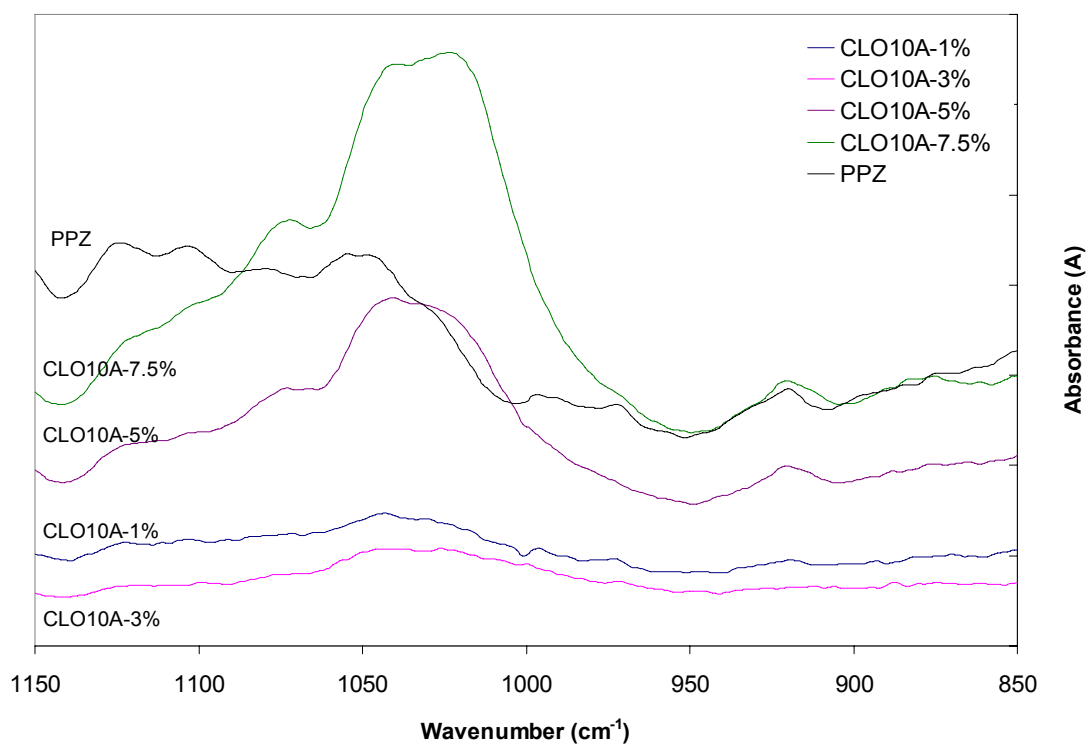
Figure 6.2. FTIR-ATR spectra of prepared CZNC-PP films in 850-1150 cm^{-1} region
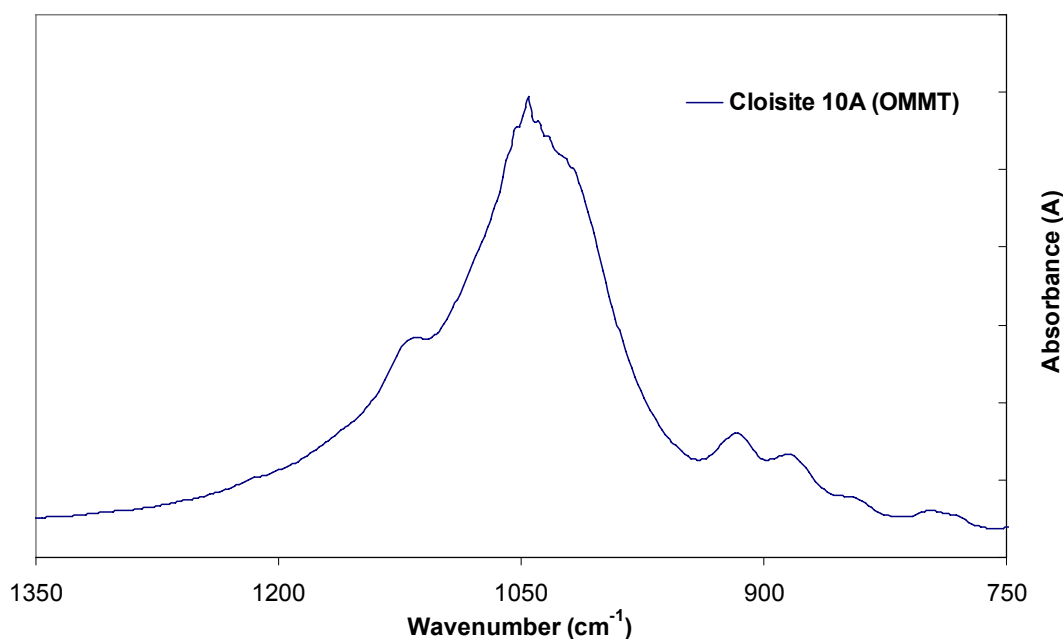
Figure 6.3. FTIR spectra of Cloisite 10A nanoclay in 750-1350 cm^{-1}

Powder FTIR patterns of packed layered silicate platelets only gave in-plane Si-O bands overlapping with each other. However, a new band appeared at the wave number of 1072 cm^{-1} for the nanocomposite coatings (Figure 6.2). The new arising band was assigned to out-of-plane Si-O bonding (bonds oriented normal to clay layer). Several nanocomposite studies reported appearance of such bands, attributed to opening of clay galleries and fine dispersion (exfoliation or partial exfoliation) of clay platelets (Yu et al., 2007; Ijdo et al., 2006; Johnston and Premachandra, 2001). Ijdo and coworkers (2006) studied organoclay delamination in solutions and LDPE nanocomposites using FTIR-ATR in their patented study. Beside appearance of new out-of-plane band, they also reported bandwidth narrowing in 850-1150 cm^{-1} region due to transition to more exfoliated state (Ijdo et al., 2006). Prepared CZNC coatings showed narrower bands for smaller clay contents, especially for very slight bands of 1 wt% and 3 wt% clay loaded samples as seen in Figure 6.2. Additional to discussed new bands at 850-1150 cm^{-1} region, two new organomodified nanoclay bands were appeared in the FTIR spectra of CZNC coatings at 522.73 cm^{-1} and 462.93 cm^{-1} wave numbers assigned to Al-O stretching and Si-O bending (Chen et al., 2001). Similar to nanoclay bands of 850-1150 cm^{-1} region, the bands of Al-O and Si-O became broader with increasing OMMT content. Positions and assignments of all FTIR bands observed for prepared CZNC were given in Table 6.2 together.

Table 6.2. Positions and assignments of characteristic bands of CZNC-PP films, corn zein and Cloisite 10A nanoclays

Sample	Wavenumber (cm-1)	Assignment
Cloisite 10A		
Si-O-Si Bands	1040	in-plane Si-O stretching
	1122	in-plane Si-O stretching
	1023.43	in-plane Si-O stretching
	1072	out-of-plane Si-O stretching
	522.73	Al-O stretching
	462.93	Si-O bending
Corn Zein		
	1637.49 - 1645.57	Amide I region (C=O stretching)
	1528.47 - 1531	Amide II region (N-H bending and C-N Stretching)

Significant bands at 1528.47cm^{-1} and 1637.49cm^{-1} in FTIR-ATR spectra of pristine corn zein can be seen in Figure 6.4. These bands were attributed to Amide II and Amide I bands of corn zein, respectively. Amide I and amide II regions are generally used to follow hydrogen bonding in corn zein. Contribution of plasticizers and water molecules to amide regions were also reported in the literature. (Gillgren et al., 2009; Gao et al., 2006) While Amide II region of nanocomposites showed wavenumber shift to 1531 cm^{-1} in CLO10A-5% sample and no change for CLO10A-7.5%; effect of organomodified nanoclay was more significant in the Amide I region. Although position of Amide I bands of CLO10A-1% and CLO10A-3% did not change significantly as seen in Figure 6.4, appearance of several smaller bands can be attributed to a possible exfoliation of nanoclays in the corn zein matrix. Since nanoclays could be oriented in several directions for exfoliated state, they might form several different hydrogen bands with corn zein matrix. Effect and degree nanoclay delamination and dispersion on the formation of H-bonding can be more significantly followed for higher clay content CZNC coatings. Amide I band of corn zein (1637.49cm^{-1}) shifted to higher wavenumbers; 1643.05cm^{-1} and 1645.57cm^{-1} for CLO10A-7.5% and CLO10A-5% coatings, respectively. Shifting of Amide I and Amide II bands to higher wavelength can be attributed to increased hydrogen bonding (Cervantes-Uc et al., 2007; Gao et al., 2006; Madejova, 2003).

C=O containing molecules of protein based biopolymers are able to form hydrogen bonding with the Si-O-Si and –OH containing galleries of MMT particles that may result in shifting of Amide bands to higher wave numbers (Yu et al., 2007; Chen and Zhang, 2006). As nanoclay delamination and the number of orientations due to effective dispersion increases, more bonding sites on nanoclay galleries will be able to form new hydrogen bonds. Based on the band shiftings in Amide I and Amide II regions, the level of hydrogen bonding was higher for 5 wt% clay loaded samples compared to 7.5 wt%. This could be attributed to more efficient dispersion of nanoclays in 5 wt% samples.
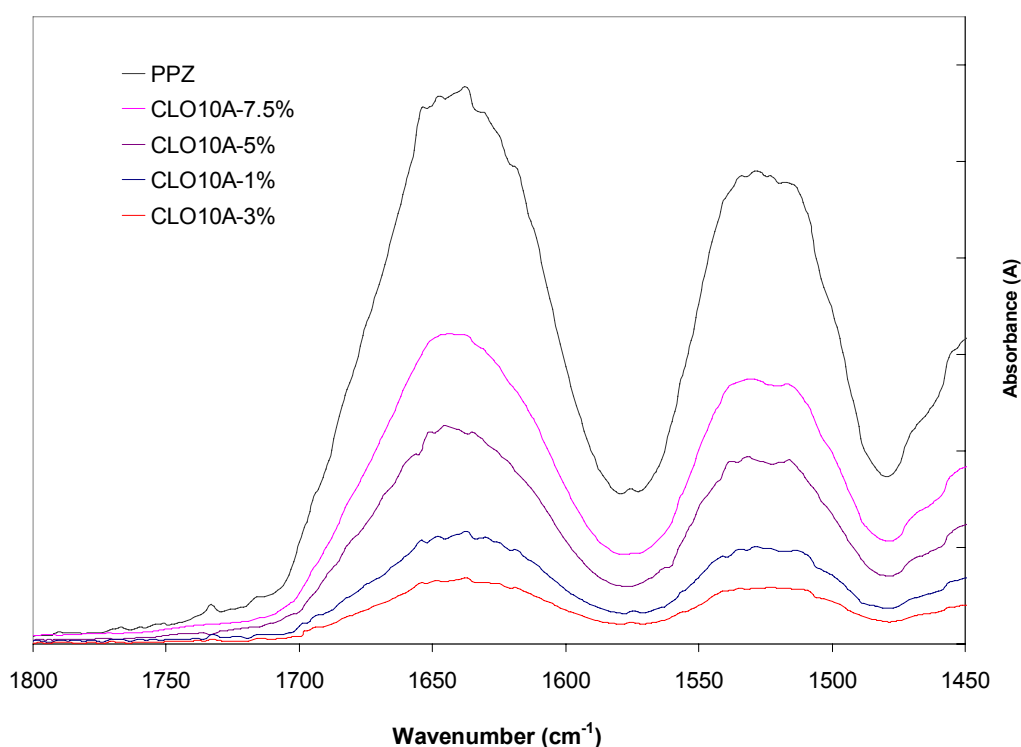
Figure 6.4. FTIR-ATR spectra of prepared CZNC-PP films in 1450-1800 cm^{-1} region. Order of samples from top to bottom follows the order given in the legend of the plot.

6.2. Barrier Properties of Corn Zein Nanocomposite Coated Films

Barrier properties of packaging materials are critical since aim of packaging is to preserve the quality of food during storage period before the end use by the customer. Ability to restrict oxygen and water vapor permeation is, therefore, important to develop

efficient barrier packaging materials. This section deals with the evaluation of oxygen and water vapor properties of prepared CZNC-PP coatings. Effect of nanoclay type and its content, as well as preparation technique of CZNC was studied in order to investigate the barrier performance of corn zein nanocomposites.

6.2.1 Oxygen Barrier Properties

Oxygen transmissions of the uncoated and coated PP films were tabulated in the Table 6.3. As seen in the table; oxygen transmission through the films was successfully reduced by coating corn zein and its nanocomposites on PP substrate.

Table 6.3. Oxygen transmission rates (OTR) of Cloisite 10A loaded CZNC coated PP films and single CZNC layers

Sample Code	Nanoclay Concentration (%wt)	OTR of CZNC-PP films (ml/m² day)	OTR of CZNC Layers (ml/m² day)
PP	-	1627.85±311.90	-
PPZ	-	605.3±49.92	131.89
CLO10A-1%	1	549.32±5.54	108.12
CLO10A-3%	3	346.38±26.63	60.22
CLO10A-5%	5	370.78±12.98	46.94
CLO10A-7.5%	7.5	403.48±81.99	57.69

Oxygen barrier performances of prepared coatings were analyzed at 23 ^{o}C and 0% RH. Oxygen barrier improvements obtained by the CZNC coatings on PP substrates were also reported as a function of nanoclay concentration in Figure 6.5. Excellent oxygen barrier of corn zein and other plant based polysaccharide and protein polymers due to the presence of polar interactions in their structure were discussed by many authors (Rhim et al., 2006; Hong and Krochta, 2003;2006; Tharanathan, 2003; Padua and Wang, 2002). As seen in the Figure 6.5, a thin layer of corn zein coating without nanoclays on substrate PP film resulted in 56% decrease in oxygen transmission through the film. Such result was expected since oxygen permeability of corn zein is significantly lower than polyolefins such as PP and PE; being comparable to well known oxygen barriers EVOH and PVDC (Tihminlioglu et al., 2010; Padua and Wang,

2002; Miller and Krochta, 1997; Cuq et al., 1998). Oxygen transmission rate of single corn zein layer was calculated by using Equation (5.1) and found as 131.89 ml/m^2 day. This value is 12 fold lower than that of PP film (1627.85 ml/m^2 day) being in consistent with the literature data. In conformance with the prepared CZNC-PP films, several studies showed significant decreases in oxygen transmission with corn zein (Tihminlioglu et al., 2010) and whey protein isolate (Hong and Krochta, 2003;2006) coatings on polyolefins. Further improvements in oxygen barrier were also obtained by the CZNC coatings on PP as seen in Figure 6.5. The maximum improvement, which is almost 75 %, was obtained for 3 wt% nanoclay loaded samples. The OTR decreased from 1627.85 ml/m^2 day to 346.38 ml/m^2 day Since no nanocomposite structure exists in substrate films, it is obligatory to investigate the effect of nanocomposite structure on oxygen transmission for single CZNC layers.
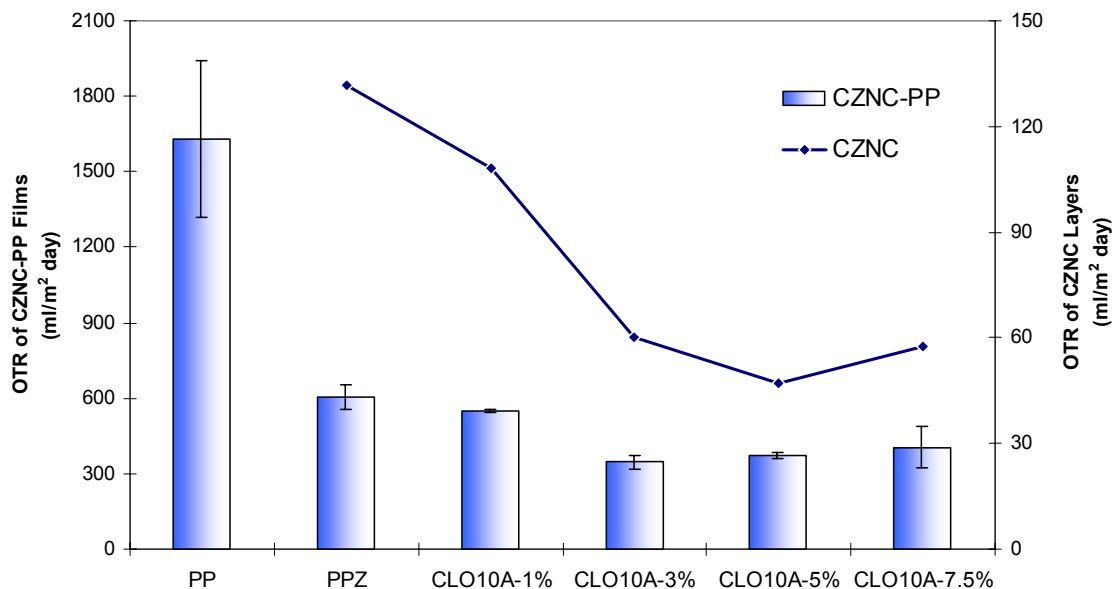
Figure 6.5. Oxygen transmission rate (OTR) values of CZNC-PP films (in columns - left y-axis) and single CZNC layers (curve – right y-axis)

Oxygen transmission rates (OTR) of CZNC layers were calculated OTR and tabulated in Table 6.3. Figure 6.5 also illustrates the OTR results of CZNC single layers together with CZNC-PP film. As evidenced from the Figure 6.5, the addition of even small amount of Cloisite 10A into corn zein decreased the oxygen transmission rate. OTR of CZNC layers decreased by 56% and 65% at 3 wt% and 5 wt% Cloisite 10A loaded corn zein coatings, respectively. Increased oxygen barrier of the CZNC layers

can be interpreted as a result of efficient delamination of nanoclays within the corn zein matrix. Improved barrier of LSNC systems are mainly attributed to the formation of more tortuous path developed by the well dispersed (partial or totally exfoliated) nanoclay platelets within the polymer matrix (Choudalakis and Gotsis, 2009; Bae et al., 2009; Paul and Robeson, 2008; Yu et al., 2007; Lape et al., 2006). Impermeable layered silicate platelets interrupt the movement of permeating gas or water vapor molecules and force the molecules to change their direction, resulting in longer permeation path to be followed (Nielsen, 1967; Bharadwaj, 2001).

Continuous decreases in oxygen transmission rates were observed for coated CZNC layers up to 5 wt% nanoclay content. This result can be attributed to effective dispersion of layered silicates in corn zein matrix. However, the CZNC layer containing 7.5 wt% Cloisite 10A showed an increase in oxygen transmission rate although nanoclay content was 50% higher. Layered silicates are more capable of reducing permeation through the film since their aspect ratio (length to thickness ratio) is very high compared to conventional fillers. (Choudalakis and Gotsis, 2009; Nielsen, 1967). At this point, effective aspect ratio must be considered for interpretation of permeability in nanocomposites since agglomeration of layered silicate platelets reduces the effective aspect ratio and length of the diffusion path must be travelled by the permeant.

Generally, a critical limit of layered silicate content was reported by many authors, due to the changes in nanostructure after certain nanoclay loadings. Decreased efficiency in barrier improvements could be observed because of the decrease tortuousity due to the poorer dispersion of layered silicate in the polymer matrix (Luecha et al., 2010; Herrera-Alonso et al., 2009; Tunc et al., 2007). In this study, the increase in the oxygen transmission rate of CLO10A-7.5% sample can be explained by the poorer delamination or agglomerations of nanoclays in the polymer matrix. The marginal effectiveness of nanoclay addition was reduced for the CLO10A-7.5% sample, even though the oxygen transmission is still significantly lower than the pristine corn zein layer.

6.2.2. Water Vapor Barrier Properties

Polypropylene; being an excellent barrier to water vapor is readily used in many packaging applications. CZNC layers applied on PP substrate also contributed to water

vapor barrier of prepared CZNC-PP films. In order to investigate the barrier performance of nanocomposite coatings, water vapor permeability (WVP) of prepared CZNC-PP films were investigated.

Although biopolymers does not have strong barrier to water vapor, their coatings can be utilized to decrease WVP of synthetic polymers additional to oxygen barrier improvements. Tihminlioglu and coworkers (2010) studied effect of corn zein coating formulations on WVP of corn zein coated polypropylene films. Although corn zein is not a known water vapor barrier, noticeable decreases in WVP of films coated with a thin layer of corn zein was reported (Tıhmınlıoğlu et al., 2010). Corn zein nanocomposite layers coated on PP substrate films also improved barrier to water vapor in our study. Water vapor permeability changes due to the existence of coated corn zein nanocomposites on PP films were presented in Figure 6.6. Compared to intense effect of CZNC coatings on oxygen transmission rates of coated films, water vapor barrier improvements were less significant. While OTR of corn zein was found to be 12 times smaller than PP, WVP analysis showed that PP and pristine corn zein layer had similar water vapor permeability, 6.62×10^{-2} g mm/m day mmHg for PP and 3.78×10^{-2} g mm/m day mmHg for corn zein. Nanocomposite coatings on PP also showed further improvement as well. 30% decrease in the WVP of CZNC-PP was achieved compared to substrate PP film for CLO10A-5% coated sample. Water vapor permeability results of CZNC coated PP films were tabulated in Table 6.4.

Table 6.4. Water vapor permeability (WVP) results of CZNC-PP films prepared by different nanoclays and processing technique

Sample Code	Nanoclay Concentration (%wt)	WVP of CZNC-PP films ($*10^{-2}$ g mm / m^2 day mmHg)	WVP of CZNC Layers ($*10^{-2}$ g mm / m^2 day mmHg)
PP	-	6.62±0.21	-
PPZ	-	6.02±0.29	3.78
CLO10A-1%	1	5.39±0.15	2.58
CLO10A-3%	3	4.96±0.14	1.99
CLO10A-5%	5	4.57±0.14	1.48
CLO10A-7.5%	7.5	4.91±0.09	2.08
NF116-1%	1	5.55±0.39	3.02
NF116-3%	3	5.62±0.09	3.06
NF116-5%	5	5.31±0.1	2.74
CLO10A(Stir)-3%	3	5.51±0.07	3.36
CLO10A(Stir)-5%	5	5.41±0.31	3.09

Figure 6.6. Water vapor permeability (WVP) values of CZNC-PP films (in columns – left y-axis) and single CZNC layers (curve – right y-axis)

Since thicknesses of CZNC layers on PP films are not the same, again single CZNC layer permeabilities were calculated from the multilayer model using the measured thicknesses. Calculated single layer permeabilities were also plotted in Figure 6.6. Comparably to the oxygen permeability plot, WVP of nanocomposite coating layers also showed distinctive decrease by increasing nanoclay content. 60% decrease for the WVP of single corn zein layers was achieved at 5 wt%, CLO10A-5% as seen in Figure 6.6. Improvements achieved in the water vapor barrier of synthetic and biopolymers by using layered silicates were reviewed by many authors in the literature (Paul and Robeson, 2008; Ray and Bousmina, 2005; Alexandre and Dubois, 2000).

As in the case of oxygen permeability, efficient dispersion of layered silicates within the polymer matrix form more tortuous path for travelling water molecules. Several studies reported decreases in the water vapor permeability for plant based biopolymer nanocomposites prepared by montmorillonite (MMT) and other layered silicates (Bae et al., 2009; Tang et al., 2008; Tunc et al., 2007). An increase in WVP was observed for CLO10A-7.5% sample which is in agreement with the oxgen transmission results that could be attributed to more intercalated rather than exfoliated character of corn zein nanocomposite layer.

Compatibility of layered silicate and polymer matrix is determining for effective dispersion of particles in a nanocomposite. Layered silicates are only compatible with

hydrophilic polymers in their natural form. In order to increase the compatibility of layered silicates with hydrophobic polymers, layered silicates are organomodified with several compounds. Since corn zein has hydrophobic character, organomodification of nanoclays is critical. In order to investigate the effect of organomodification on the permeability properties of nanocomposites, CZNC layers were also prepared by using unmodified nanoclays, Nanofil 116, and coated on to the PP films. WVP values of films coated with Nanofil116 incorporated CZNC were given in Table 6.5 together with modified clay, Cloisite 10A, incorporated samples for comparison.

Table 6.5. WVP results of CZNC-PP films prepared by using modified Cloisite 10A and unmodified Nanofil 116 nanoclays

Sample Code	Nanoclay Concentration (%wt)	WVP of CZNC-PP films (*10^{-2} g mm / m^2 day mmHg)	WVP of CZNC Layers (*10^{-2} g mm / m^2 day mmHg)
PPZ	-	6.02±0.29	3.78
CLO10A-1%	1	5.39±0.15	2.58
CLO10A-3%	3	4.96±0.14	1.99
CLO10A-5%	5	4.57±0.14	1.48
NF116-1%	1	5.55±0.39	3.02
NF116-3%	3	5.62±0.09	3.06
NF116-5%	5	5.31±0.1	2.74

CZNC layers prepared by using unmodified Nanofil 116 nanoclays exhibited lower barrier improvements compared to modified nanoclay samples. WVP of NF116 samples were 15-30% higher than CLO10A samples. This is due to the incompatibility problem between layered silicate and corn zein polymer matrix that was reported by several authors for different polymer-layered silicate systems (Herrera-Alonso et al., 2009; Magalhaes and Andrade, 2009; Tang et al., 2008).

Effect of processing on WVP of coated films was also investigated. As it is seen in Table 6.6, CZNC layers prepared by employing stirring instead of sonication exhibited very low improvements in water vapor barrier. Lower performance of stirring samples can be attributed to ineffective entering of zein chains between nanoclay platelets because of low mechanical forces exerted to the system. The WVP decrease seems to be only due to the existence of impermeable clay platelets rather than tortuosity formed by dispersed layered silicates. This situation is more evident when 5% samples are compared. Although both CLO10A and CLO10A(Stir) samples have same

content and type of nanoclays in corn zein matrix, permeation of water molecules in the stirred samples is 2 times more than sonicated samples.

Table 6.6. WVP results of CZNC-PP films prepared by different techniques. While CZNC layer of CLO10A and NF116 films were prepared by using sonication, CLO10A(Stir) samples were prepared by stirring only

Sample Code	Nanoclay Concentration (%wt)	WVP of CZNC-PP films ($*10^{-2}$ g mm / m^2 day mmHg)	WVP of CZNC Layers ($*10^{-2}$ g mm / m^2 day mmHg)
PPZ	-	6.02±0.29	3.78
CLO10A-3%	3	4.96±0.14	1.99
CLO10A-5%	5	4.57±0.14	1.48
NF116-3%	3	5.62±0.09	3.06
NF116-5%	5	5.31±0.1	2.74
CLO10A(Stir)-3%	3	5.51±0.07	3.36
CLO10A(Stir)-5%	5	5.41±0.31	3.09

6.2.3. Evaluation of Nanocomposite Performance on Oxygen and Water Vapor Barrier of Single CZNC layers

Effect of Cloisite 10A montmorillonite content on WVP is analogous with the oxygen transmission rate results of the CZNC layers. Oxygen and water vapor permeability trends were plotted relative to pristine corn zein coating layer for convenience in Figure 6.7 together. Depending on the degree of layered silicate nanoclay dispersion in the polymer matrix, permeability of water vapor decreased as in the case of oxygen due to the tortuous path formed for permeating water molecules. Decreasing oxygen and water vapor permeability due to tortuosity can also be explained by the employment of permeability models on coated corn zein nanocomposite layers.
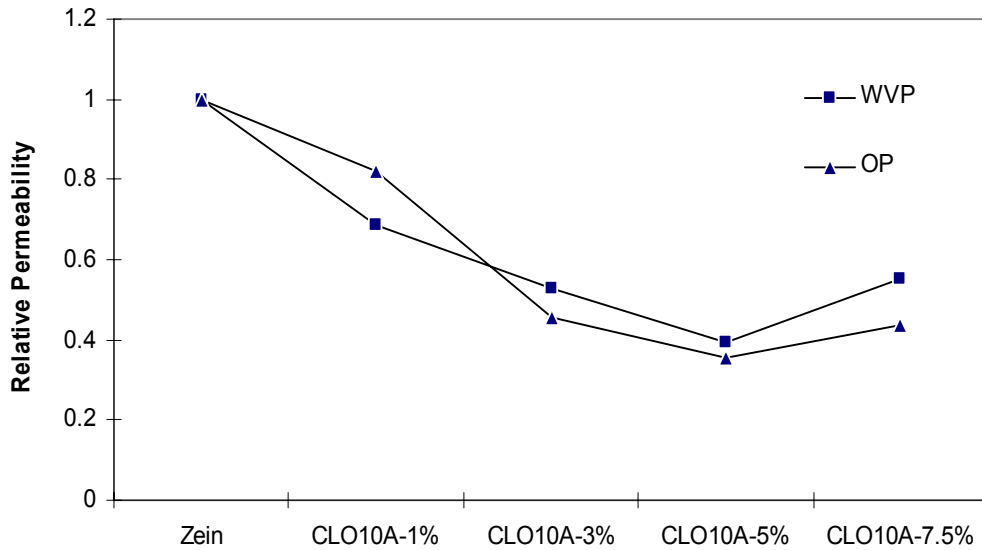
Figure 6.7. Oxygen and WVP values of CZNC layers relative to permeability of pristine corn zein layer

Several permeability models were developed to understand the effect of fillers on the permeability of molecules in composite structures. Permeability models differ in their assumptions and considered filler geometry. Models based on rectangular flakes can be applied to layered silicate nanocomposite systems. Although theoretical models were proposed for conventional microcomposites; tortuosity effect of conventional fillers and nanofillers are similar. (Choudalakis and Gotsis, 2009; Sun et al., 2008). Permeability models applied on prepared CZNC layers, and their basic assumptions were tabulated in Table 4.1. Although theoretical permeability models were developed to predict permeability of composite systems for considered aspect ratio of filler, they can also be used in reverse form to predict the average aspect ratio of fillers by using experimental permeability data. Figure 6.8 shows the relative water vapor permeability and oxygen permeability of the single CZNC layer as a function of volume fraction of nanoclay. Both water vapor and oxygen experimental permeability data were used for fitting of the models given in Table 4.1.

Figure 6.8. Permeability models fitted to experimental OTR and WVP data of Cloisite 10A samples. Aspect ratios found for best fitting models were also reported

As seen in Figure 6.8, the Nielsen Model (Nielsen, 1967) and Bharadwaj Model (S=0 case, random silicate platelet orientation included version of Nielsen Model) (Bharadwaj, 2001) gave the best fitting to experimental OTR and WVP data. Both Nielsen and Bharadwaj models gave aspect ratios around 94 and 283, respectively for OTR and WVP data , which is in good agreement with the reported aspect ratio range (10-1000) for layered silicates (Choudalakis and Gotsis, 2009; Ray and Bousmina, 2006). Bharadwaj model with S=1 gives the same aspect ratio with Nielsen model. S=0 case of Bharadwaj Equation generally results in higher aspect ratios for exfoliated systems since it considers different orientations of silicates resulting in theoretically possible shorter paths for permeants. While S=1 situation considers the longest path available for permeating molecules and gives same result with Nielsen Model since they both consider same nanoclay platelet alignments with same assumptions. Figure 6.9 illustrates schematic representations of S=1 and S=0 cases.

S = 1   S = 0
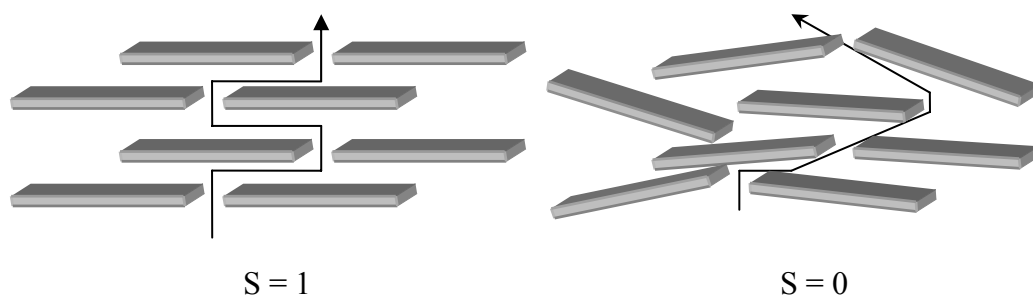
Figure 6.9. Schematic representations of S=1 (regular array, also same for Nielsen Model) and S=0 (random array) cases of Bharadwaj Model (Source: Bharadwaj, 2001)

WVP results of CZNC layers prepared by using unmodified Nanofil 116 were also investigated by using permeability models. Models fitted on experimental WVP data was given in Figure 6.10. Similar to modified Cloisite 10A nanoclay samples, again the best fitting models were Nielsen and random Bharadwaj (S=0) models. According to the models, the effective aspect ratio was estimated as 23 and 68, respectively from the Nielsen Model and Bharadwaj Model which is quite lower than modified Cloisite 10A loaded samples.
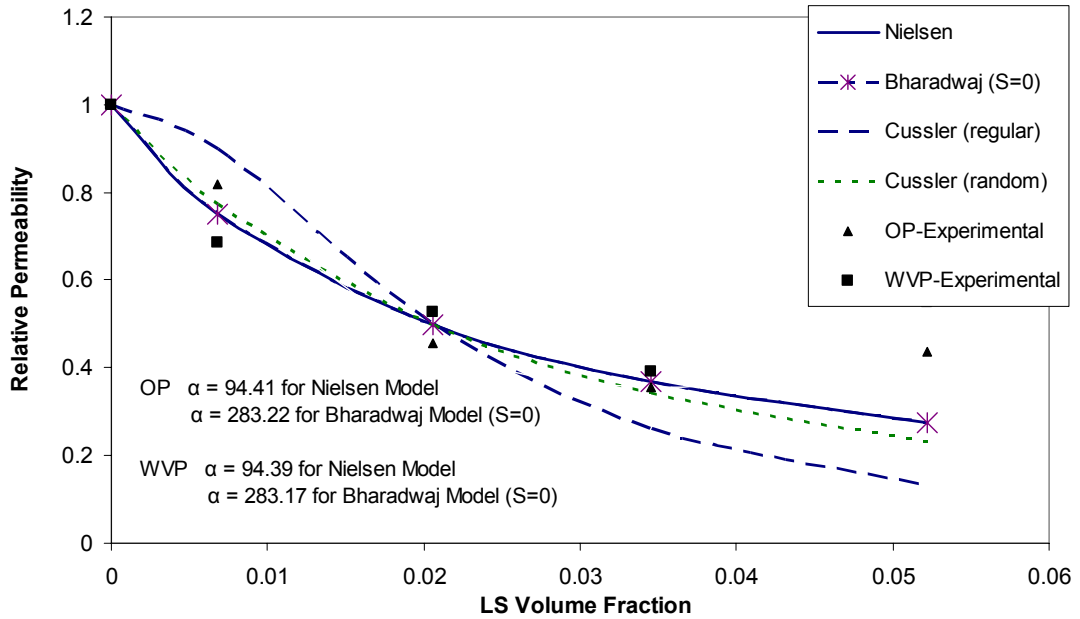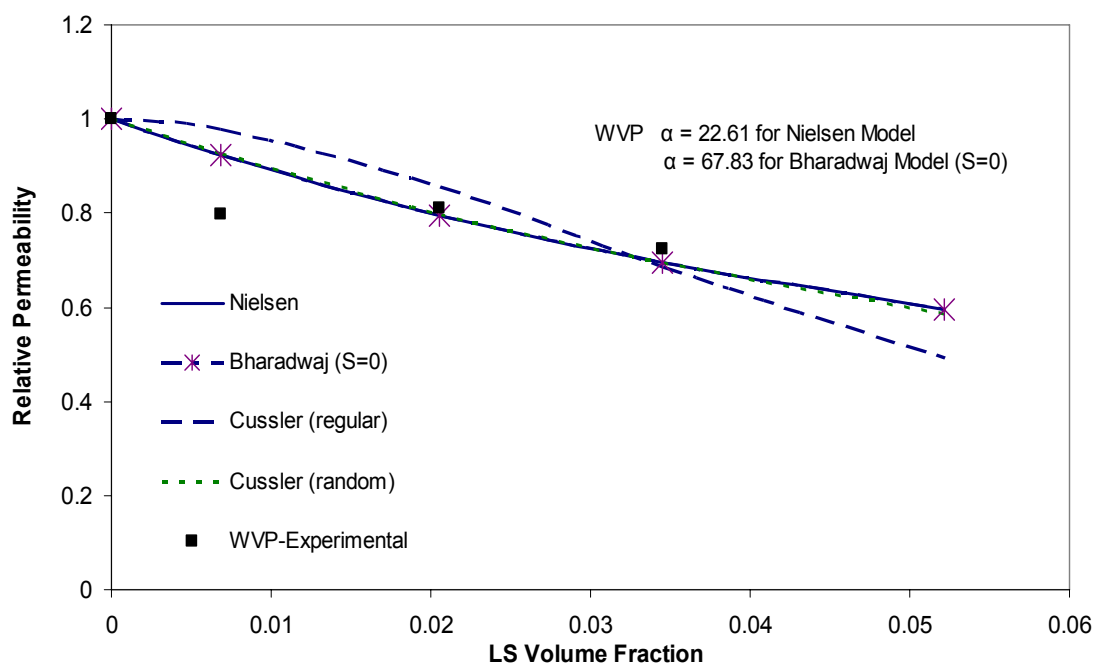

Figure 6.10. Permeability models fitted to experimental WVP data of Nanofil 116 samples. Aspect ratios found for best fitting models were also reported

Predicted effective aspect ratio could also be used to examine the delamination efficiency of layered silicates in the polymer nanocomposites. Layered silicate platelets are characterized by large aspect ratios in a broad range in their delaminated form (Paul and Robeson, 2008). Therefore, the higher calculated aspect ratio could be attributed to more exfoliated nanocomposite structures. But it must be emphasized that the applied models are only considering available area and/or effective path of permeating molecule. Enhanced interactions between clay and polymer matrix and crystallinity changes are not considered in these models.

6.3. Mechanical Properties

Mechanical properties of the corn zein nanocomposite coated polypropylene films were determined by tensile testing. Mechanical characteristics of plant based biopolymer coatings tend to rely strongly on the synthetic substrate of composite structure (Lee et al., 2008; Hong et al., 2004; 2005). In this study mechanical characteristics of prepared films were mainly coming from the polypropylene base film. However, tensile properties of PP films were observed to be significantly affected by the corn zein nanocomposite coatings. Sample stress – strain curves representing the effect of CZNC coating on polypropylene was given in Figure 6.11.
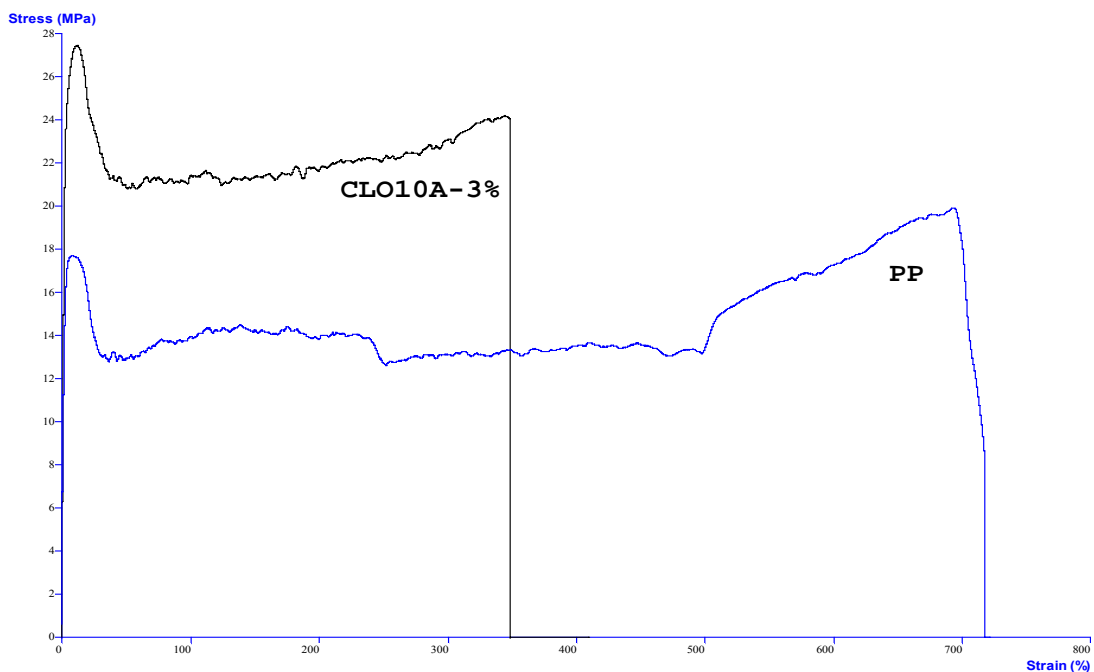
Figure 6.11. Sample stress-strain curves representing the effect of CZNC coating

The most significant changes were obtained in the elastic (Young's) modulus of CZNC-PP films. Elastic modulus is the measure of the required force to deform the film by a given amount of tension. It is also a measure of stiffness related with the rigidity of the film. As long as an acceptable level of elongation before breaking of the film is satisfied, high modulus (stiff) materials are desired in food packaging. Elastic modulus of prepared CZNC coated PP films were affected by the corn zein coatings at different extends depending on the nanoclay type and loading as well as preparation method. Elastic modulus of prepared CZNC-PP films evaluated from the stress-strain curves of tensile testing are tabulated in the Table 6.7 below.

Elastic modulus of the base film was unsurprisingly found to be enhanced by the corn zein coatings, since stiff but brittle CZNC layer on the PP surface acts like filler in composite structure. Improved stiffness of the films became more evident by the incorporation of Cloisite 10A as seen in Figure 6.12.

Table 6.7. Elastic modulus of the prepared CZNC-PP films

Sample	Nanoclay Content in CZNC Layer (%)	Elastic Modulus (*100 MPa)
PP	-	5.83±0.29
PPZ	-	8.21±0.48
CLO10A-1%	1	9.12±0.51
CLO10A-3%	3	10.27±0.31
CLO10A-5%	5	11.59±0.43
CLO10A-7.5%	7.5	10.54±0.38
NF116-5%	5	9.54±0.39
CLO10A(Stir)-3%	3	8.27±0.93
CLO10A(Stir)-5%	5	8.20±0.69
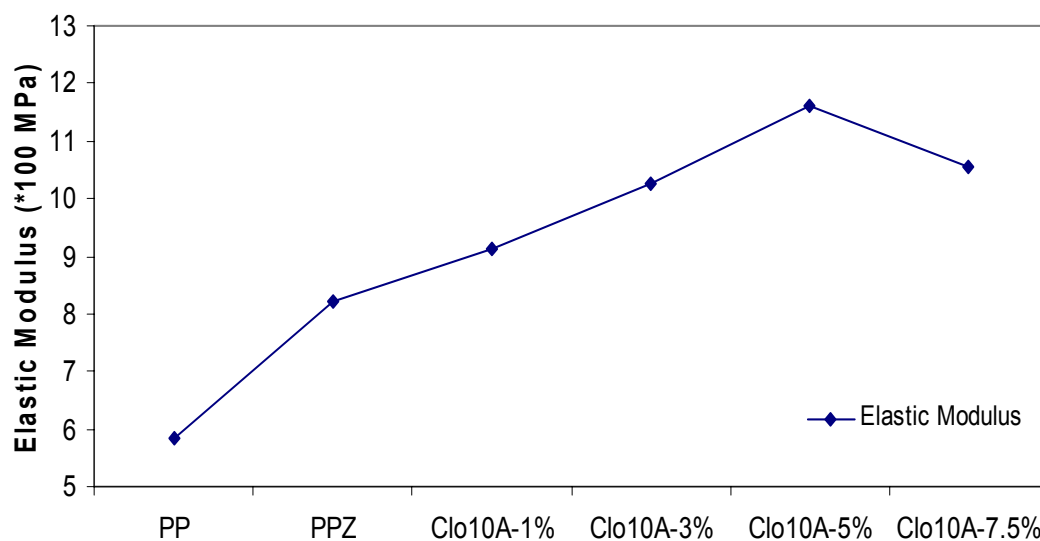
Figure 6.12. Elastic modulus of the base PP film and CZNC-PP films

Modulus of CZNC-PP films increased continuously up to 5 wt% Cloisite 10A content and then decreased for Clo10A-7.5% samples. As in the case of conventional composites, layered silicate nanocomposites moduli also exhibits strong increases due to fine dispersion of mechanically strong clay (Ray and Bousmina, 2006; Alexandre and Dubois, 2000). Beside existence of high moduli nanoclay, strong interactions due to higher aspect ratio of nanoclays thought to be playing an important role on improved stiffness in nanocomposites compared to conventional composite structures (Pavlidou and Papaspyrides, 2008; Paul and Robeson, 2008; Petersson and Oksman, 2006; Alexandre and Dubois, 2000). Moreover improved stiffness and durability, more brittle character of various nanocomposite systems was also reviewed by Pavlidou and Papaspyrides (2008) in detail. In our study,5 wt% Cloisite 10A loading can be accepted as the optimum clay concentration where interactions between zein matrix and nanoclays were maximum; doubling the elastic modulus of base PP film. Nanoclay content above 5 wt% resulted in decreased reinforcement, as it was also in good agreement with the barrier properties of prepared films. Degree of reinforcement can be attributed to the changes in intermolecular forces due to exfoliation/intercalation of layered silicates within the corn zein matrix. Decreased marginal or overall efficiency of reinforcing after a critical limit was reported in several protein based nanocomposites (Yu et al., 2007; Huang and Netravali, 2006; Chen and Zhang, 2006).

Reinforcement effect of CZNC layers on CZNC-PP films were differed by the compatibility of nanoclays within the corn zein matrix and preparation method. Elastic modulus of CZNC-PP films containing 5 wt% nanoclay samples were compared and tabulated in Table 6.8. Similar to WVP results, better compatibility of organomodified Cloisite 10A was resulted in higher modulus improvement compared to unmodified Nanofil 116 montmorillonites. Effectiveness of sonication for the preparation of CZNC layers of coated films was again evident. While sonicated Cloisite 10A sample successfully increased modulus about 40% compared to pristine zein coated film; modulus of stirring sample was nearly the same with the zein coated film.

Table 6.8. Elastic modulus of CZNC-PP films containing 5 wt% nanoclay

Sample	Nanoclay Content in CZNC Layer (%)	Elastic Modulus (*100 MPa)
PPZ	-	8.21±0.48
CLO10A-5%	5	11.59±0.43
NF116-5%	5	9.54±0.39
CLO10A(Stir)-5%	5	8.2±0.69

Corn zein has different mechanical characteristics compared to polyolefins. Corn zein is a brittle biopolymer, breaking up before plastic deformation without yielding (Selling and Sessa, 2007; Lawton, 2004; Gennadios, 2002). CZNC-PP films exhibited yielding that is inherent to substrate PP. Brittle character of corn zein did not alter the yielding point of PP films. Moreover, the addition of nanoclay into corn zein increased yielding strength of the coated films depending on the nanoclay used and preparation method. Yield strength of CZNC-PP films were tabulated in Table 6.9. Improvements in yielding strength can be followed from the Figure 6.13 for Cloisite 10A loaded samples. Coated CZNC layers improved the mechanical durability of the base PP films. While the yielding strength of corn zein coated films were about 25MPa, modified montmorillonite loaded CZNC layers delayed yielding of coated films to 30.9MPa for CLO10A-7.5% films.

Table 6.9. Yield strength of the CZNC-PP films

Sample	Nanoclay Content in CZNC Layer (%)	Yield Strength (MPa)
PP	-	17.51±0.35
PPZ	-	24.68±0.79
CLO10A-1%	1	28.09±1.18
CLO10A-3%	3	27.91±1.15
CLO10A-5%	5	30.17±0.86
CLO10A-7.5%	7.5	30.87±0.96
NF116-5%	5	26.92±1.96
CLO10A(Stir)-3%	3	24.68±0.32
CLO10A(Stir)-5%	5	25.28±1.36
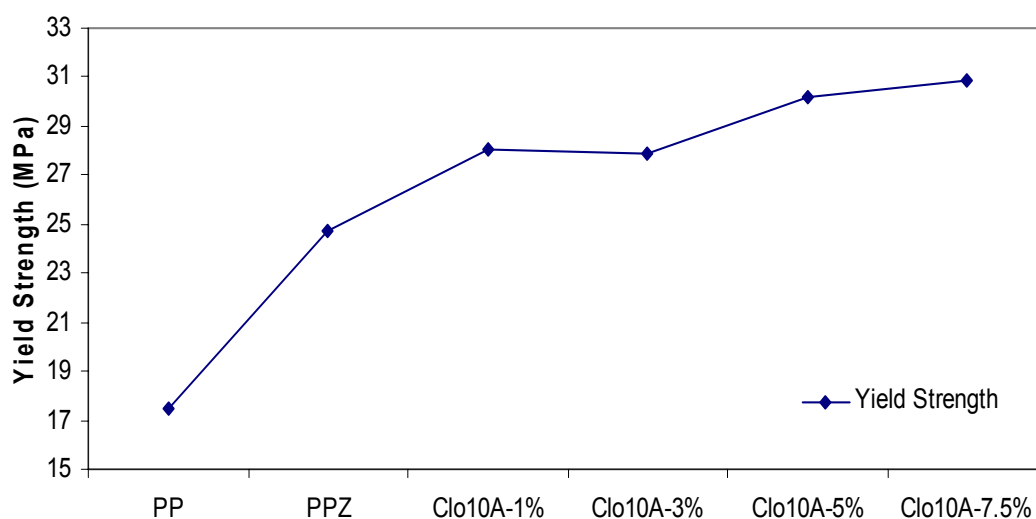
Figure 6.13. Yield Strength results of the base PP film CZNC coated PP films

Since corn zein is a weak and brittle polymer compared to PP with lower tensile strength and flexibility; separation of zein coatings was expected for higher strain values. It was observed that, corn zein and nanocomposite coatings were loosing their mechanical integrity around yielding point of coated films although PP substrate was continuing to elongate. Though zein coating layer was broken around yielding, coating layer adhered on PP substrate. Breaking of the coatings was changed depending on the clay content in the CZNC coatings. While pristine corn zein and CLO10A-1% samples were breaking homogeneously from several points throughout the surface of the film,

samples containing 3 – 7.5 wt% clay resulted in a couple or single breaking points (Figure 6.14). Change in breaking characteristics of CZNC coatings could be attributed to increased strong interactions between organomodified Cloisite 10A and zein matrix with increasing clay concentration as it was also evidenced from FTIR results.
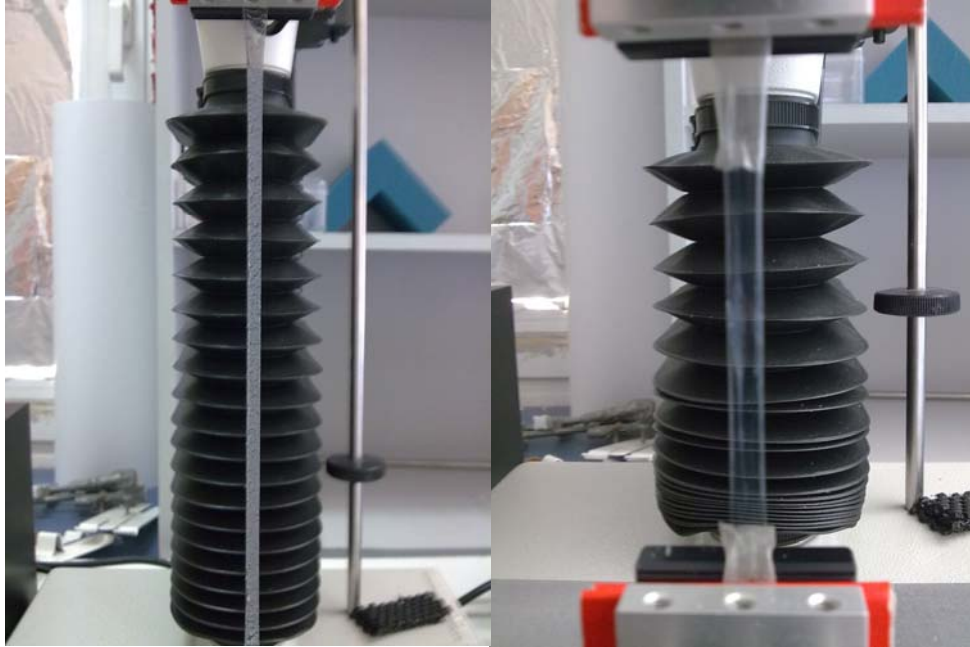
Figure 6.14. Breaking of the CZNC layers after yielding. Photo on the left shows the homogeneous breaking of CZNC layers from several points before breaking of CLO10A-1% film. Photo on the right shows the breaking of CZNC layer after yielding for CLO10A-5%.

Effect of stronger CZNC layers on yield strength of CZNC-PP films is obvious as it can be followed from Table 6.9. Stronger H-bonding between layered silicates and corn zein chains results in durable CZNC layers. Effect of processing and organomodification on the yield strength and elongation at break values of CZNC-PP films containing 5 wt% clay were investigated and compared in Tables 6.10 and 6.11. Level of improvement in yield strength was significantly higher for organomodified Cloisite 10A containing films compared to unmodified Nanofil 116 containing films. Efficient delamination of nanoclays and their dispersion in corn zein matrix achieved by sonication also reinforced zein layer better compared to stirring samples.

Table 6.10. Yield strength of CZNC-PP films containing 5 wt% nanoclay

Sample	Nanoclay Content in CZNC Layer (%)	Yield Strength (MPa)
PPZ	-	24.68±0.79
CLO10A-5%	5	30.17±0.86
NF116-5%	5	26.92±1.96
CLO10A(Stir)-5%	5	25.28±1.36

Although effective reinforcement provided by organomodified Cloisite 10A due to increased interactions with zein matrix in CZNC coatings brought in desirable properties such as enhanced elastic modulus and higher yield strength, elongation at break of coated PP films decreased dramatically with increasing clay concentration as seen in Figure 6.15. As mentioned before, CZNC layer coated on PP surface acts like a fiber in a composite structure. Stiffer and stronger corn zein layers formed by the dispersion of nanoclays lowered the elasticity of prepared films by creating stress concentrated regions on substrate film. Unmodified clay containing and stirring samples gave higher elongation at break values compared to modified ones (Table 6.11) Continuous decrease in elongation at break was observed in CZNC-PP samples prepred by using organomdified Cloisite 10A nanoclay. The elongation value of zein coated PP decreased from 683% to 247%. Although flexibility of the all prepared films decreased, the maximum elongation before break was still much higher than the yielding strain of the films where integrity of the CZNC coating and PP substrate film altered.
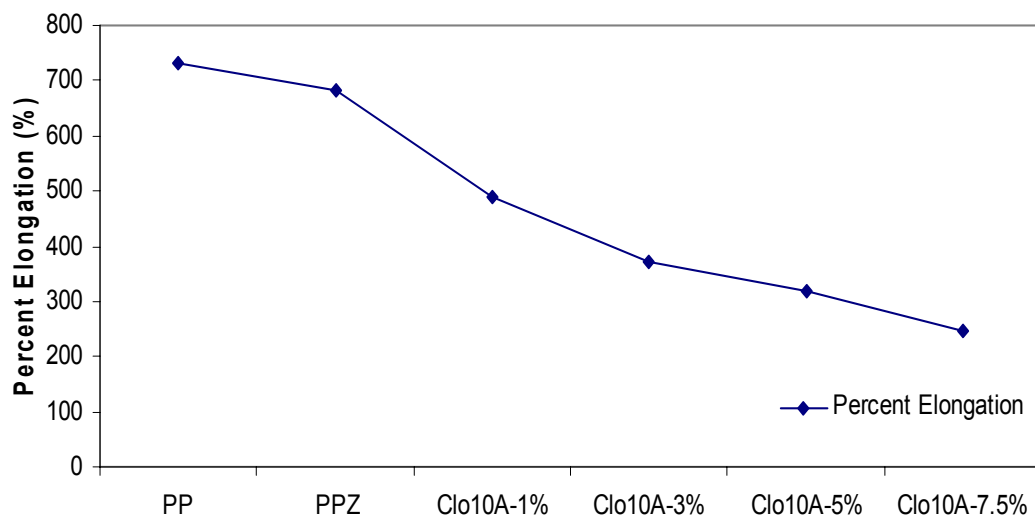
Figure 6.15. Percent Elongation at break values of CZNC-PP and base PP films

Table 6.11. Effects of clay amount/type and preparation method on the percent elongation at break values of CZNC films

Sample	Nanoclay Content in CZNC Layer (%)	Percent Elongation at Break (%)
PP	-	732.89±56.11
PPZ	-	683.76±67.93
CLO10A-1%	1	487.49±37
CLO10A-3%	3	372.19±180.31
CLO10A-5%	5	320.16±25.22
CLO10A-7.5%	7.5	247.1±30.77
NF116-5%	5	427.78±139.78
CLO10A(Stir)-3%	3	581.54±60.65
CLO10A(Stir)-5%	5	385.82±164.85

6.4. Optical and Surface Properties

Effect of nanoclay content, type and processing method on the optical and surface hydrophobicity properties of CZNC layers were also investigated. Surface hydrophobicity of the CZNC-PP films were evaluated by contact angle measurements. Optical properties of the films were investigated by conducting color measurements, examining the total color change.

6.4.1. Contact Angle Measurements

Initial contact angle measurements were conducted in order to observe the effect of organomodified montmorillonite (Cloisite 10A) content on corn zein nanocomposite coated polypropylene films. Contact angle is the measure of hydrophobicity of a substance. As hydrophobicity of the surface decreases, water molecules tend to spread on surface more readily. Measured water contact angles of the PP substrate and CZNC coated films were given in Table 6.12. Values denoted by θ, are the angle of tangent line to water drop with the surface as seen in Figure 6.16.
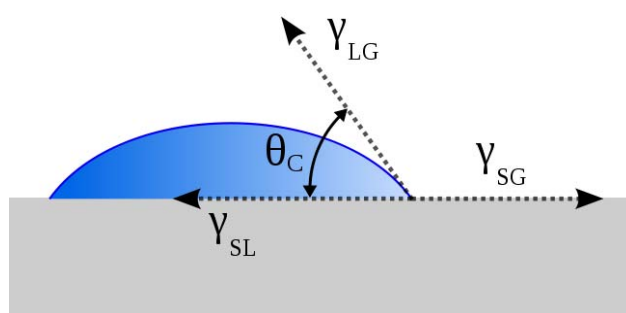
Figure 6.16. Definition of contact angle used in this study

Zein coating reduced the contact angle of the film surface from 88.90^0 to 54.25^0, due to more hydrophilic nature of corn zein. Measured contact angle value for zein coating is in good agreement with previously reported glycerol plasticized zein films and coatings (Tihminlioglu et al., 2010; Atik et al., 2007; Ghanbarzadeh et al., 2006). Addition of even small amount of organomodified Cloisite 10A nanoclay into corn zein increased hydrophobicity of CZNC coatings. Increase in hydrophobicity can be attributed to the addition of Cloisite 10A with hydrophobic character into the corn zein polymer. Effect hydrophobic or hydrophilic character of nanofillers on contact angles of nanocomposite films were also reported previously. Decrease in contact angle reported by the use of hydrophilic unmodified montmorillonites (Tunc et al., 2007) while hydrophobic organomodified MMT increased hydrophobicity of the surface (Rhim et al., 2006).

Table 6.12. Initial contact angles measured for CZNC-PP samples

Sample Code	Left Angle (θ)	Right Angle (θ)	Avg. Contact Angle (θ)
PP	89.34±0.67	88.45±1.07	88.90±0.82
PPZ	54.93±1.18	53.57±2.03	54.25±1.45
CLO10A-1%	56.43±1.31	55.68±0.95	56.06±1.02
CLO10A-3%	57.06±1.01	56.17±3.34	56.62±1.93
CLO10A-5%	61.90±0.57	60.36±1.21	61.13±0.89
CLO10A-7.5%	62.38±1.79	60.95±1.76	61.66±1.68
CLO10A-15%	64.76±4.37	61.47±5.65	63.12±4.88

Measured initial contact angles of the CZNC coatings were in good accordance with the water vapor permeability results. The degree of surface hydrophobicity increased with increasing OMMT concentration. As degree of surface hydrophobicity increased, WVP of CZNC-PP films decreased indicating a possible relationship between contact angle changes and water vapor barrier due to changes in the nanocomposite structure in the polymer matrix. WVP of the coatings would be decreased by the presence of exfoliated OMMT on the surface by limiting water molecules to be absorbed by CZNC matrix. Another possibility is that affinity to water molecules is decreased due to the more hydrophobic zein coating.

In this study, contact angles measured for various Cloisite 10A concentrations showed small deviations; that can be interpreted as an indication of homogeneous surface. Effect of high nanoclay content can be seen in Table 6.12 for CLO10A-15% sample. Measured contact angle for CLO10A-15% was higher than all CZNC-PP films. Standard deviation of the measurements was also significantly higher than other samples that can be attributed to altered homogeneity of the surface due to inefficient dispersion of layered silicates.

6.4.2 Color Changes of Films

Color of corn zein nanocomposite coated polypropylene films are as important as barrier and mechanical properties for their possible use as a packaging film. Polypropylene is widely used in food packaging applications where display of food is

desired. Since PP is an accepted colorless polymer; the effect of CZNC coatings on polypropylene were evaluated by using Hunter Method by taking the commercial PP film as reference. The total color differences (ΔE) of the coated films were calculated by using the L, a, b parameters for different CZNC formulations.

Results of the color analysis showed that nanoclay type and loading as well as preparation method of CZNC coating layers has significant effect on the color of the films. The total color difference of the films represents the cumulative effect of three color parameters; L, a, and b. The luminosity or lightness parameter L can have values between 0 and 100. As ability of film to reflect light increases, the value of L converges to 100. As seen in Table 6.13, the luminosity of the films did not change by the CZNC coating. Second color parameter a, is the measure of redness-greenness. Values of a changes between -60 (green) and 60 (red); as the material become greener, its value converges to -60. As seen in Table 6.13, increase in the clay content resulted in very slight change of b parameter in the direction of green color.

Table 6.13. The total color difference (ΔE) and color parameters of prepared CZNC coated PP films for different formulations

Sample Code	OMMT (%wt)	L	a	b	Total Color Difference (ΔE)
PP	-	90.38	0.27	-0.13	(Reference)
PPZ	-	90.25	-0.07	2.03	2.19
CLO10A-1%	1	90.11	-0.10	2.11	2.28
CLO10A-3%	3	90.15	-0.02	2.35	2.51
CLO10A-5%	5	90.12	-0.20	2.71	2.89
CLO10A-7.5%	7.5	90.19	-0.20	2.72	2.89
NF116-1%	1	89.26	-0.40	3.95	4.28
NF116-3%	3	89.06	-0.37	3.56	3.97
NF116-5%	5	89.19	-0.59	4.58	4.93
CLO10A(Stir)-3%	3	89.71	-0.50	4.05	4.31
CLO10A(Stir)-5%	5	89.81	-0.26	4.62	4.81

The most significant contribution to total color change was done by the yellowness index b. As materials become yellower, the value converges to 60. The applied polymer layers onto the substrate in laminated (Weller et al., 1998) or coated (Lee et al., 2008) structures change the color depending on the characteristics of applied layer. Higher yellowness of CZNC coated PP films is unsurprising, since corn zein is

yellow in its standalone form (Weller et al., 1998). Corn zein coatings were also reported to change the color of PP films yellower in different extends depending on the plasticizer type (Lee et al., 2008). As seen in Table 6.13, even 6 micron corn zein coating without nanoclay loading resulted in increased b value.

Blending and composting the polymers change the color of resulting films. Several studies reported the color change together with transparency that is an indication for the miscibility of components (Su et al., 2010; Rotta et al., 2009). Since human eye is insensitive to color differences below the value of 3; generally color changes below this limit is acceptable in many applications (Hong et al., 2005). The color measurement results for CLO10A set of prepared films were tabulated in Table 6.14. Corn zein nanocomposite coatings prepared by using Cloisite 10A at different loadings exerted only small changes to total color difference values. Since the total difference values were maximum 2.89, it can be said that the color change is insignificant due to the fine delamination of nanoclay platelets within the corn zein matrix as it was also evidenced from the FTIR-ATR results. As seen in Tbale 6.14, the loaded filler amount increases, the color of CZNC becomes slightly yellower. Casariego and coworkers (2009) reported only very slight yellowish color change of chitosan nanocomposites, due to fine dispersion of nanoparticles.

Table 6.14. The total color difference (ΔE) and color parameters of Cloisite 10A loaded CZNC coated PP films

Sample Code	OMMT (%wt)	L	a	b	Total Color Difference (ΔE)
PP	-	90.38	0.27	-0.13	(Reference)
PPZ	-	90.25	-0.07	2.03	2.19
CLO10A-1%	1	90.11	-0.10	2.11	2.28
CLO10A-3%	3	90.15	-0.02	2.35	2.51
CLO10A-5%	5	90.12	-0.20	2.71	2.89
CLO10A-7.5%	7.5	90.19	-0.20	2.72	2.89

Besides the nanoclay content; the chemistry of the clay – pristine or organomodified montmorillonite, and processing type were observed to be influential on the color changes of the corn zein nanocomposite coating layers. Though CZNC layers prepared by sonication of Cloisite 10A organomodified montmorillonites showed

insignificant color differences compared to base PP film, films coated with zein layers containing unmodified Nanofil 116 and coatings prepared without sonication resulted in significant total color changes. Effect of modification of montmorillonite and preparation technique on the color changes were observed to be more evident in coatings prepared by incorporation of 5% nanoclay in CZNC layer. Total color differences evaluated for 5% nanoclay content in CZNC layers were tabulated in Table 6.15 for comparison.

Table 6.15. Total color difference (ΔE) and color parameters of 5% nanoclay loaded CZNC coated PP films

Sample Code	OMMT (%wt)	L	a	b	Total Color Difference (ΔE)
PP	-	90.38	0.27	-0.13	(Reference)
PPZ	-	90.25	-0.07	2.03	2.19
CLO10A-5%	5	90.12	-0.20	2.71	2.89
NF116-5%	5	89.19	-0.59	4.58	4.93
CLO10A(Stir)-5%	5	89.81	-0.26	4.62	4.81

As seen in Table 6.15, inefficient dispersion of layered silicates resulted in significant color changes, even detectable by naked eye. Yellowness and total color difference of 5% samples prepared by unmodified MMT and without sonication were higher compared to CLO10A-5% nanocomposite coating.

CHAPTER 7

CONCLUSION

In this study, corn zein nanocomposites (CZNC) prepared by solution intercalation method were coated onto polypropylene (PP) films in order to develop a novel film system for food packaging applications. The study was focused on the effects of montmorillonite addition into corn zein coating layer. Effect of nanoclay content, type and processing of CZNC layers on the oxygen and water vapor barrier as well as mechanical properties, optical and surface characteristics of corn zein nanocomposite coated PP films (CZNC-PP) were investigated. The final films showed good compatibility between CZNC coating and PP in terms of appearance and adhesion. CZNC coatings applied on PP showed improvements in the barrier properties of the bilayer PP films depending on the level of nanoclay content and type in CZNC coating. CZNC coating with a thickness of only 5.9 μm successfully improved the barrier properties of PP film. Nanocomposite coating reduced the oxygen transmission rates (OTR) of prepared films by 4 times compared to base PP film, meanwhile WVP decreased by 30% for the films prepared with 5wt% OMMT in the CZNC coating.

Effect of nanocomposite structure on barrier properties of single corn zein layers was also investigated. Extend of barrier improvements were also in good accordance with the interactions between layered silicate nanoclays and zein matrix as well as nanoclay loading since FTIR-ATR results revealed new bonds within the coated CZNC structure due to fine layered silicate delamination. Independent of coating thickness, addition of 5wt% Cloisite 10A organomodified nanoclay to corn zein decreased the OTR and WVP of single zein coating layers by 65% and 60%, respectively. The decreases in permeabilities of the films is believed to be due to the presence of dispersed particle layers with large aspect ratios in the polymer matrix. This forces permeating molecules to follow a tortuous path through the polymer matrix by increasing the effective path length for diffusion. Permeation data was fitted to various phenomenological tortuosity based models predicting the permeability of polymer nanocomposite filled with nanoclay as a function of clay concentration and aspect ratio of nanoplatelets. Since effective aspect ratio is somehow related to level of delamination

in the structure, the barrier property improvements are in accordance with the aspect ratio. CZNC layer showed higher OTR and WVP for 7.5% wt nanoclay loaded sample attributed to reduced exfoliation and possibly some degree of agglomeration of nanoclays in nanocomposite structure. Surface characteristics were also in agreement with the permeability results. Higher modified nanoclay content increased hydrophobicity of CZNC surfaces.

Mechanical properties of prepared films (elastic modulus and yield strength) were significantly improved by the addition of organomodified montmorillonites. While elastic moduli of the prepared films were doubled and yield strengths increased by 75% compared to PP film; elongation at break of the films decreased due to less flexible zein coating.

Optical properties of CZNC-PP films were found to be affected by the nanoclay amount and organomodification. Organomodified montmorillonites finely dispersed in corn zein layer changed the color of the films very slightly, and not detectable by naked eye. Meanwhile, addition unmodified nanoclay and stirring employed instead sonication lead to deterioration of the color of the films. Additionaly, incompatibility between zein and unmodified nanoclays resulted in lower barrier and mechanical performance of CZNC-PP films. Similarly, stirring was found to be ineffective for the preparation of CZNC layers since no significant achievements were obtained compared to the samples prepared by sonication.

In summary, excellent barrier properties of corn zein nanocomposites were successfully combined with mechanically strong PP as an eco-friendly promising alternative to conventional barrier packaging systems. A novel strategy was proposed to put corn zein in use for food packaging applications by nanocomposites.

REFERENCES

Akbari, Z.; Ghomashchi, T.; Moghadam, S. Improvement in Food Packaging Industry with Biobased Nanocomposites. *International Journal of Food Engineering.* **2007**, 3, 1-24

Alexandre, M.; Dubois, P. Polymer - Layered Silicate Nanocomposites: Preparation, Properties and Uses of A New Class of Materials *Materials Science and Engineering.* **2000,** 28, 1-63

Bae, H.J.; Park, H.I.; Hong, S.I.; Byun, Y.J.; Darby, D.O.; Kimmel, R.M.; Whiteside, W.S. Effect of Clay Content, Homogenization RPM, pH, and Ultrasonication on Mechanical and Barrier Properties of Gelatin/Montmorillonite Nanocomposite Films. *Food Science and Technology.* **2009**, 42, 1179-1186

Handbook of Biodegradable Polymers, 1st ed. Bastioli, C.; Rapra Technology Limited, 2005; Chapter 1, pp. 2-3

Bharadwaj, R.K. Modelling the Barrier Properties of Polymer-Layered Silicate Nanocomposites. *Macromolecules.* **2001**, 34, 9189-9192

Brachet, P.; Høydal, L.T.; Hinrichsen, E. L.; Melum, F. Modification of Mechanical Properties of Recycled Polypropylene from Post-consumer Containers. *Waste Management.* **2008**, 28, 2456-2464

Burgentzle, D.; Duchet, J.; Gerard, J.F.; Jupin, A.; Fillon, B. Solvent Based Nanocomposite Coatings I. Dispersion of Organophilic Montmorillonite in Organic Solvents. *Journal of Colloid and Interface Science.* **2004**, Vol. 278, pp.26-39

Butkinaree, S.; Jinkarn, T.; Yoksan, R. Effect of Biodegradable Coating on Barrier Properties of Paperboard Food Packaging. *Journal of Metals, Materials and Minerals.* **2008**, 18, 219-222.

Casariego, A.; Souza, B.W.S.; Cerqueira, M.A.; Teixeira, J.A.; Cruz, L.; Diaz, R.; Vicente, A.A. Chitosan/clay Films' Properties as Affected by Biopolymer and Clay Micro/Nanoparticles' Concentrations. *Food Hydrocolloids.* **2009**, 23, 1895-1902

Chandra, R. Biodegradable Polymers. *Progress in Polymer Science.* **1997***, 23, 1273–1335

Chen, G. X.; Hao, G. J.; Guo, T. Y.; Song, M. D.; Zhang, B. H. Crystallization Kinetics of Poly(3-Hydroxybutyrate-co-3-Hydroxyvalerate)/Clay Nanocomposites. *Polymer Science.* **2003***, 93, 655-661

Chen, P.; Zhang, L. Interaction and Properties of Highly Exfoliated Soy Protein/ Montmorillonite Nanocomposites. *Biomacromolecules*. **2006**, 7(6), 1700-1706.

Chiellini, E.; Chiellini, F.; Cinelli, P. *in Degradable Polymers Principles and Applications* Scott, G.; 2nd ed, Kluwer Academic Publishers, 2002; pp.163-233.

Cho, S.Y.; Park, J.W.; Rhee, C. Properties of Laminated Films from Whey Powder and Sodium Caseinate Mixtures and Zein Layers. *Lebensm.-Wiss. U.-Technol*. **2002**, 35, 135-139.

Choudalakis, G.; Gotsis, A.D. Permeability of Polymer/Clay Nanocomposites: A Review. *European Polymer Journal*. **2009**, 45, 967-984

Comstock, K.; Farrell, D.; Christina G. C; Xi, Y. *From Hydrocarbons to Carbohydrates: Food Packaging of the Future*, 1st ed, John Wiley, New York; 2004; pp. 1-25.

Cutter, C. N. Opportunities for Bio-based Packaging Technologies to Improve the Quality and Safety of Fresh and Further Processed Muscle Foods. *Meat Science*. **2006**, 74, 131-142.

Cuq, B.; Gontard, N.; Guilbert, S. Proteins as Agricultural Polymers for Packaging Production. *Cereal Chemistry*. **1998**, 75, 1-9

Dean, K.M.; Do, M.D.; Petinakis, E.; Yu, L. Key Interactions in Biodegradable Thermoplastic Starch/poly(Vinyl Alcohol)/Montmorillonite Micro- and Nanocomposites. *Composites Science and Technology*. **2008**, 68, 1453-1462

DeRocher, J.P.; Gettelfinger, B.T.; Wang, J.; Nuxoll, E.E.; Cussler, E.L. Barrier Membranes with Different Sizes of Aligned Flakes. *Journal of Membrane Science*. **2005**, 254, 21-30

Dean, K.; Yu, L. in *Biodegradable Polymers for Industrial Applications*, Smith, R., 1st ed., Woodhead Publishing, Cambridge, 2005; pp. 289-307

Eitzman, D.M.; Melkote, R.R.; Cussler, E.L. Barrier Membranes with Tipped Impermeable Flakes. *AIChe Journal*. **1996**, 42, 2-9

Gao, C.; Stading, M.; Wellner, N.; Parker, M.L.; Noel, T.R.; Mills, E.N.C.; Belton, P.S. Plasticization of a Protein-Based Film by Glycerol: A Spectroscopic, Mechanical and Thermal Study. *Journal of Agricultural and Food Chemistry*. **2006**, 54, 4611-4616

Ghanbarzadeh, B.; Musavi, M.; Oromiehie, A.R.; Rezayi, K.; Razmi, E.; Milani, J. Investigation of Water vapor Permeability, Hydrophobicity and Morphology of Zein Films Plasticized by Polyols. *Iranian Polymer Journal*. **2006**, 15 (9), 691-700

Ghanbarzadeh B.; Musavi M.; Oromiehie A.R.; Jomeh Z. E.; Rad E. R.; Milani J. Effect of Plasticizing Sugars on Water Vapor Permeability, Surface Energy and Microstructure Properties of Zein Films. *Food Research International.* **2006**, 39, 882-890

Ghanbarzadeh, B.; Oromiehie, A.R.; Musavi, M.; Falcone P.M.; D-Jomeh, Z.E.; Rad, E.Z. Study of Mechanical Properties, Oxygen Permeability and AFM Topography of Zein Films Plasticized by Polyols. *Packaging Technology and Science.* **2007**, 20, 155-163

Ghanbarzadeh, B.; Oromiehi, A.R. Biodegradable Biocomposite Films Based on Whey Protein and Zein: Barrier, Mechanical Properties and AFM Analysis. *International Journal of Biological Macromolecules.* **2008**, 43, 209-215

Gioia, L. D.; Guilbert, S. Corn Protein-Based Thermoplastic Resins: Effect of Some Polar and Amphiphilic Plasticizers. *Journal of Agricultural Food Chemistry.* **1999**, 47, 1254-1261.

Gioia, L. D.; Cuq, B.; Guilbert, S. Mechanical and Water Barrier Properties of Corn-protein Based Biodegradable Plastics. *Journal of Material Research.* **2000**, 15 (12), 2612-2619.

Gillgren, T.; Barker, S.A.; Belton P.S.; Georget, D.M.R.; Stading, M. Plasticization of Zein: A Thermomechanical, FTIR and Dielectric Study. *Biomacromolecules.* **2009**, 10, 1135-1139

Hablot, E.; Bordes, P.; Pollet, E.; Averous L. Thermal and Thermo-mechanical Degradation of Poly(3-hydroxybutyrate)-Based Multiphase Systems. *Polymer Degradation and Stability.* **2008**, 93, 413-421

Haugaard, V. K.; Udsen, A. M.; Mortensen, G.; Høegh, L.; Petersen, K.; Monahan, F. Potential Food Applications of Biobased Materials-An EU-Concerted Action Project. *Starch/Starke.* **2001**, 53, 189-200.

Han, J. H., 2005. *Innovations in Food Packaging, 1st ed., CRC Press;* pp.12-23

Herald, T. J.; Obuz, E.; Twombly, W. W.; Rausch, K. D. Tensile Properties of Extruded Corn Protein Low-Density Polyethylene Films. *Cereal Chemistry.* **2002,** 79 (2), 261-264.

Hernandez-Izquerdo, V.M.; Krochta, J.M. Thermoplastic Processing of Proteins for Film Formation – A review. *Journal of Food Science.* **2008,** 73 (2), 30-39

Herrera-Alonso, J.M.; Marand, E.; Little, J.C.; Cox, S.S. Transport Properties in Polyurethane/Clay Nanocomposites as Barrier Materials: Effect of Processing Conditions. *Journal of Membrane Science.* **2009,** 337, 208-214

Hong, S. I.; Krochta, J. M. Oxygen Barrier Properties of Whey Protein Isolate Coatings on Polypropylene Films. *Journal Of Food Science.* **2003**, 68, 224-228.

Hong, S. I.; Han, J. H.; Krochta, J. M. Optical and Surface Properties of Whey Protein Isolate Coatings on Plastic Films as Influenced by Substrate, Protein Concentration, and Plasticizer Type. *Journal of Applied Polymer Science.* **2004**, 92, 335-343.

Hong, S. I.; Lee, J. W.; Son, S. M. Properties of Polysaccharide-coated Polypropylene Films as Affected by Biopolymer and Plasticizer Types. *Packaging Technology and Science.* **2005**, 18, 1-9

Hong, S. I.; Krochta, J. M. Oxygen Barrier Performance of Whey-protein Coated Plastic Films as Affected by Temperature, Relative Humidity, Base Film and Protein Type. *Journal of Food Engineering.* **2006**, 77, 739-745.

Huang, X.; Netravali, A.N. Characterization of Nano-Clay Reinforced Phytagel-Modified Soy Protein Concentrate Resin. *Biomacromolecules.* **2006**, 7, 2783-2789

Krochta, J.M. A. in Protein Based Films and Coatings, Gennadios, A., 1st ed., CRC Press, 2002; pp. 1-41

Kvien, I.; Sugiyama, J.; Votrubec, M.; Oksman, K. Characterization of Starch Based Nanocomposites. *Journal of Materials Science.* **2007**, 42, 8163-8171

Lai, H. M.; Padua, G.W. Properties and Microstructure of Plasticized Zein Films. *Cereal Chemistry.* **1997**, 74(6), 771-775.

Lape, N.K.; Nuxoll, E.E.; Cussler, E.L. Polydisperse Flakes in Barrier Films. *Journal of Membrane Science.* **2004**, 236, 29-37

Lawton, J. W. Zein: A History of Processing and Use. *Cereal Chemistry.* **2002**, 79, pp. 1-18.

Lawton, J. W. Plasticizers for Zein: Their Effect on Tensile Properties and Water Absorption of Zein Films. *Cereal Chemistry.* **2004**, 81, pp. 1-5.

Lee, J.W.; Son, S. M.; Hong, S.I. Characterization of Protein-coated Polypropylene Films as a Novel Composite Structure for Active Food Packaging Application. *Journal of Food Engineering.* **2008**, 86, 484-493.

Lu, C.; Mai, Y.W. Permeability Modeling of Polymer-Layered Silicate Nanocomposites. *Composites Science and Technology.* **2007**, 67, 2895-2902

Luecha, J.; Sözer, N.; Kokini, J.L. Synthesis and Properties of Corn zein /Montmorillonite Nanocomposite Films. *Journal of Materials Science*. **2010**, 45, 3529-3537

Madeka, H.; Kokini, J. L. Effect of Glass Transition and Cross-Linking on Rheological Properties of Zein: Development of a Preliminary State Diagram. *Cereal Chemistry*. **1996**, Vol. 73 (4), 433-438.

Magalhaes, N.F.; Andrade, C.T. Thermoplastic Corn Starch/Clay Hybrids: Effect of Clay Type and Content on Physical Properties. *Carbohydrate Polymers*. **2009**, 75, 712-718

Maiti, P.; Batt, C. A.; Giannelis, E. P. New Biodegradable polyhydroxybutyrate /Layered Silicate Nanocomposites. *Biomacromolecules*. **2007**, 8, 3393-3400.

Marsh, K.; Bugusu, B. Food Packaging – Roles, Materials, and Environmental Issues. *Journal of Food Science*. **2007**, 72, 39-55

Miguel, O.; Fernandez-Berrini, M. J.; Iruin, J. J. Survey on Transport Properties of Liquids, Vapors, and Gases in Biodegradable Poly(3-hydroxybutyrate) (PHB). *John Wiley & Sons*. **1996**, 1849-1859

Miller, K. S.; Krochta, J.M. Oxygen and Aroma Barrier Properties of Edible Films: A Review. *Trends in Food Science & Technology*. **1997**, 8, 228-237.

Mohanty, A. K.; Misra, M.; Hinrichsen G. Biofibres, Biodegradable Polymers and Biocomposites: An Overview. *Macromolecular Materials Engineering*. **2000**, 276, 1-24

Mohanty, A. K.; Misra, M.; Drzal L. T. Sustainable Bio-Composites from Renewable Resources: Opportunities and Challenges in the Green Materials World. *Journal of Polymers and the Environment*. **2002**, 12, 19-26

Muthuselvi, L.; Dhathathreyan, A. Contact Angle Hysterisis of Liquid Drops as Means to Measure Adhesive Energy of Zein on Solid Substrates. *Pramana-Journal of Physics*. **2006**, 66(3), 563-574

Nayak, P. L. Biodegradable Polymers: Opportunities and Challenges. *Macromolecular Chemical Physics* . **1999**, 39, 481-505

Nielsen, L.E. Models for the Filled Polymer System. *J. Macromol. Sci. Chem.* **1967**, A1, 929-942

Okamoto, M., 2005 in *Handbook of Biodegradable Polymeric Materials and their Applications*, Mallapragada, S.; Narasimhan, P., American Scientific Publishers, Vol.1, 2005; pp. 1-45

Olabarrieta, I. Strategies to Improve the Aging, Barrier and Mechanical Properites of Chitosan, Whey and Wheat Gluten Protein Films. *KTH Fibre and Polymer Technolgy.* **2005***, 42, 12-22

Padua, G.W., Wang, Q. in *Protein Based Films and Coatings*, Gennadios, A., CRC Press, 2002; pp. 43-67

Pandey, J.K.; Singh, R.P. Green Nanocomposites from Renewable Resources: Effect of Plasticizer on the Structure and Material Properties of Clay-filled Starch. *Starch / Stärke.* **2005***, 57, 8–15

Paramawati, R.; Yoshino, T.; Isobe, S. Properties of Plasticized-Zein Film as Affected by Plasticizer Treatments. *Food Science Technology.* **2001***, 7 (3), 191-194.

Park, J.W.; Whiteside, W.S.; Cho, S.Y. Mechanical and Water Vapor Barrier Properties of Extruded and Heat-Pressed Gelatin Films. *LWT.* **2008**, 41, 692-700

Petersen, K.; Nielsen, P. V.; Bertelsen, G.; Lawther, M.; Olsen M. B.; Nilsson, N. H.; Mortensen, G. Potential of Biobased Materials for food Packaging. *Trends in Food Science and Technology.* **1999***, 10, 52 – 68

Paul, D.R.; Robeson, L.M. Polymer Nanotechnology: Nanocomposites. *Polymer.* **2008**, 49, 3187-3204

Pavlidou, S., Papaspyrides, C.D. A review on Polymer-Layered Silicate Nanocomposites. *Progress in Polymer Science.* **2008**, 33, 1119–1198

Petersson, L.; Oksman, K. Biopolymer Based Nanocomposites: Comparing Layered Silicates and Microcrystalline Cellulose as Nanoreinforcement. *Composites Science and Technology.* **2006**, 66, 2187-2196

Rao, Y. Gelatin – Clay Nanocomposites of Improved properties. *Polymer.* **2007**, 48, 5369-5375

Ray, S.S.; Okamoto, K.; Okamoto, M. Structure-Property Relationship in Biodegradable Poly(butylene succinate)/Layered Silicate Nanocomposites. *Macromolecules.* **2003**, 36, 2355-2367

Ray, S.S.; Okamoto, M. Polymer/Layered Silicate Nanocomposites: A Review from Preparation to Processing. *Progress in Polymer Science.* **2003**, 28, 1539-1641

Ray, S. S.; Bousmina, M. Biodegradable Polymers and Their Layered Silicate Nanocomposites: In Greening The 21st Century Materials World. *Progress in Materials Science.* **2005**, 50,962–1079

Ray, S.S, Bousmina, M.M. 2006, in *Polymer Nanocomposites*, Mail, Y.W.; Yu, Z.Z.; 1st ed, Woodhead Publishing, Cambridge, 2006, pp.57-129

Rhim, J.W.; Lee, J.H.; Hong, S.I. Water Resistance and Mechanical Properties of Biopolymer (alginate and soy protein) Coated Paperboards. *LWT*. **2006**, 39, 806-813

Rotta, J.; Ozorio, R.A.; Kehrwald, A.M.; Barra, G.M.O.; Amboni, R.D.M.C.; Barreto, P.L.M. Parameters of Color, Transparency, Water Solubility, Wettability and Surface Free Energy of Chitosan/Hydroxypropylmethylcellulose (HPMC) Films Plasticized with Sorbitol. *Materials Science and Engineering*. **2009**, C29, 619-623

Ryu, S.Y.; Rhim, J.W.; Roh, H.J.; Kim, S.S. Preparation and Physical Properties of Zein-Coated-High Amylose Corn Starch Film. *Lebensm.-Wiss. U.-Technol.* **2002**, 35, 680-686

Robertson, G. L.; *Food Packaging Principles and Practice – 2nd Ed.,* CRC Press, 2005, pp. 18-46

Santosa, F.X.B.; Padua, G.W. Thermal Behavior of Zein Sheets Plasticized with Oleic Acid. *Cereal Chemistry*. **2000**, 77(4), 459-462

Selling, G.W.; Sessa, D.J.; Palmquist, D.E. Effect of Water and tri(ethylene) glycol on the Rheological Properties of Zein. *Polymer*. **2004**, 45, 4249-4255

Selling, G.W.; Sessa, D.J. Sample Preparation and testing Methods Affect the Physical Properties and Evaluation of Plasticized Zein. *Industrial Crops and Products*. **2007**, 25(3), 266-273.

Shukla, R.; Cheryan, M. Zein: the Industrial Protein from Corn. *Industrial Crops and Products*. **2001**, 13, 171-192.

Smith, R. Biodegradable Polymers for Industrial Applications, 1st ed., CRC Press, 2005, pp. 134-176

Sothornvit, R.; Hong, S.I.; An, D.J.; Rhim, J.W. Effect of Clay Content on the Physical and Antimicrobial Properties of Whey Protein Isolate/Organo-clay Composite Films. *Food Science and Technology*. **2010**, 43, 279-283

Su, J.F.; Yuan, X.Y.; Huang, Z.; Xia, W.L. Properties Stability and Biodegradation Behaviors of Soy Protein isolate/poly (vinyl alcohol) Blend Films. *Polymer Degradation and Stability*. **2010**, 95, 1226-1237

Sun, L.; Boo, W.J.; Clearfield, A.; Sue, H.J.; Pham, H.Q. Barrier Properties of Model Epoxy Nanocomposites. *Journal of Membrane Science*. **2008**, 318, 128-136

Tang, X.; Alavi, S.; Herald, T.J. Barrier and Mechanical Properties of Starch-Clay Nanocomposite Films. *Cereal Chemistry.* **2008**, 85, 433-438

Tharanathan, R. N. Biodegradable Films and Composite Coatings: Past, Present and Future. *Trends in Food Science & Technology.* **2003**, 14, 71-78.

Tice, P., 2003, Packaging Materials 4. - Polyethylene for Food Packaging Applications. *ILSI Europe Packaging Material Task Force.*

Tihminlioglu, F.; Atik, İ.D.; Özen, B. Water Vapor and Oxygen-Barrier Performance of Corn-Zein Coated Polypropylene Films. *Journal of Food Engineering.* **2010**, 96, 342-347

Tillekeratne, M.; Eastel, A.J. Modification of Zein Films by Incorporation of Poly(ethylene glycol)s. *Polymer International.* **2000**, 49, 127-134

Tran, N.H.; Dennis, G.R.; Milev, A.S.; Kannangara, G.S.K.; Williams, P.; Wilson, M.A.; Lamb, R.N. Dispersion of Modified Clays within n-alcohols. *Journal of Colloid and Interface Science.* **2006**, 297, 541-545

Tunc, S.; Angellier, H.; Cahyana, Y.; Chalier, P.; Gontard, N.; Gastaldi, E. Functional Properties of Wheat Gluten/Montmorillonite Nanocomposite Films Processed by Casting. *Journal of Membrane Science.* **2007**, 289, 159-168

Wang, Y.; Padua, G. W. Tensile Properties of Extruded Zein Sheets and Extrusion Blown Films. *Macromolecular Materials and Engineering.* **2003**, 288, 886-893.

Wang, Y.; Rakotonirainy, M.A.; Padua, G. W. Thermal Behavior of Zein-based Films. *Starch.* **2004**, 55, 25-32

Wang, Y.; Padua, G. W. Water Sorption Properties of Extruded Zein Films. *Journal of Agricultural Food Chemistry.* **2004**, 52, 3100-3105.

Wang, Y.; Filho, F. L.; Geil P.; Padua, G. W. Effects of Processing on the Structure of Zein/Oleic Acid Films Investigated by X-Ray Diffraction. *Macromolecular Bioscience.* **2005**, 5, 1200-1208.

Weber, C.J. *Biobased Packaging Materials for the Food Industry: Status and Perspectives*, KVL, 2005, pp.15-69.

Weber, C. J.; Haugaard, V.; Festersen, R.; Bertelsen, G. Production and Applications of Biobased Packaging Materials for the Food Industry. *Food Additives and Contaminants.* **2002**, 19, 172-177

Weller, C.L.; Gennadios, A.; Saraiva, R.A. Edible Bilayer Films from Zein and Grain Sorghum Wax or Carnauba Wax. *Lebensm.-Wiss. U.-Technol*. **1998**, 31, 279-285.

Yu, J.; Cui, G.; Wei, M.; Huang, J. Facile Exfoliation of Rectorite Nanoplatelets in Soy Protein Matrix and Reinforced Bionanocomposites Thereof. *Journal of Applied Polymer Science.* **2007**, 104, 3367-3377